THE USE OF VIBRATION MEASUREMENTS TO MONITOR THE CONDITION OF THE DIE IN THE DIEBOX IN THE STEEL WIREDRAWING PROCESS

by

Sergije Hlistunov

Submitted as part of the requirements for
the degree of M. Sc. (Acoustics)

UNIVERSITY OF NEW SOUTH WALES

1984

CONTENTS

ACKNOWLEDGEMENTS

I wish to express my sincere thanks to my Supervisor, Associate Professor, Anita Lawrence for her critical appraisal of this work and her guidance during its preparation.

I am indebited to my immediate supervisor Dr. Robert W. Harris for his invaluable guidance and assistance throughout the project and particularly wish to thank for the use of facilities of CSIRO at Lucas Heights.

A special appreciation is given to my employer, Australian Wire Industries - Sydney Wiremill for granting me study leave etc. to attend the course and conduct my project.

I take this opportunity to thank my wife who supported me and encouraged me throughout the course and last but not least Mrs. Annette Morris for the care and patience taken with the typing.

ABSTRACT

The use of vibration monitoring to assess the mechanical integrity of components in a manufacturing facility where motion occurs, is reviewed. The operation of a steel wiredrawing process is described with particular emphasis on wear mechanisms and how vibration monitoring can be used in this situation.

An accelerometer was used to monitor the vibration of the die assembly in a steel wiredrawing unit by tape recording at selected times the output of the transducer and subsequently the acquired data was analysed in the frequency domain by computing the power spectral density. The power spectral densities and quantities derived from them such as the mean, median and variances, were examined for correlations with the various physical parameters associated with the wiredrawing process such as tensile strength, die wear (the parameter of real interest), wire speed, wire diameter etc. The results showed general trends, however, since the wire speed was observed to be a dominating factor, it was difficult to assess die wear using the observed data, although a new die did tend to give a broader spectrum at lower frequencies than a worn die. A very exhaustive investigation using 100% monitoring of vibration and other parameters would be required to determine definitely if die wear can be assessed by vibration monitoring.

1. INTRODUCTION

The measurement of vibration of a machine or a plant can provide data on its mechanical condition. The data obtained from vibration monitoring has been used in the assessment of the mechanical integrity of rotating machinery, process plants, power stations, aircraft, space vehicles, ships etc. Thus condition monitoring, using the results of the analysis of vibration signals has become an important diagnostic tool.

Vibration is generated by forces within machinery thus detection and analysis of this vibration will yield information on the nature of these forces.

Although vibration signals can usually only be measured at external surfaces, information may be obtained about the machine's interior provided that a good mechanical path exists from the sources to the external surface, Vibration monitoring can allow the condition of the machine to be determined during normal operation which is very useful in both preventive or predictive maintenance, so that the three major functions of detection, analysis and correction can be implemented.

Vibration monitoring has proved most successful when used on rotating or reciprocating machinery. This investigation will examine the possible application of vibration monitoring to study the mechanical integrity of the die used in a steel wiredrawing process. The primary analytical tool to be used on the vibration signals is the computation of the Power Spectral Density (P.S.D.). The results will be interpreted in terms of

the various physical parameters associated with the wiredrawing process such as die geometry, lubrication, wire speed, wire size, percentage of reduction, tensile strength of the wire, intermittent operation of plant, surface texture of the wire etc. If possible, it is hoped that the onset of cracking in the die will be ascertained and the time from detection to final failure may be estimated.

Knowledge gained from this study may provide a basis for prevention and detection of early failure of the die through cracking and for extending the normal allowable die wear life.

There exists a large amount of research concerning the determination of the mechanical integrity of the components in a processing plant using the analyses of vibration signals. Unfortunately there are no reports on the use of vibration signals to determine the integrity of the die in a wiredrawing/extrusion process, however, an examination of the literature does yield some guidlines to assist in this area and has been included here for completeness.

The main emphasis has been on rotating machinery. This can be broadly categorised as:

1.1 Machinery Vibration
1.2 Bearings
1.3 Gears
1.4 Motors
1.5 Turbines and Generators
1.6 Fans
1.7 Pumps
1.8 Compressors

Another field, which has been of particular interest in the nuclear industry, is loose parts monitoring.

TABLE 1.1 VIBRATION FREQUENCIES AND LIKELY CAUSES
From Fox [14]

Frequency in terms of rpm	Most likely causes	Other possible causes and remarks
1 X rpm	Imbalance	1) Eccentric journals, gears or pulleys. 2) Misalignment or bent shaft—if high axial vibration. 3) Bad belts if rpm of belt. 4) Resonance. 5) Reciprocating forces. 6) Electrical problems.
2 X rpm	Mechanical looseness	1) Misalignment if high axial vibration. 2) Reciprocating forces. 3) Resonance. 4) Bad belts if 2 X rpm of belt.
3 X rpm	Misalignment	Usually a combination of misalignment and excessive axial clearances (looseness).
Less than 1 X rpm	Oil whirl (less than ½ rpm)	1) Bad drive belts. 2) Background vibration. 3) Sub-harmonic resonance. 4) Beat vibration.
Synchronous (a-c line frequency)	Electrical problems	Common electrical problems include broken rotor bars, eccentric rotor, imbalanced phases in poly-phase systems, unequal air gap.
2 X synchronous frequency	Torque pulses	Rare as a problem unless resonance is excited.
Many times rpm (harmonically related frequency)	Bad gears	Gear teeth X rpm of bad gear.
	Aerodynamic forces	Number of fan blades X rpm.
	Hydraulic forces	Number of impeller vanes X rpm.
	Mechanical looseness	May occur at 2, 3, 4 and sometimes higher harmonics if severely loose.
	Reciprocating forces	
High frequency (not harmonically related)	Bad antifriction bearings	1) Bearing vibration may be unsteady—amplitude and frequency. 2) Cavitation, recirculation and flow turbulence cause random, high frequency vibration. 3) Improper lubrication of journal bearings (friction excited vibration). 4) Rubbing.

1.1. MACHINERY VIBRATION

Mechanical signature analysis has been used to monitor the condition of many types of rotating machinery - pumps, fans, compressors, turbines and electric motors.

For instance, if there is a large vibration component at the frequency corresponding to the speed of rotation of the machine, this indicates an out-of-balance condition, whereas if a large vibration component occurs at twice this frequency it indicates misalignment in the couplings.

When vibration increases or becomes excessive, some mechanical trouble is usually the reason. Each mechanical defect, unbalance, misalignment, worn gears, looseness etc. generates vibration in its own unique way and different machinery troubles cause different frequencies of vibration. Thus when analysing machinery vibration to pinpoint problems, it is possible to identify a problem positively by simply measuring and noting its vibration characteristics. Table 1.1 lists the frequencies of vibration produced by rotating machinery and most likely causes for each [14].

Periodic vibrations and noise level readings obtained with hand-held meters are normally recorded on data sheets. Using a simple meter, one person can take noise and vibration readings on critical machinery in a

TABLE 1.2 VIBRATION IDENTIFICATION
REPRODUCED FROM FOX [14]

Cause	Amplitude	Frequency	Phase	Remarks
Imbalance	Proportional to imbalance. Largest in radial direction.	1 X rpm	Single reference mark.	Most common cause of vibration.
Misalignment of couplings or bearings, and bent shaft.	Large in axial direction, 50% or more of radial vibration.	1 X rpm usual, 2 and 3 X rpm sometimes.	Single double or triple.	Best found by appearance of large axial vibration. Use dial indicators or other method for positive diagnosis. If sleeve bearing machine and no coupling misalignment balance the rotor.
Bad bearings—anti-friction type.	Unsteady—use velocity measurement if possible	Very high, several X rpm.	Erratic.	Bearing responsible most likely the one nearest point of largest high-frequency vibration.
Eccentric journals.	Usually not large.	1 X rpm	Single mark.	If on gears largest vibration in line with gear centers. If on motor or generator vibration disappears when power is turned off. If on pump or blower attempt to balance.
Bad gears or gear noise.	Low—use velocity measure if possible.	Very high—gear teeth X rpm.	Erratic.	...
Mechanical looseness.		2 X rpm	Two reference marks. Slightly erratic.	Usually accompanied by unbalance and/or misalignment.
Bad drive belts.	Erratic or pulsing.	1, 2, 3 and 4 X rpm of belts	One or two depending on frequency. Usually unsteady.	Strobe light best tool to freeze faulty belt.
Electrical.	Disappears when power is turned off.	1 X rpm or 1 or 2 X synchronous frequency.	Single or rotating double mark.	If vibration amplitude drops off instantly when power is turned off cause is electrical.
Aerodynamic or hydraulic forces.	...	1 X rpm or number of blades on fan or impeller X rpm	...	Rare as a cause of trouble except in cases of resonance.
Reciprocating forces.	...	1, 2 and higher orders X rpm	...	Inherent in reciprocating machines; can only be reduced by design changes or isolation.

relatively short period of time. However, some machines are not well suited for spot check manual monitoring, and continuous monitoring is necessary. Vibration analyses conducted to determine the machine faults are concerned with monitoring forces which can cause wear, failure and inferior performance.

Table 1.2 is an alternative rearrangement of the data of Table 1.1 listing the most common causes of vibration together with amplitude and frequency of the resulting vibration and strobe picture characteristics [14]. Eshleman [15] also states that fault identification can be made directly from the measured and analysed data in many cases. The frequency of the vibrations monitored is related to both the excitation frequencies and the sum and difference of these excitation frequencies. When chronic problems occur, it is prudent to take into account the factors in Table 1.3.

In a linear system, the frequency of the monitored vibration is the same as the frequency of the exciting force. Thus forcing frequencies can be identified directly. Allison [16] has presented a method for calculating the known dynamic forces from measured vibrations of the systems to which the forces are applied. When the system stiffness becomes non linear, higher harmonics of the basic forcing frequency are present. This situation usually indicates the presence of faults such as misalignment or excessive loading.

Design	Manufacturing and Installation	Wear
critical speeds	mass unbalance	looseness
resonance	bow	mass unbalance
oil whirl	casing distortion	coupling
self-excited vibration	misalignment	gears
process induced excitation including slider crank, blades, vanes, etc.	foundation distortion	bearings seals
	repair	shafts

TABLE 1.3 DIAGNOSIS OF DESIGN, INSTALLATION AND WEAR DEFECTS REPRODUCED FROM ESHLEMAN [15]

Fault	Correction*
critical speeds	change bearing stiffness and/or damping change coupling size and type alter machine operating speed
resonance	alter stiffness of structure alter mass of structure add damping coatings, films, etc. alter forcing frequency
oil whirl	change oil temperature increase load on bearing change bearing geometry and/or type – pressure dam, lobe, tilting pad
self-excited vibration	eliminate rubs change bearing characteristics eliminate hysteresis from built-up parts
process induced excitation: slider cranks, blades, vanes, etc.	usually not much can be done unless trade-offs between process efficiency and vibration excitation has not been fully utilized

*more extreme alterations required for correction not listed.

TABLE 1.4 MACHINE DESIGN FAULTS AND CORRECTIONS FROM ESHLEMAN [15]

Fault	Correction
mass unbalance	single, two, or multiplane balancing depending on rotor configuration change critical speed for decreased balance sensitivity
bow	replace rotor local planing or hot spot application balancing
casing distortion and resonance	loosen bolts and apply shims add mass and/or stiffness to remove resonance
misalignment	hot and/or cold alignment change coupling* to decrease sensitivity
foundation distortion, looseness, and resonances	apply grout to foundation apply shims to remove distortion pour concrete in foundation to add mass add steel braces to increase stiffness
piping distortion and resonance	check pipe supports, isolators, and connectors check pressure pulsations

*hen couplings are changed possible critical speed changes should .e investigated.

TABLE 1.5 MACHINE MANUFACTURING AND INSTALLATION FAULTS AND CORRECTIONS FROM ESHLEMAN [15]

There are three basic methods in machine and structural fault correction and vibration control other than a replacement of worn parts:-

1. Excitation reduction - change both in amplitude and frequency of input forces to decrease vibration

2. Tuning and isolation - change both mass and stiffness to alter natural frequencies and mode shapes so that maxima in the vibration response will not coincide with maxima in driving force.

3. Damping - applications of bearings, film coatings, composite structures and other structures to dissipate vibrational energy in the form of heat.

Table 1.4 lists machine design faults and possible correction methods while Table 1.5 lists faults and possible correction methods applicable to manufacturing and installation. Computer analyses are often required to calculate critical speeds and vibration responses, so that corrections can be applied. These calculation techniques have been adequately developed but the physical data needed as input which characterises the equipment is often non-existent or inaccurate. Thus, it is often difficult to carry out analyses yielding precise results [15].

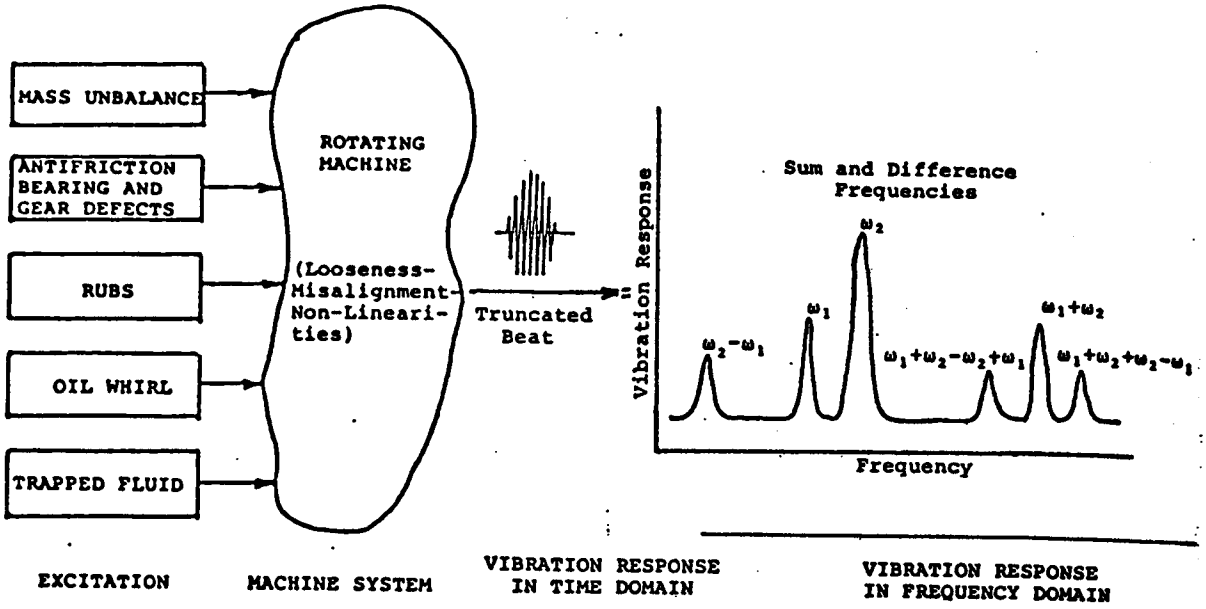

FIGURE 1.1 HYPOTHETICAL VIBRATION RESPONSE EXHIBITING TRUNCATED BEAT FREQUENCY

Sideband Frequencies		Center Frequencies		Sideband Frequencies		Harmonic Zone No.
—		0		$(\omega_2-\omega_1)$		0
$(2\omega_1-\omega_2)$		ω_1	ω_2	$(2\omega_2-\omega_1)$		1
$(3\omega_1-\omega_2)$	$2\omega_1$	$(\omega_1+\omega_2)$	$2\omega_2$	$(3\omega_2-\omega_1)$		2
$(4\omega_1-\omega_2)$	$3\omega_1$	$(2\omega_1+\omega_2)$	$(\omega_1+2\omega_2)$	$3\omega_2$	$(4\omega_2-\omega_1)$	3
		etc.				

FIGURE 1.2 SCHEMATIC REPRESENTATION OF THE PROCESS OF GENERATION OF SUM AND DIFFERENCE FREQUENCY IN ROTATING MACHINERY

Fault identification can be made directly from measured and analysed data in many cases. Excitations such as mass unbalance, anti-friction bearing and gear defects, oil whirl, trapped fluid and rubs cause rotor vibration at discrete frequencies. Due to misalignment, looseness and stiffness nonlinearities, the stator vibration wave form caused by the rotor vibration is truncated. The amount and shape of the truncation (shown in the time domain) depends on physical characteristics (stiffness, damping and mass) [17].

When a beat signal is truncated as in Figure 1.1, a number of sum and difference frequencies are obtained. The truncated wave form is a periodic function of the beat frequency $(\omega_2 - \omega_1)$, thus it can be expressed as a series of harmonic functions using a Fourier series. The truncation of the "beat frequency" induces strong harmonics at the sum and difference frequencies $(\omega_1 + \omega_2)$ and $(\omega_2 - \omega_1)$. Frequencies in the range of third harmonics $(2\omega_1 + \omega_2)$ and $(\omega_1 + 2\omega_2)$ are generated. In addition, the sum and difference frequency components are accompanied by side band frequency components separated by $(\omega_2 - \omega_1)$ from centre bands.

The presence of the sum and difference frequencies and their amplitude determine the source of the vibration problem. The severity of the defect whose frequency is present in the vibration response system, is determined by the ratio of the side band to centre frequency amplitudes. Taylor (18) has applied this theory to bearings, gears and general machinery conditions.

Figure 1.2 contains a schematic representation of the process of generation of sum and difference frequencies in rotating machinery.

1.2 BEARINGS

The failure of ball and roller bearings - assuming proper design and maintenance - usually results from sub-surface fatigue caused by the high cyclic contact load between the balls, rollers and the race. Surface fatigue spalls or any other surface defects disturbs the rolling motion. The results are growth of the defect area, an increase in friction and ultimately an increase in wear rate. The defects become so large that the bearing no longer functions properly and serious damage occurs.

Local defects in the inner or outer race of a bearing are hit by the ball each time it passes over them. A surface defect on the ball will also strike the inner and outer race. The rate at which these impacts occur depends upon bearing speed and location of the defect. Other defects arise from overload or misalignment. High frequency vibrations (which produce squeaks) are symptoms of lubricating failure.

Methods are available to enable calculation of the frequencies generated by rolling elements, for example those given by Babkin [19] and Mitchell [20]:-

$$fr = \frac{\omega}{60} \qquad \text{Fundamental frequency} \qquad (1.1)$$

$$fc = \frac{1}{2}\left[1-\left(\frac{d}{D}\right)\cos\alpha\right] \qquad \text{Defect in outer race} \qquad (1.2)$$

$$fi = \frac{1}{2}\left[1+\left(\frac{d}{D}\right)\cos\alpha\right] \qquad \text{Defect in inner race} \qquad (1.3)$$

$$fb = \frac{D}{2d}\left[1-\left(\frac{d}{D}\right)^2\cos^2\alpha\right] \qquad \text{Ball defect} \qquad (1.4)$$

Further are the equations for vibrational orders that would be found for various types of surface inperfections:

Inner Race	Eccentricity	1	
	Waviness	$nZf_i \pm 1$	(1.5)
	Rough spot	nZf_i	
Outer Race	Waviness, rough spot	nZf_o	(1.6)
Ball	Diameter variation	f_o	
	Waviness	$2nf_b \pm f_o$	(1.7)
	Rough spot	$2nf_o$	

where:

= inner race rotational speed, rpm
d = diameter of ball element.
D = pitch diameter of bearing
= contact angle of the ball to the raceway
Z = number of the balls
n = index number

Corben [21] gives different formulae for the vibrational frequencies to be anticipated from defective ball/roller bearings; as follows:-

Shaft rotational frequency	$f_1 = N_{Hz}$	(1.8)
Irregularity (rough spot or indentation) on the cage	$f_2 = \frac{(R-r)}{2R} N$ Hz	(1.9)
Spin frequency or rolling element	$f_3 = \frac{R+r}{r} \times f_2$ Hz	(1.10)
Irregularity of an element causes vibrational frequency striking on the inner and outer raceway	$f_4 = 2\frac{(R+r)}{r} f_2$ Hz	(1.11)
Irregularity on the inner raceway	$f_5 = (f_1 - f_2)n$ Hz	(1.12)
Irregularity on the outer raceway	$f_6 = f_2 n$ Hz	(1.13)

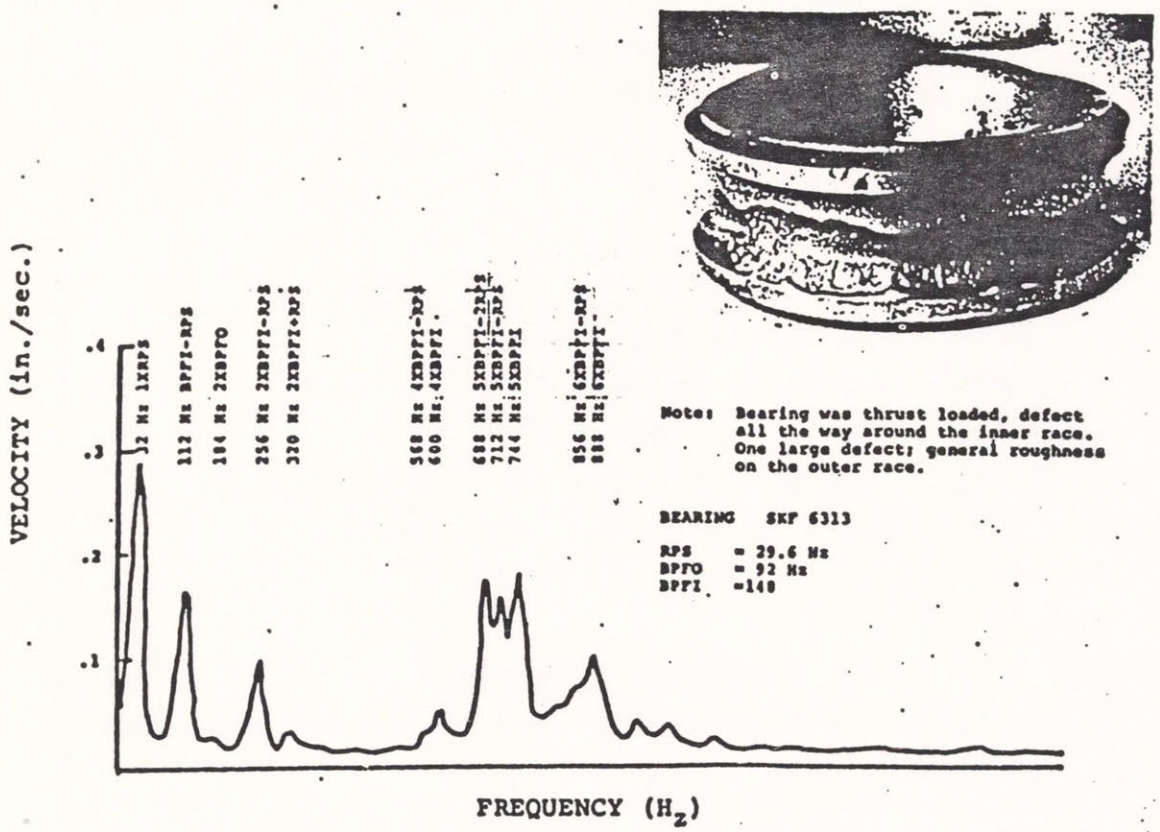

FIGURE 1.3 VIBRATION SPECTRUM OF A BEARING WITH MULTIPLE DEFECTS ON THE INNER RACE
from Eshleman [17]

f_1 - f_6 are the fundamental frequencies due to the various causes and often accompanied by the harmonics.

Where:

N = Speed of Shaft rev/sec.
R = Pitch circle diameter
r = Ball/Roller Radius
n = Number of Balls/Rollers

When a motor bearing is damaged, apart from the vibration components generated by the bearing, the bearing wear allows the rotor to run off-centre, giving rise to mechanical and magnetic unbalance, misalignment, unequal air-gaps around electric motor, unequal blade clearances at impellers, poor meshing of gear teeth etc.

Eshleman [17] describes the effects of defects that occur in anti-friction bearings on the races, balls and cages, which have been associated with five vibration frequencies of the rotating unit and bearing. He has identified bearing defects with spectrum discrete frequencies in the spectrum and also the shape and amplitudes of spectral peaks particularly for sum and difference frequencies and has shown that side bands are generated as defect size increases. The side bands are sum and difference frequencies involving both bearing ball pass or spin frequencies and shaft revolutions per minute (rpm), depending on the location of the defect.

Figure 1.3 shows a vibration spectrum of a bearing with multiple defects on the inner race. Multiples of inner race ball pass frequency are modulated by the rotating frequency of the unit. The sum and difference frequencies therefore are due to the frequencies generated as a result of mass unbalance of the unit and inner race defects.

Houser [22] applied modelling techniques to rolling elements and bearing faults, where the ball, cage and race frequencies may be easily predicted using Babkin [19] formulae. Methods for predicting high frequency resonances of bearing races have also been developed.

A few methods of analysing vibration signals of bearings will now be discussed:-

1. Direct spectrum analysis of a complex vibration signal is obtained either from a velocity pick-up or from an accelerometer attached to a bearing cap. With some training and a great deal of experience, an analyst can recognise clear changes as a bearing develops a defect and the defects grow to a point so that it must be replaced [18].

2. A second method of extracting the same type of information is based on the observation of the bearing characteristic frequencies by their modulation of the higher bearing or structural resonant frequencies. The signal is usually obtained by using a high frequency accelerometer.

3. A third method is to average the vibration signal obtained in the time domain over a time period associated with the frequency of the characteristics to be analysed. This form of signal averaging acts to emphasise frequency components of interest.

4. Vibration monitoring using acceleration measurements are usually analysed initially into broad bands rather than into individual components. Specific bands of interest may be analysed into narrower components. The advantage of octave analysis is that a wide frequency band can be analysed rapidly into a fixed number of

octaves. The disadvantage, of course, is that in a complex machine with many vibration sources more than one source may be located within the same octave band and identification of the source is not precise.

The previous analytical procedures require some form of comparison between graphs such as power spectral densities. Other methods of rolling bearing analysis all attempt to simplify the procedure so that only a few defect parameters are needed. The first method is to calculate the crest factor or the ratio between peak and RMS components of wideband vibration signals obtained from an accelerometer attached as close as possible to the bearing. Defects in the bearing produce sharp spikes or pulses as the defects produce transient contacts with mating member. The larger the defect the sharper the spikes, thus a high or increasing crest factor implies a larger or increasing defect. One problem with crest factor measurements is that in bearings with multiple or spreading defects, the crest factor may be low or decreasing due to an increasing RMS amplitude.

A similar argument about bearing damage is used for the kurtosis method. Kurtosis expresses the "flatness" of the probability density function of the signal and is computed as the fourth moment about the mean divided by the square of the second moment. (See Section 4.5).

Kurtosis provides a measure of the occurrence of extreme or peak values in the signal. Swanson [24] quotes Dyer and Stewart (1978) who suggest that kurtosis provides a reasonable compromise between using only the insensitive low order moments and highly sensitive high orders of a signal.

It has been observed that early bearing damage is manifested by high kurtosis values in the low frequency bands, as damage progresses the kurtosis values approach that for a normal distribution (3.0) in the low frequencies but increases in the high frequency bands [36]

Other methods used for bearing monitoring are acoustic flaw detection and shock pulse monitoring [23] [32].

1.3 GEARS

Gears generate mechanical signatures (power spectral densities) that are periodic and related to the meshing frequency which depends on the number of teeth and shaft speed. The main frequency at which vibration will be generated is the tooth passing frequency [25].

$$\text{Frequency (Hz)} = \frac{NT}{60}, \qquad (1.14)$$

where:

T = number of teeth on smaller gear

N = Rpm of the smaller gear

The meshing of two teeth produces impacts even if the gears are operating properly. Gears can also have such local defects as worn or chipped teeth and the defects can be distributed due to pitch diameter errors or shaft eccentricity. The last two faults cause side bands to develop at several orders of the rotational speed of shaft.

Forces causing gear tooth vibration are of two main types. The first is the force pulse generated when one tooth slides over its mating tooth. This is termed the pitch line impulse. The other is termed the engagement impulse and is caused by an imperfect engagement of gear teeth as they come into contact. The main factors that influence the size of these forces are: type of gear, pressure angle, contact ratio, tooth face width alignment, resonance, surface, finish, gear pitch, profile, load etc.

Manufacturing errors are known to have a major influence on the dynamic performance and integrity of gears. Lees [26] in his study of large mill drive trains found that some of the low speed gears are so heavily loaded that they suffer significant wear quite early in life. Usually there is not enough metal in the teeth to give many years of service, and in addition profile errors in gear construction give increased dynamic geartooth forces which also affects other gears in the train. The degree of precision in the geometry of the gear profile can have a crucial effect on the machine vibration. Coupling between torsional and flexural modes is usual and occurs predominantly at lower frequencies. The most common cause of gearbox failure in mill drives is the excessive torque fluctuation in the whole drive due to the badly worn profile of girth gear teeth. In conclusion, Lees found that a direct link between vibration and gear forces has been established and tooth-pitch errors give rise to components in the vibrational spectrum at other frequencies associated with the basic speed of rotation of the gearbox.

Bhattacharayya [27] investigated the effects of transmission error on the dynamic loading of two meshing gears under actual working conditions, and showed that a dynamic loading is produced which is predominantly a forced vibration phenomenon, in which certain resonance harmonics are excited.

Detection of gear faults is relatively easy, but interpreting the mechanical signature in terms of actual gear conditions is often difficult. The reason is that many faults show up at the gear mesh frequency. Gear

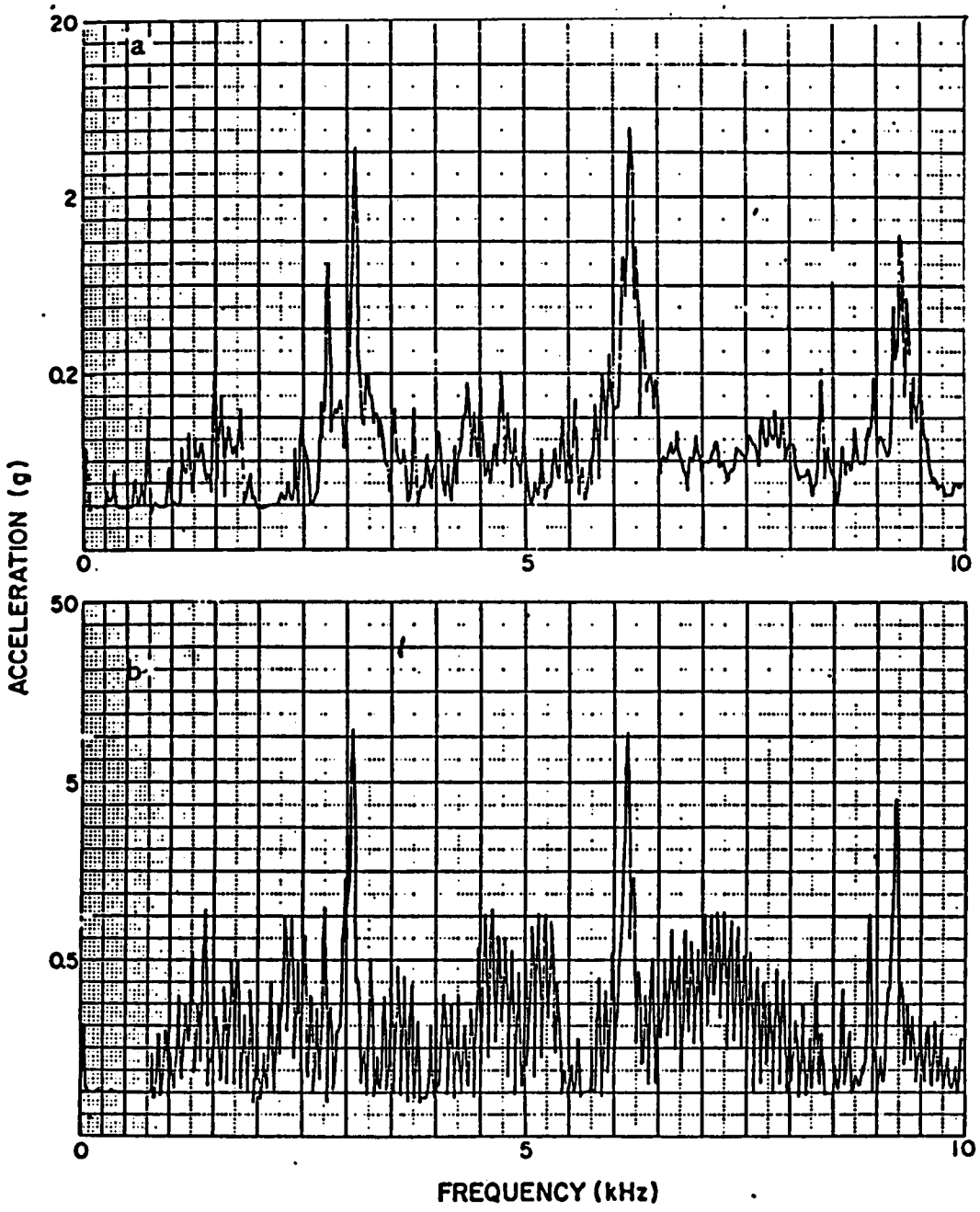

FREQUENCY SPECTRA FOR RUNNING GEARS

FIGURE 1.4 a) GOOD GEAR

FIGURE 1.5 b) GEAR WITH PITCH LINE PIT ON A SINGLE TOOTH

defects can often be identified using the sum and difference frequencies in the power spectral densities. Gear mesh frequencies modulated by rotational frequencies are indicative of defects in the gear mesh teeth. Defects include loading, bottoming, backlash and eccentricity of the teeth of the gear. Taylor [18] has published examples of vibration spectra measured on gearboxes. Side bands were obtained at sum and difference frequencies of one or two times running speed, depending on the number and nature of gear tooth defects plus or minus the gear or pinion mesh frequency. Sum and difference frequencies resulting from a defective gear tooth can be obtained because it causes ringing of the gear sets at system natural frequencies [18]. These sum and difference frequencies are comprised of a gear tooth frequency (or frequencies depending on the excitation) at multiples of shaft speed and/or system or component natural frequencies. The pulse amplitude caused by ringing governs the number and amplitude of the sum and difference frequencies generated and thus it is an indicator of the severity of the gear defects. Thus this technique is of value for identifying defective components. An extensive quantitative assessment of these defects has not been yet reported, probably because of the complexity of mechanical equipment.

Houser [22] used a technique of pattern recognition based on frequency data for the detection of faulty gears and bearings. Figure 1.4 & 1.5 show reference and running data for a gear having a single pitch line pit. An interesting result from the figures is that the gear mesh frequency side bands were found to be the result of

torque oscillation in the system which was due to coupling misalignment. The fault appears to give a very predominant periodicity at multiples of the shaft frequency. A second less noticeable periodicity occurs at the first torsional natural frequency of the system.

Gearbox vibration spectra contain many side bands spaced around the tooth mesh frequencies and their harmonics. Changes in the number and the strength of such side bands generally indicate a deterioration in condition and the side band spacing gives valuable diagnostic information as to a source of the modulation [44]. An analytical tool is required to emphasise any variations from a true harmonic sequence in a multi-peaked spectrum. This can be achieved using the cepstrum which is defined basically as a spectrum of the logarithmic spectrum. The cepstrum is computed by determining the power spectral density of a signal; taking the logarithm of the values of the power spectral density) this is equivalent to using a dB scaling); and then taking a further Fourier transform to obtain the cepstrum. The existence of harmonics in a logarithmic spectrum gives a periodic sequence of peaks and the subsequent further spectrum calculation will give only one peak in the "sequency" domain for this harmonic sequence. Thus, the cepstrum not only aids in separating the various families of fundamental frequencies and their harmonics but it also gives a measure of their relative importance. Uniformly distributed wear will only increase the components at the tooth mesh frequency. A typical cause of amplitude modulation is caused by the eccentricity of the pitch circle with respect to the centre of rotation causing a variation in tooth contact pressure once per revolution and this will be apparent in the various peak amplitudes in the cepstrum.

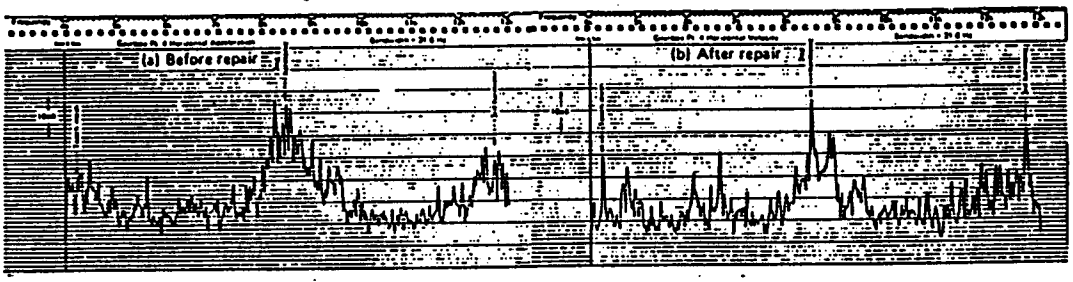

FIGURE 1.6 CONSTANT BANDWIDTH GEARBOX VIBRATION SPECTRA

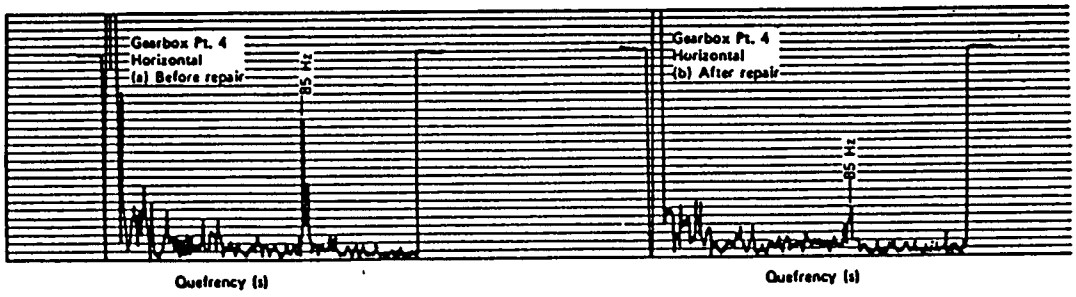

FIGURE 1.7 CEPSTRA CORRESPONDING TO FIGURE 1.6
From Randall [28]

Frequency modulation arises from variations in the tooth meshing rate due to either non-uniform tooth spacing or speed fluctuations and this will cause deviations from the harmonic sequences which will be readily apparent in the cepstrum.

Load fluctuations would also give frequency modulation due to varying tooth load. Thus, it is normally of interest to distinguish between both amplitude and frequency modulation and focus attention on the fundamental forcing frequencies rather than the complete harmonic sequences which cepstrum accomplishes. Thus the Cepstrum and on the other hand the spacing of side bands in the spectrum gives directly the fundamental modulating frequency, sufficient to trace the source.

It is a useful supplement to normal spectrum analysis of gearbox vibration signals. Determination of the basic modulating frequencies and ability to detect spectrum periodicity not immediately apparent to the eye, is advantageous.

An example of such measurements made on a gearbox is shown here. The tooth meshing frequency and its harmonics were difficult to determine from 3% bandwidth spectra, however, the cepstra corresponding to the spectra (Figure 1.6 & 1.7) shows up the difference more clearly and at the same time confirms that virtually all the modulation is occurring at the speed of the high speed shaft at 85 Hz [28].

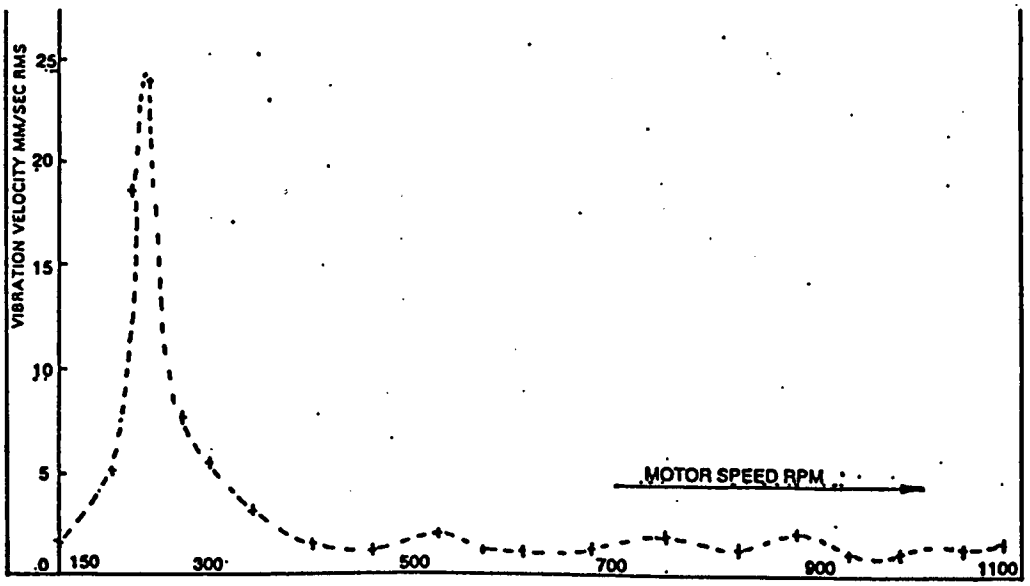

FIGURE 1.8 ON SITE VIBRATION PERFORMANCE

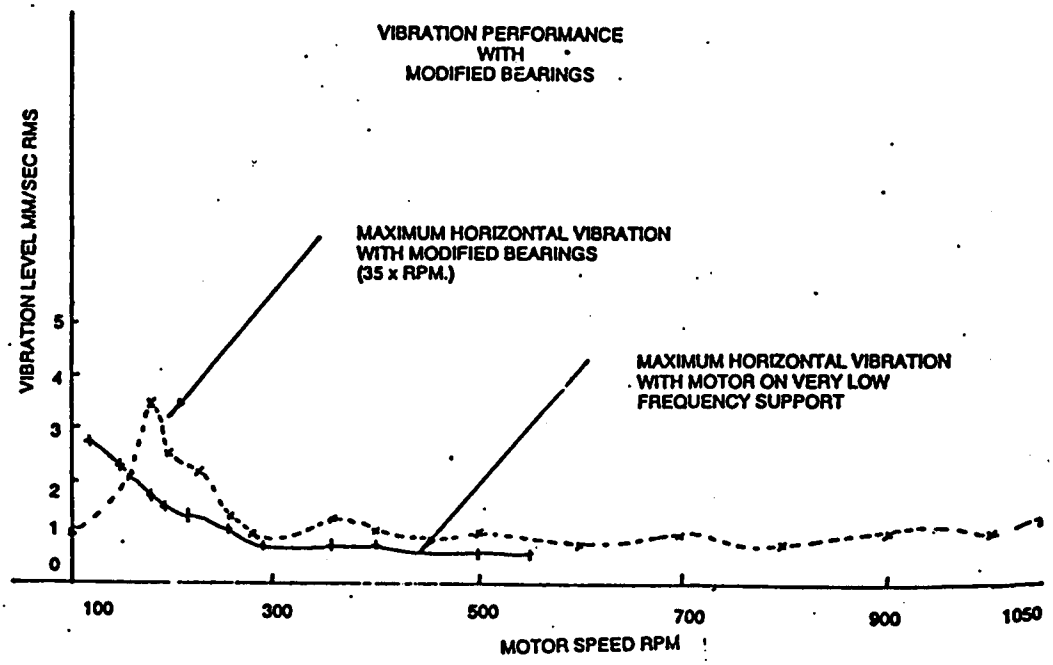

FIGURE 1.9 VIBRATION TEST RESULTS SOFT MOUNTED BEARING OPTION
From France [29]

1.4 MOTORS

Mechanical vibratory forces in motors may be produced by several means including out-of-balance conditions of the rotor, bent shafts, misalignment with the driven machine and rubbing and rolling actions in the bearings. France and Grainer [29] described various steps taken to identify the excitation force and determine the characteristics of the resonant modes of vibration. The vibration frequency was found by multiplying the number of rotor slots by the rotational speed and so distinct resonant regions were evident within the motor operating speed range. Various solutions to reduce resonant vibrations were considered and described and a solution to the problem was achieved by use of an elastomeric mounting arrangement for the motor bearing. A typical situation is represented in Figures 1.8 and 1.9.

Initial results indicated that the problem was purely due to the motor. When the motor was decoupled for frequencies associated with 1000 rpm and the resultant vibration levels showed clearly that the residual unbalance at low speeds was reduced and a number of well damped resonant regions were now observed. Figure 1.8 is the vibration spectrum prior to any treatment and Figure 1.9 that after treatment. Thus, soft mounting of the rotor in its bearings was shown to decrease the strong coupling and resulted in a machine with acceptable vibration levels.

1.5 TURBINE/GENERATORS

Many different types of signals are generated by turbines/generators and since it is difficult to gather and analyse sufficient data, signature analysis for these situations must be considered in its infancy. Signature analysis using vibration signals up to 250 Hz is an area where sufficient experience and knowledge is available so it can be used effectively for preventive-maintenance planning purposes. [30] [31]. Vibration analysis can accurately identify such operating problems as permanent unbalance, temporary unbalance, impacting, bearing and spindle instability and double moment of inertia [30] [31]. These phenomena are described below.

Permanent unbalance is created by permanent displacement of the centre of gravity of the shaft. The frequency associated with permanent balance is the frequency associated with the running speed.

Temporary unbalance occurs when the centre of gravity shifts due to transient conditions causing spindle distortion such as transient energy inputs to the shafts; heating effects which could be caused by the rubbing of seals; other effects causing transient energy extraction.

Impacting exists when a rotating and stationary component come into contact. Its characteristic frequency is often a subharmonic of the running speed frequency and the closest sub-harmonic to the natural frequency of the shaft will be emphasised.

Cause of Vibration	Identifying Frequency	Solution to Problem
Permanent unbalance	Running speed frequency	Balance rotor
Temporary unbalance	Running speed frequency	Rotor balancing may be necessary; however, other causes of vibration - such as component distortion and running - may also require correction.
Impacting	Subharmonic: 1/2, 1/3 or 1/4 of running speed frequency	Eliminate contact between rotating and stationary parts
Bearing instability - oil whip	Less than 1/2 of running speed frequency	Improve bearing parameters (1) increase loading (2) increase oil temperature, (3) design new bearing
Resonant whirl	Natural frequency of system	Improve damping characteristics of journal bearing and/or diminish excitation forces
Out-of-round journals	Harmonic: 2,3 or 4 times running-speed frequency	Machine journals round
Rocking journal bearings	Harmonic: 2, 3 or 4 times running speed frequency	Prevent rocking with additional pads.
Double moment of inertia	Harmonic: 2, 3 or 4 times running speed frequency	Equalize shaft flexibility in all directions

TABLE 1.6 ANALYZING TURBINE VIBRATION TO IDENTIFY OPERATING PROBLEMS
From Shattoff [30]

Bearing instability is a self excited bearing vibration which occurs when the oil film between the journal and the bearing is not tapered and so a thick wedge of oil is present. The bearing can be made stable by either increasing its natural frequency so that no vibration is excited or increasing the bearing displacement parameter so that a wedge of oil does not occur.

Spindle instability or resonant whirl describes the spindle vibrating at is own natural frequency. The associated dominant frequency of vibration is either slightly less than, or slightly greater than half of the running speed frequency. One possible cause is an uneven seal clearance. Another possible cause is an excitation force produced by the steam flow across the tips of turbine blades. Rocking of the bearing on its pads produces a frequency at either half or twice the running speed.

The double moment of inertia condition can be detected as the harmonic 2, 3, or 4 times of running speed frequency. It occurs when the shaft is not equally flexible in all direction and is common on 3600 rpm generators, due to design. When such a turbine rotor exhibits a double moment of inertia condition, it could indicate that a crack is present that is deep enough to affect the flexibility of the shaft. A solution to problem is to equalise shaft flexibility in all directions.

Table 1.6 shows Analysing Turbine Vibration to identify operating problems.

1.6 FANS

To solve vibration control problems, it is necessary to determine the frequency of the disturbing force as the part of the design criteria. In fan and motor systems, the fan speed produces the lowest value for the frequency. By providing adequate flexibilities in the structure for satisfactory isolation of this frequency one automatically provides some protection against transmission of the frequencies caused by electrical hum, motor unbalance or fan blades to the rest of the structure so as to minimise belt and bearing wear. Also the fan and motor shafts must be parallel and fan and the motor must be mounted on a rigid common base.

Most fans and blowers have their own unique type of trouble. Some are subjected to abrasive wear, which will cause increased vibration due to unbalance. This unbalance is caused by an uneven build-up of deposited material from the abrasion causing a misalignment. The changes in vibration occur at or near the rotation frequency and can be monitored effectively [32]. A rotor may be in a perfect static balance and yet produce vibration at its bearing by the rocking motion associated with misalignment. Fan shafts are designed with sufficient stiffness to keep the running speed below the first critical speed at all times. The critical speed [47] is given by:

$$Nc = \frac{\omega}{2\pi} = \frac{1}{2\pi}\sqrt{\frac{k}{M}} \qquad (1.15)$$

where:

ω = angular velocity
k = stiffness
M = mass

Fans are designed to operate with mechanical stresses below the ultimate stress of the material of construction.

Vibrational frequency	Types of problems	Cause
0–40% running speed (RS)	Oil-whip resonance, friction-induced whirl, loose bearing, loose seals, bearing damage, bearing-support resonance, case distortion, poor shrink fit, torsional critical	1
40–60% RS	Half-speed whirl, oil-whip resonance, worn bearings, support resonance, coupling damage, poor shrink fit, bearing-support resonance, rotor rub (axial), seal rub, torsional critical	1
60–100% RS	Loose bearing, loose seals, poor shrink fit, torsional critical	1,2
Running speed	Unbalance, lateral critical, torsional critical, transient torsional, foundation resonance, bearing-support resonance, bent shaft, bearing damage, thrust-bearing damage, bearings eccentric, seal rub, loose impeller, loose coupling, case distortion, shaft out-of-round, case vibrations	3
2 X RS	Misalignment, loose coupling, seal rub, case distortion, bearing damage, loose coupling, support resonance, thrust-bearing damage	1,2,3
n X RS	Blade or vane frequency, pressure pulsations, misalignment, case distortion, seal rub, gear inaccuracy	3,4
Very high frequency	Shaft rub: seals, bearings, gear inaccuracy, bearing chatter, poor shrink fit	3,4
Nonsynchronous frequencies > RS	Piping vibrations, foundation resonance, case resonance, pressure pulsations, valve vibrations, noise, shaft rubs, cavitation	5

1. *Bearing-related problems*
   - Low-stability-type bearing
   - Excessive bearing clearance
   - Loose liners
   - Impurities in oil
   - Improper oil properties (viscosity, temperature)
   - Frothing of oil due to air or process fluid
   - Poor lubrication
   - Worn bearings
2. *Seal-related problems*
   - Excessive clearance
   - Loose retainers
   - Too-tight clearance
   - Worn seals
3. *Unit-design-related problems*
   - Critical speed
   - Loose coupling sleeves
   - Thermal gradients
   - Shaft not concentric
   - Inadequate support stiffness
   - Pedestal or support resonance
   - Case distortion
   - Thrust bearing or thrust balance deficiencies
   - Unbalance
   - Coupling unbalance
   - Bent shaft
   - Loose shrink fits
4. *System-related problems*
   - Torsional criticals
   - Pedestal resonances
   - Foundation resonances
   - Misalignment
   - Excessive piping loads
   - Gear tooth inaccuracies/wear
   - Piping mechanical resonances
5. *System-flow-related problems*
   - Pulsation
   - Vortex shedding
   - Piping shell resonances
   - Inadequate flow area
   - Inadequate NPSH
   - Acoustic resonance
   - Cavitation

TABLE 1.7 - TYPICAL PROBLEMS AND CAUSES
CENTRIFUGAL PUMPS [48]

1.7 PUMPS

Pumps are more likely to develop misalignment due to variations in temperature, load and other factors during normal operation. The pump rotors are subjected to numerous loads such as torsion, bending, whirling and axial loadings.

Centrifugal pumps have a relatively flexible cantilevered housing, so that a large portion of the dynamic force developed by the rotor is transmitted across the bearings and only a small motion is transmitted to the structure. Sensors attached to the bearing housing in the plane of least stiffness provide the best response to induced vibrations and therefore the best indicators of mechanical condition. The signal from the casing sensor must be analysed into frequency bands which can be related to a specific mechanical component or components. The first band including the frequencies around the running speed frequency should analyse a parameter proportional to velocity so that it can be related to force, since it is the mechanical impedance times the velocity.

A different monitoring scheme, uses high frequency (100 kHz) sensors to monitor pulses of energy above an adjustable threshold. It can check rolling bearings and be used to provide early warning at an impending failure. [32]

Table 1.7 lists typical problems found in centrifugal pumps and their causes and can be used in trouble-shooting vibration problems.

1.8 COMPRESSORS

Vibration signature analysis using a microcomputer - based fast Fourier transform analysis is being applied to the evaluation and surveillance of compressor performance. [45] Three areas of application include:

1. new blade design and prototype compressor evaluation.

2. corrective and preventive maintenance of machinery components.

3. evaluation of machinery health.

The system is used to monitor signals from accelerometers mounted on the load-bearing housings. Vibration monitoring of the machinery will be used to reduce equipment failures and possibly to prevent more serious failures. Vibration signature analysis also has been used to assist in the design of the axial-flow compressor blades. The key to any signature analysis application is an understanding of the mechanisms of failure for the compressor components. Effectively monitoring machinery health with signature analysis depends upon the following factors:

1. having an accelerometer with sufficient sensitivity and frequency response.

2. obtaining the location and direction of measurement that will contain the components that are representative of machinery condition.

3. transmitting the signals

4. analysis equipment with sufficient frequency resolution.

It was found that blades experience "g" forces during surges or shutdowns, two or three times those experienced under steady-state conditions. Blade fatigue cracks which initiate during vibrations are either in the first bending or torsional modes. The best location found for the accelerometer was on the torque side of the load bearing cap. As the range of compressor operating speed is known, so blade passing frequencies generated can be calculated. If any blade resonances fall within these driving frequencies, it points potential blade failures.

Power spectral density signals on the load bearing showed considerably energy around 4600 Hz. A visual examination of rotor shaft seal showed excessive wear. The presence of excessive oil whirl is usually indicated by a large subharmonic of the rotor fundamental. Structural resonance also gives rise to various components.

A good deal of judgement is required in the high frequency range in terms of deciding when to shutdown plant. This is especially true in cases where the source or cause of the higher frequency component cannot be identified. Of the three parameters, (displacement, velocity and acceleration) acceleration provides the greatest amount of information regarding the machine condition.

CONCLUSION

From the preceding literature review it can be seen that there are many techniques for exploiting the vibration signatures of machinery or systems to determine their condition or to diagnose the cause of faults. Many applications exist and many mechanical signature analysis techniques are available and there is no single "best" technique, as it depends on the application. In most cases a mechanical signature analysis alone is sensitive enough to indicate the condition of a system, but in other cases measurements of other performance or operating parameters might also be necessary to indicate the condition of a system. Mechanical signature analysis is a viable technique since laboratory studies and field experiments have shown that monitoring the vibration in a system or its components can be analysed to identify defects.

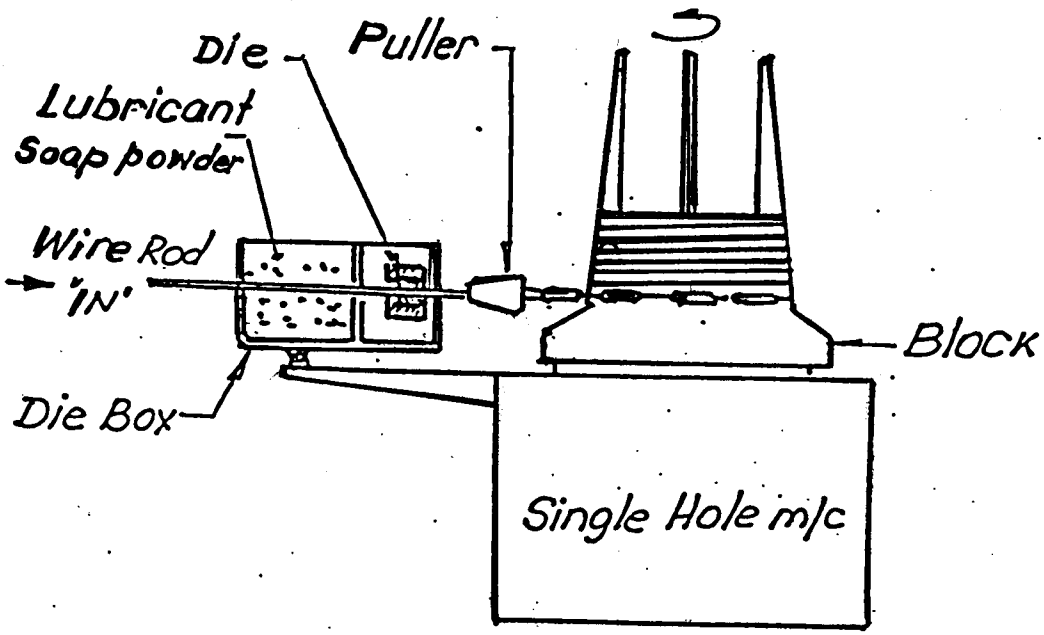

FIG. 2.1 TYPICAL SINGLE HOLE WIRE DRAWING PROCESS

2. WIRE DRAWING

In this chapter, the important characteristics of the wire drawing operation are described.

2.1. Basics

The wiredrawing operation involves the forcing of metal through a die by means of a tensile force applied to the exit side of the die. The wire passes through the die and is reduced in diameter while undergoing plastic flow. Most of the plastic flow is caused by the compressive force which arises from the reaction of the metal with the die. Wire drawing is usually carried out at room temperature, however, because large deformations are usually involved, there can be a considerable temperature rise during the drawing operation.

The rod* is pointed with either a swager or a pointer** so that it can be inserted through the die and clamped by the jaws of the puller. The draw speed varies depending on the reduction of the rod wire diameter.

* It should be noted that rod becomes a wire when it is drawn through a die as shown in Fig. 2.1.

** For drawing the end of the wire is pointed by working it backwards and forwards between two grooved rollers or by swagging or other suitable means. Figure 2.1 is a schematic of the wiredrawing process.

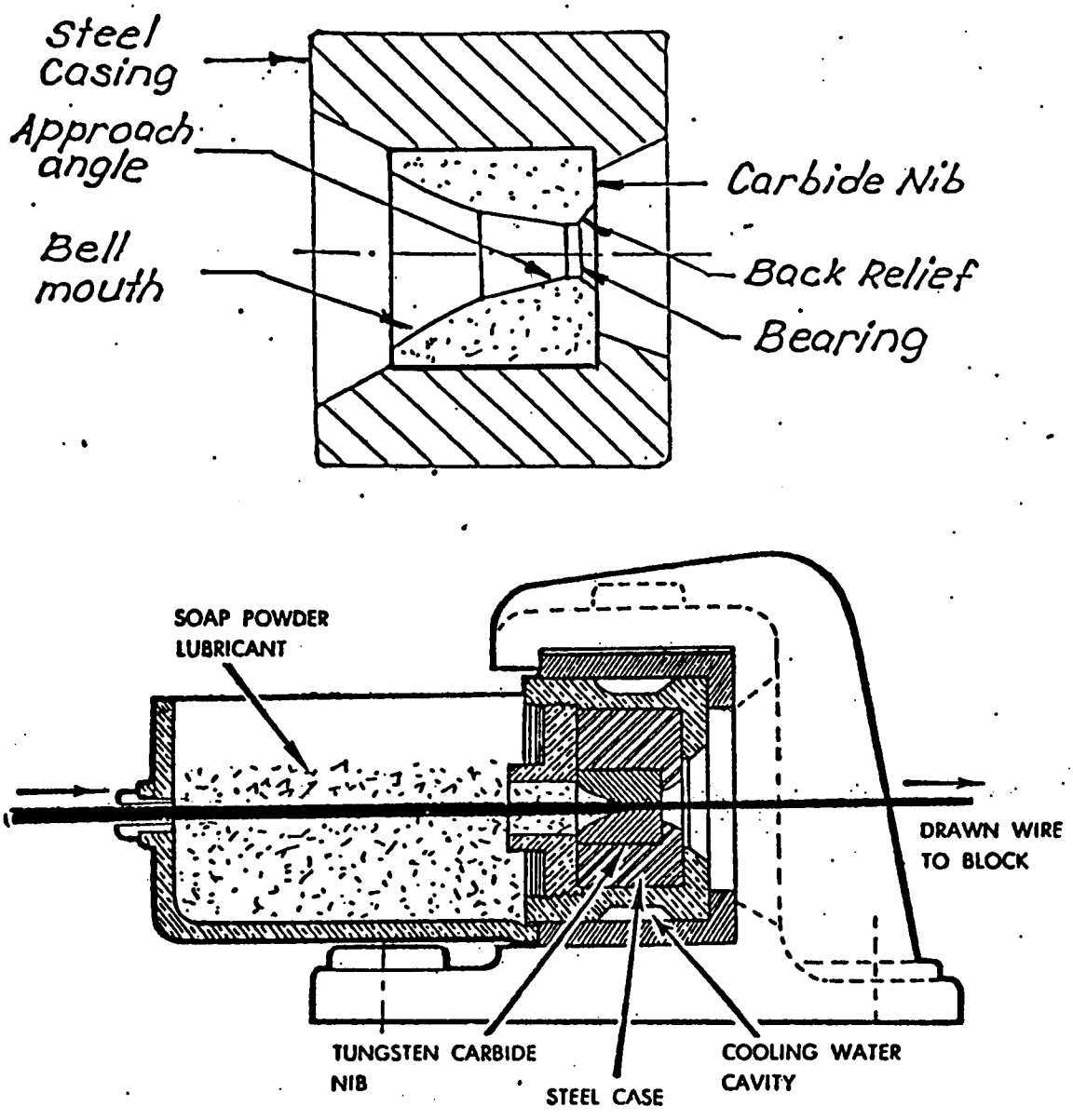

FIG. 2.2 CROSS SECTION OF A SOAP BOX AND DIE

The sequence followed in wiredrawing is first to clean the rod by pickling to remove any scale which would otherwise lead to surface defects and hence excessive die wear. Then the wire rod is coated with lime, to serve as an absorber so as to carry off lubricant during any drawing and to neutralise any acid remaining from pickling. In dry drawing the lubricant is soap powder. Figure 2.2 shows a cross section of a die and soap box.

In practice it is found the die life is erratic; dies mainly fail due to wear and breakage. The causes of failure are three fold: worn out size, scratched and broken. Not only do worn dies cost money to replace or recondition, but die inspection takes time, the machine has to be stopped, the die taken out and visually inspected and worst of all, die wear is often undetected before substantial quantities of out of size (worn-out die) or blenished and/or scratched-up wire (cracked die) have been produced. Dies are often gauged by checking the diameters of drawn wire through the die which does not always represent the true condition of the die.

This project attempted to examine the use of vibration signals to monitor the condition of the die in the die box. It was hoped that knowledge gained from this study may provide a basis for monitoring for the prevention and detection of early failure of the die, through cracking, and the normal allowable die wear life.

2.2. Construction of Wire Drawing Dies

The introduction of the tungsten carbide (T.C.) die for wiredrawing in 1929's was an important step towards the development of high speed multi-hole wiredrawing machines and the T.C. die also replaced expensive diamond dies. The tungsten carbide used in wiredrawing dies is usually a mixture of approximately 91% tungsten carbide and 9% cobalt. When pressed to shape and sintered it forms an extremely hard compound [1]. Wire drawing is usually done with dies having from 6% to 13% cobalt content. Below 6% the wear accelerates because of inadequate bonding, while over 15% the wear accelerates because of insufficient density [2] [3].

Tungsten carbide is extremely hard and has great resistance to abrasion or wear and dies made of it can produce a large tonnage of even gauge wire. There are other properties which makes it valuable as a wiredrawing material; it has very small elastic extension with correspondingly high modulus of elasticity, great compressional strength and great resistance to deformation up to temperatures of $1000^{o}C$. The coefficient of thermal expansion is half that of steel and this must be taken into consideration when it is mounted in a steel cage during die manufacture. The tungsten nib is shrink fitted into a carbon steel case. The nib is held in compression, to gain support from the lower elastic modulus steel case.

Dies may be round or profiled to various shapes, such as a wedge, a square and rectangular. There are four sections in a die as shown in Fig. 2.2 [3]

The Bell Radius: the section of the die used to guide the incoming rod which has an angle of about 45^{o}.

The Approach Angle: this is the most important section of the wiredrawing die. The entire reduction of area and the compacting of lubricant onto the incoming rod or wire occurs here.

The efficiency of any die is determined by its design and accuracy. It is cut to an accurate conical angle with a smooth surface finish. For example, 16^{o} included approach angle is the accepted standard for drawing low carbon steel wire.

The Bearing (Parallel): is where control of wire diameter, roundness and straightness takes place. The length of bearing is important [4] and is usually not greater than 3/4 D (D = diameter) in bright wire or not greater than 1/3 D for galvanised wire.

The Back Relief: is the area designed to strengthen the exit of the die and to prevent breakage of the carbide nib.

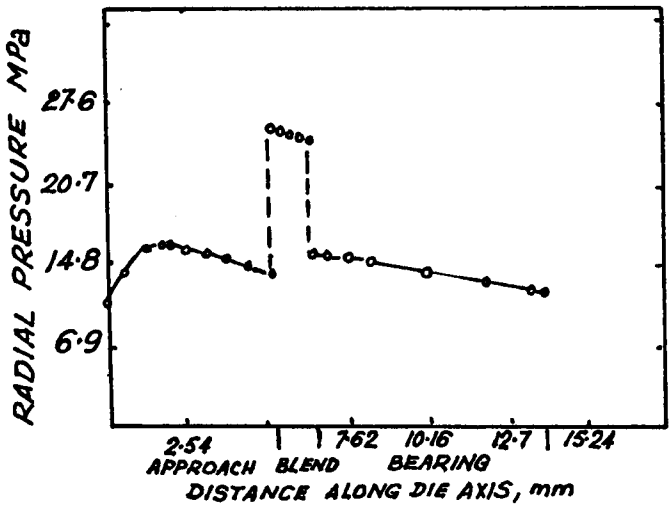

FIGURE 2.3 RADIAL STRESSES AS A FUNCTION OF POSITION ALONG THE DIE

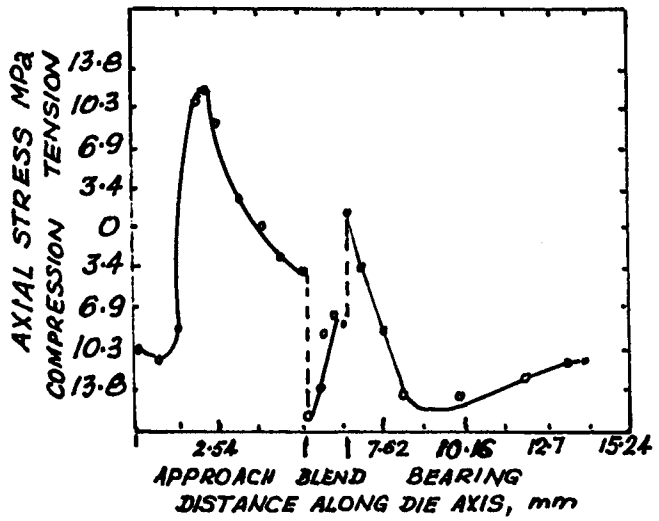

FIGURE 2.4 AXIAL STRESSES AS A FUNCTION OF POSITION ALONG THE DIE
From Verduzco/Daly [5]

2.3 Working Stresses

It was established that a large number of factors affect the failure of the drawing dies and the study by Verduzco and Daly [5] was initiated to determine which of these factors most strongly influenced the failure rate in the drawing operation. They have used a three dimensional analysis of the stresses acting in a die during drawing, based on a photoelastic technique using a celluloid model. They have determined that a high stress concentration exists at the entrance of die. Abrupt changes in the stresses occur along the die contour where a sharp transition in geometry exists. In addition, axial stresses are found to develop at the surface of the die during the drawing in the region around the point where the wire first contacts the die. The presence of axial tensile stresses in the die also suggests a possible cause for the failure of the drawing die. See Figures 2.3 & 2.4.

Carbide dies are normally shrunk into a steel cage thus introducing large compressive hoop (circumferential) stresses in the die nib which tends to counteract the action of the tensile hoop stresses produced during drawing. In the axial direction drawing dies are not prestressed and therefore support the full value of tensile stress developed during drawing. Other observations pertaining to the mode of fracture of carbide dies indicate the importance of tensile stresses acting in the axial direction.

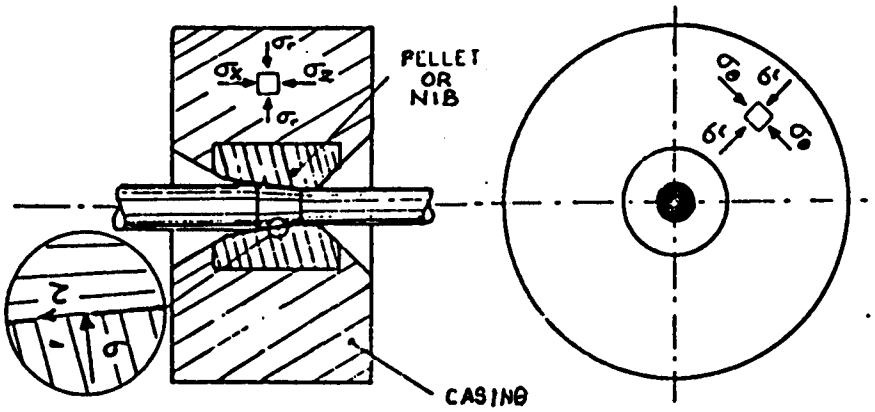

FIGURE 2.5 INDICATION OF WORKING STRESSES IN THE DIE
From Felder [2]

Figure 2.5 indicates the approach used by Felder [2] in obtaining estimates of the stresses.

where: σ_r = radial stress
σ_θ = circumferential stress
$\sigma_{x,z}$ = axial stress
τ = friction

The working stresses arise from stresses due to the encasing; stresses induced by the wire drawing and heating along the working surface.

Wire oxides probably cause die abrasion and sudden jerks observed in the running wire probably induce wear by fatigue. The length of life of the tungsten carbide (T.C.) dies depends considerably upon surface roughness and cooling effectiveness. The life increases if the grain size is slightly increased and the cobalt content is higher.

The strain due to dimensional change according to the analysis by Felder [2] is:-

$$\varepsilon = \ln \left(\frac{A_o}{A_f} \right) , \qquad (2.1)$$

where: A_o and A_f are the initial and final cross sectional areas of the wire respectively.

The minimum work needed to reduce a cross sectional area of metal (Smith/Cooper [6]) is:

$$\sigma = \bar{Y} \ln \frac{1}{1-r} , \qquad (2.2)$$

where:

σ = drawing stress
$\bar{Y}$ = mean yield stress
r = fractional reduction of area.

The stress at the wire expressed as a frictional shear, τ is related to the die pressure P and co-efficient of friction, μ by[7].

$$\tau = \mu P, \qquad (2.3)$$

The average die pressure P can be found using the relation.

$$\frac{P}{\sigma} \simeq \frac{\Delta}{4} + 0.6 , \qquad (2.4)$$

where: σ is the average wire flow stress and Δ the deformation zone shape paramater i.e. ratio of the height of deformation zone to its length. [7]

It is commonly known that the dies used in drawing practice usually fail by cleavage on a plane perpendicular to the direction of drawing indicating excessive axial stresses. It is clear that axial stresses in the nib cause failure which suggests that the mechanism for the fracture of the carbide nib is axial stresses exceeding the tensile strength of the die material.

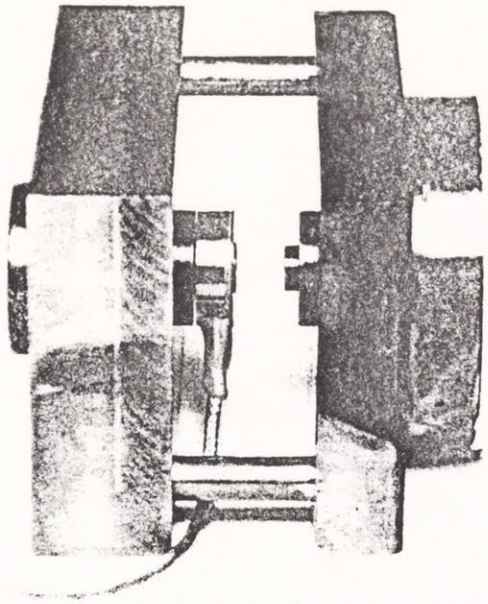

Fig. 2.6 Load washer fixture. Side view showing load washer, hardened steel inserts and guide pins. Also seen are an R5 drawing die (left) and the drawbox mounting fitting (right).

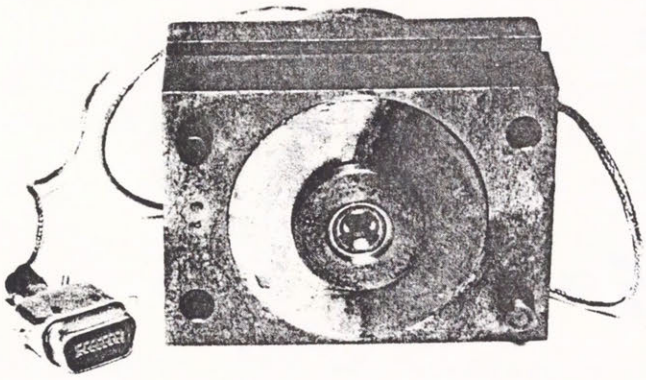

Fig. 2.7 Load washer fixture. Front view showing die and adaptor ring. The Amphenol connector for the transducer indicator plug-in is seen at the left.

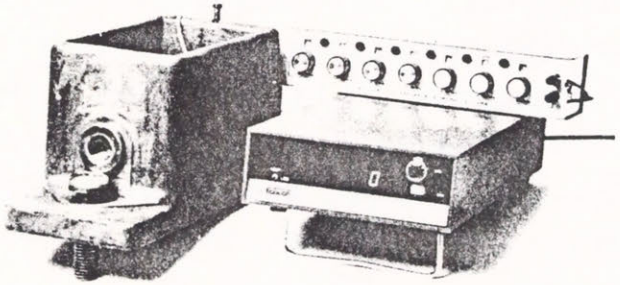

Fig. 2.8 Draw force measuring system. Load washer fixture is hidden in draw box. The digital transducer indicator and decade resistance box are shown at the right.

Reid [8] describes how an analysis of the wire drawing process can be carried out by computer reduction of the data from a load cell measuring the force on the die. This force can then be used to compute the amount of energy used in the wire drawing process and the energy loss due to friction. This data together with measurements of die geometry (die angle, bearing diameter, bearing length, diameter ratio) and the co-efficient of friction allows some evaluation of the effects of lubricants. The actual draw force measuring system consisted of load washer and load washer fixture consisting of two hardened steel inserts mounted in two 25 mm steel plates with digital force transducers. The plates slide together along two hardened steel guide pins. The fixture ensures uniform loading on the load washer; fits into the recess of the die wall of the draw box; and accommodates (by means of adaptor rings) die casings up to 75 mm in diameter. (See Figures 2.6, 2.7 and 2.8).

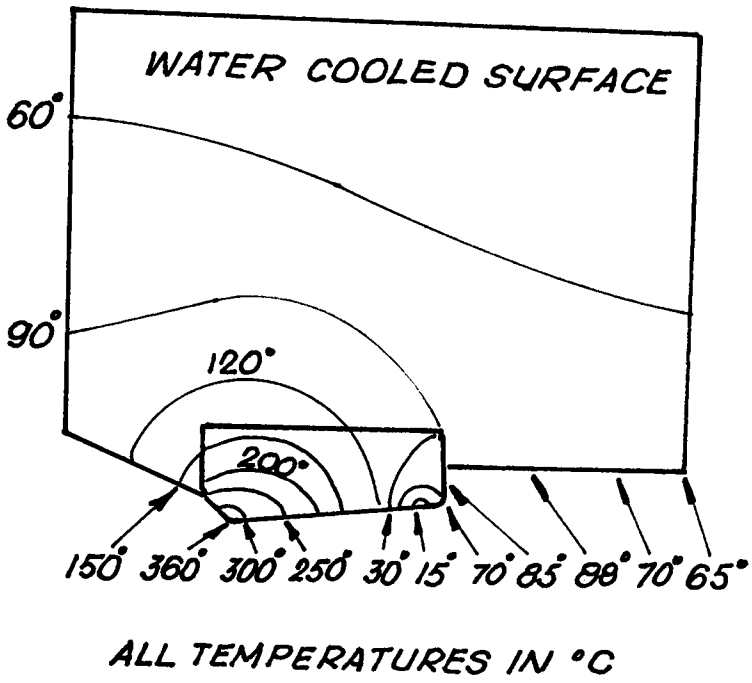

FIG. 2.9 TEMPERATURE DISTRIBUTION IN DIE AT 7M/SEC
(From Steel Wire Handbook [1])

2.4. Process Heating

The wire drawing produces a marked heating during drawing producing temperature increases of a few hundred degrees Celsius. The heating is most pronounced at the wire surface. Excessive heating can bring undesirable metallurgical changes, compromise lubricant performance, aggravate die wear and can result in poor drawn wire surface quality. [1] [10] [11] Measurements and calculations of actual temperature distributions in the drawing die have been performed by several investigators.

Two principal sources of wire heating during drawing are deformation work and friction work. Wire deformation work (Wd) can be approximated by:

$$Wd = (TS) \ln \left(\frac{Ao}{Af}\right), \qquad (2.5)$$

where TS is Tensile strength
A_o is initial cross section area
A_f is as drawn cross section area

One theoretical equation for the temperature rise during wire drawing is [1]

$$T = \frac{P}{A\ hd} \times 1.069 \times 10^{-4} \quad \text{(Imperial Units)} \qquad (2.6)$$

where T is the temperature rise in ^{o}F, A the area of the wire leaving the die in $in.^2$, P the die pull in lbs, h the specific heat (steel = 0.115) and d the density of the metal drawn in lbs/in^3. Since about 90% of the drawing energy is converted into heat, high cooling rates are necessary.

Another theoretical expression for the temperature rise is [13].

$$T = \frac{\sigma}{\rho S} \ln \left(\frac{Ao}{Af}\right), \qquad (2.7)$$

(metric units)

where σ is the flow stress of the wire in kg/mm^2, ρ is density, S is specific heat and T is in ^{o}C. Heat extraction from the die has been shown to be inversely proportional to speed for conventional die cooling [1]

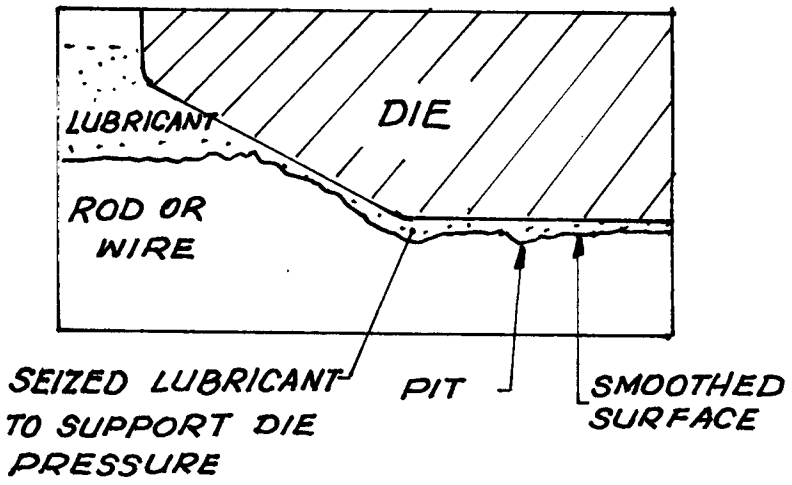

FIGURE 2.10 SCHEMATIC DIAGRAM ILLUSTRATING AN INTERFACE BETWEEN DIE AND WIRE
from Nakamura [11]

2.5. Lubrication

In wire drawing, lubrication is an important factor allowing higher drawing speeds, lower drawing temperatures and reduced die wear to be attained. Lubrication is also needed because the surfaces of the dies and wire are never perfectly smooth. Figure 2.10 shows a schematic representation of the interface betwen the wire and the die.

Lubrication in the wire drawing operation is especially needed to provide a suitable separating layer between the die and the wire being pulled. This separating layer is especially necessary to prevent scratching of the wire or the formation of a martensitic surface on the wire surface. [1] [6] [7] [11]

In steel wire drawing there are four principal lubricating methods:-

- dry drawing using powdered soap
- wet drawing employing soap solutions
- grease drawing
- prior deposition of lubricant upon the wire employing an aqueous mixture of compound.

The most common lubrication procedure is to draw the wire through a dry powdery lubricant.

2.6 Wire Drawing Power

One formula for calculating the force needed to draw wire through a die is [1].

$$P = \overline{UTS} \times \varepsilon \times A_f \times f(x) \quad , \qquad (2.8)$$

where P is wire drawing load, $\overline{UTS}$ is mean UTS (ultimate tensile strength) using the values before and after die, ε is true strain, given by $\varepsilon = \ln\left(\frac{A_o}{A_f}\right)$ where Ao and Af are initial and final cross sectional areas of wire; f (x) some function of x which depends on the die geometry (wire moves in x-direction).

An alternative formula for the force required to draw wire is,

$$H.P. = \frac{d^2 \times S \times N^{1.2} \times R}{97.6 \times \pi \times E} \quad , \qquad (2.9)$$

where H.P. is the horsepower of the motor
d is the diameter of the finishing wire in mm
S is the speed of finished wire in m/min.
N is the number of drafts (reductions) required
R is the average percentage reduction per pass
E is the percentage mechanical efficiency of the machine.

OR

$$HP = \frac{\text{Die Pull (kg)} \times \text{metres per sec.}}{75} \quad \text{metric units}$$

The force required to pull a wire through a conical die is also given by [13]

$$\frac{P}{A_f K} = \left(1 + \frac{1}{\mu \cot\alpha}\right)\left[1 - \frac{A_f}{A_o}\cot\alpha\right] + \frac{2}{3}\alpha^2\left(\frac{A_f}{A_o - A_f}\right) \qquad (2.10)$$

where P = drawing force
A_f = area of wire entering die
A_o = area of wire leaving die
K = flow stress of material
μ = coefficient of friction
α = semi-angle of cone

2.7 Die Wear and Life

A variety of factors controls both the wear of and expected life of a die. Die wear is dependent on the mechanical abrasion, compression forces, thermal stress, chemical reaction [2] [3] [4] and the amount of cooling. The composition of the die material is an important factor and increasing the amount of Cobalt in the alloy tends to decrease the life of the die. Wire preparation is, of course, an important factor as oxides on the wire surface can increase the abrasion of the die. Changes in the production, particularly jerkiness in the wire drawing have a detrimental effect on the die.

Cumulative fatigue must be considered but it is difficult to define what is the equivalence to cyclic loading in a wire drawing process and the only data available is for cyclic three point loading of a sample plate of three tungsten carbides cemented with cobalt using a cycling frequency of 50 Hz which withstood 10^7 cycles before failure [2].

Ideally the wire should enter the die normal to its plane and on-centre, however, vibrations in the wire do occur which produce off-centre entry conditions, generating larger, undesirable forces which accelerate the wear and fatigue. This could be an important factor is explaining accelerated wear at the die entry point [7].

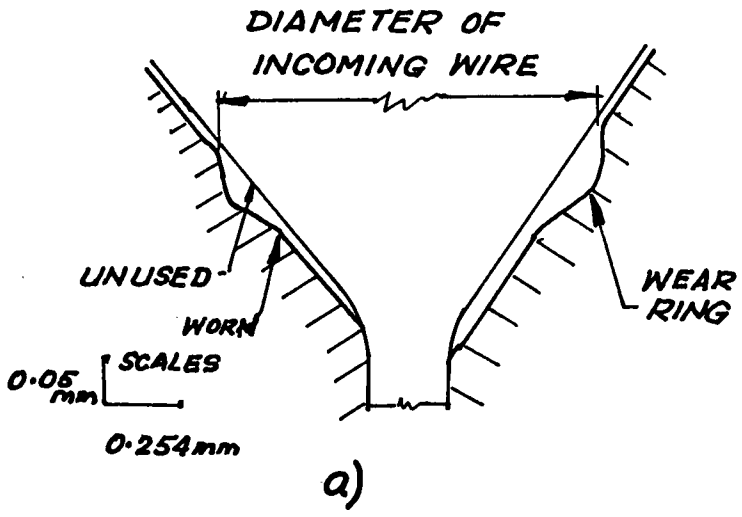

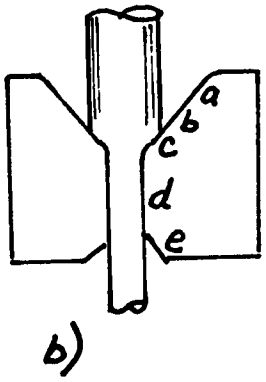

	FUNCTION
a = BELL	TRAPS LUBRICATION
b = APPROACH ANGLE	RECEIVES WIRE AND DECREASES ITS CROSS SECTIONAL AREA
C = WEAR RING	DEFECT THAT TRARS LUBRICANT
d = BEARING	SIZES AND POLISHES FINAL WIRE
e = BACK RELEIF	EXIT OF WIRE, FREE OF CONTACT

FIGURE 2.11 SCHEMATIC OF A DRAWING DIE SHOWING:

a) PROFILE OF A TYPICALLY WORN DIE [7]

b) RELATIVE LOCATION OF THE WEAR RING

Frictional and geometrical forces along the wire generate tensile loads in the nib parallel to the wire frequently resulting in failure on a plane perpendicular to the die centre line at the wear ring zone [7].

The wear of the die generally proceeds in stages, for if the diameter of drawn wire is plotted against the amount of wire drawn, then it will be observed that the increase in diameter (or rate of a die wear) is relatively rapid during the early life of a die, then becomes a slower uniform at lower rate and finally increases sharply in the later stages. The initial rapid wear is attributed to a wearing-down of peak heights to form a smooth surface and the final rapid wear is attributed to the "wear-ring" of the die. (See Figure 2.11)

With use, the die will develop erosion in the reduction zone at the point where the incoming wire contacts the die. This eroded area is called a wear ring. The wear ring should not be permitted to wear too deeply before being polished out otherwise it will cause an increase in the friction in the drawing die. Figure 2.11 shows graphically how this will increase the required drawing force of the wire in the die. When the pull required exceeds the strength of the wire the wire will break. The wear ring acts as a notch and if it is allowed to become very deep, the die becomes more susceptible to damage permitting the die to crack. The wear ring should be polished out with little or no effect on the size of the bearing. Cracks in the die bore wall due to inappropriate machining (resulting from local overheating in sintered carbide during erosion) reduces die life. Defects in the sintered carbide material, errors in geometry of the die core and flaws in the surface, accompanied by an unfavourable drawing sequence with severe stressing of the die all lead to increased wear and reduced die life.

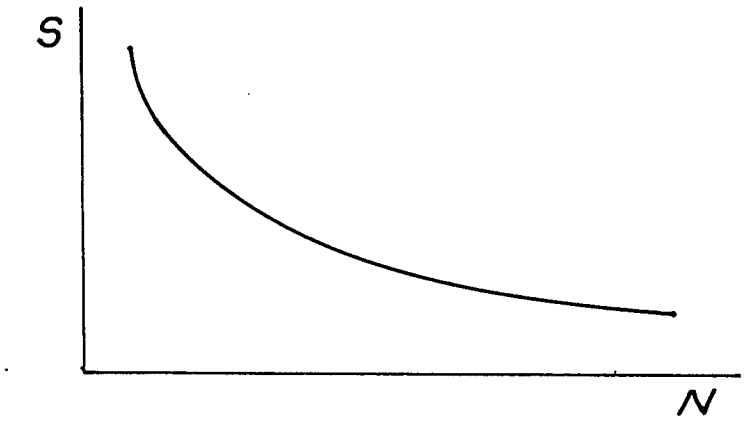

FIG. 2.12 TYPICAL S/N CURVE

A good brief survey which forms a basis for theoretical fatigued life estimates is by J. T. Broch [33].

The commonest form of mechanical failure due to vibration is fatigue failure caused by gradual propagation of cracks in the region of high stress under high alternating stresses. The fact that cracks propagate faster for higher alternating stresses is generally expressed by means of an experimentally determined S-N curve. Here S denotes the stress amplitude and N the number of cycles of stress (of fixed amplitude S) which causes failure. To obtain a reasonably accurate estimate of die life, it is necessary to combine theoretical predictions with practical test experiments. The first thing to do is to construct a S/N curve (stress level versus number of cycles to failure) (see Figure 2.12).

The change in slope of the S/N curve is due to changes in the rate of crack growth, $\frac{dx}{dN}$ given by:

$$\frac{dx}{dN} = C\, e_r^{\,m}\, x^n \qquad (2.11)$$

where x = crack length
N = number of stress reversals
C = constant depending on material
e_r = relative strain
$m = 2$; $n = 1$

The Palmgren-Miner rule (33) is used to extend regular cyclic fatigue data to cover random vibration. A factor Di as defined in equation (2.12) is used and the failure occurs when D defined by equation (2.13) becomes unity.

$$D = \frac{n_i}{N_i}, \qquad (2.12)$$

where n_i = No. of stress reversals at stress level i
N_i = Total number of stress reversals for failure for stress level i

$$D = \sum_i \frac{n_i}{N_i}, \qquad (2.13)$$

The statistics of the exciting force can now be used to obtain expressions for the number of stress reversals over a small range (equation [2.11]) and then this information can be used to obtain an estimate of the fatigue life, T (equation [2.13])

$$n(x) = f_o \; Tp(x)\, dx \qquad (2.14)$$

where $p(x)$ = peak probability density function
dx = small amplitude interval
$n_{(x)}$ = number of stress reversals for range x to x + dx
fo = force amplitude factor

Partial damage

$$Dx = \frac{n(x)}{N(x)} = f_o T \frac{p(x)dx}{N(x)}, \qquad (2.15)$$

$$T = \frac{1}{f_o \int \frac{p(x)}{N_{(x)}}\, dx}, \qquad (2.16)$$

L.W. Root [34] gives results of a study to verify a technique for predicting the random fatigue curve from the results of sinusoidal fatigue measurements by making use of the Palmgren-Miner hypothesis of fatigue damage accumulation. J. H. Tait [35] presented a method of analysis relating the total available kinetic energy of both sinusoidal and random vibration programs.

R. G. Lambert [36] describes a cumulative fatigue damage analysis which uses linear elastic fracture theory as its basis. The applied stress can be sinusoidal or random. Fatigue life can be is expressed in several ways such as median cycles to failure; probability of failure of N applied stress cycles, and cycles to first failure.

Failure occurs when

$$\sum_{j=1}^{N} Dj\ Xj, = 1 \qquad (2.17)$$

Also

$$Nm_n = Nf_n \times D_n \qquad (2.18)$$

where Nm_n = Fatigue life as median cycles to failure at the nth stress level.
Dj = Damage function of jth stress level.
Xj = Correction factor
n = Total number of stress levels

Expressions were also developed to evaluate the fatigue curves

$$S = \frac{\Delta S}{2} = \bar{A}\ Ns^{1/\beta}\ , \qquad (2.19)$$

$$\sigma = \bar{c}\ \bar{N}r^{-1/\beta}\ , \qquad (2.20)$$

where $\bar{A}$ and $\bar{c}$ are material fatigue curve constants β is slope diameter and ΔS is cyclic sine stress range.

A damage function, which is the derived probability density function of D, is given by:

$$p(D) = \frac{\bar{A}}{D\beta\,\Delta\sqrt{2\pi}}\left(\frac{\bar{D}}{D}\right)^{1/\beta} \exp\left[-\frac{\bar{A}^2\left\{\left(\frac{\bar{D}}{D}\right)^{1/\beta}-1\right\}}{2\,\Delta^2}\right] \qquad (2.21)$$

where: $\bar{A}$ = average value of A

D = cycle ratio damage function

$\bar{D}$ = median values of above cycle ratio

Δ = standard deviation of A

β = fatigue curve slope paramater.

Fatigue microcrack nucleation (i.e. initiation) occurs at only one percent of the total fatigue life. Microcracks undergo two stages of crack growth, then combine into macrocrack which eventually propagates in the material to cause fracture. The crack will grow in a stable fashion until the crack length "a" reaches a critical value "ac" which expresses when the magnitude of the stress fluctations at the crack tip reaches the material critical value ΔKc (fracture toughness), at which time the crack growth becomes unstable and the part fails catastrophically.

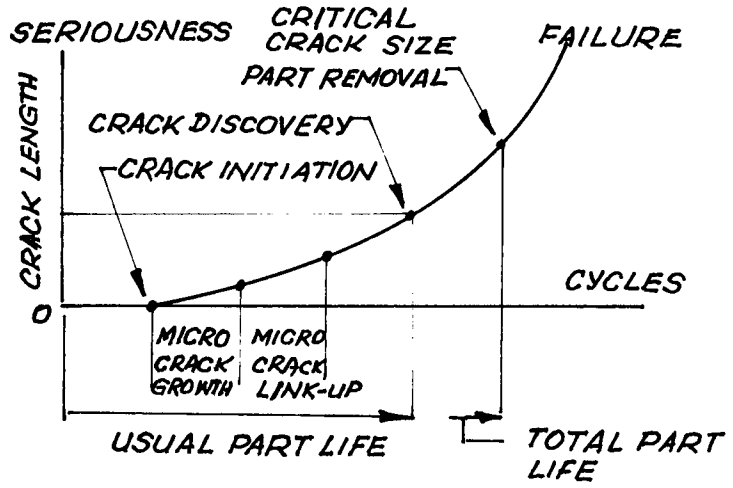

FIGURE 2.13 PROPAGATION OF CRACK
From Machine Design [46]

Figure 2.13 shows how the propagation of the crack length depends on the number of stress cycles.

Lambert's [37] formula for calculating critical crack length is:

$$a_c = \left(\frac{\Delta K_c}{Y \Delta S}\right)^2 \quad \text{metre,} \qquad (2.22)$$

where:

$$Y = \sqrt{2\pi}\left(\sec \frac{\pi a}{2b}\right)^{1/2} \qquad (2.23)$$

hence:

$$\Delta K_c = Y \Delta S \sqrt{a_c} \quad \text{MPa Metre} \qquad (2.24)$$

In the stable crack propagation region the rate of crack growth is:

$$\frac{da}{dN} = C_o (\Delta K)^{\theta} \quad \text{metre/cycle,} \qquad (2.25)$$

where: N = the number of applied cy cles
C_o = material constant
θ = material constant
ΔK_c = material's fracture toughness
a_c = critical crack half length
Y = geometrical paramater
ΔS = sinusoidal stress range - twice stress amplitude

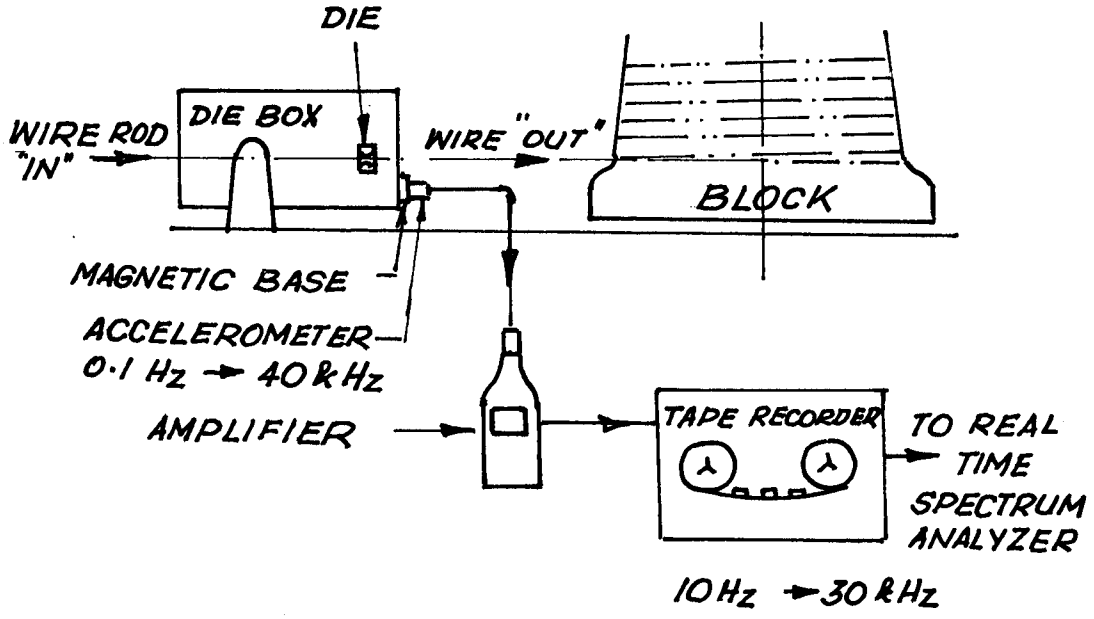

FIG. 3.1 BASIC VIBRATION MONITORING ARRANGEMENT

3. VIBRATION INSTRUMENTATION

3.1 Introduction

The vibration associated with the wire drawing process has been monitored by recording a two minute sample of the acceleration every hour at the die box. Figure 3.1 shows the basic arrangement.

It is not practicable to mount a transducer directly on the die. However, since a good mechanical path exists from the die to the outer casing of the die box, most of the essential information about the vibration of the die may be obtained from a monitor at this point, although the analysis of the data becomes more difficult.

Mechanical vibrations can be simply defined as movements of a mass about a reference point. The movement could be described in terms of:

Displacement: The distance moved by the mass from its natural position. Units in metres (m).

Velocity: The speed at which the mass moves. Units in metres/second (ms^{-1}).

Acceleration: The rate of change of velocity of the masses. Units in metres/second/second (ms^{-2}) or gravitational constant "g"*.

* An acceleration of 1g = 9.81 ms^{-2}

For oscillating motion at a single frequency.

$$\text{Velocity} = \frac{\text{Acceleration}}{2\pi f}$$

$$\text{Displacement} = \frac{\text{Acceleration}}{(2\pi f)^2}$$

Where f = frequency

The choice of the parameter for a particular measurement depends on the nature of the vibration and the purpose of the measurement.

Displacement is usually preferred for measuring low frequency vibrations. (Machine unbalance and vibration of structural support).

Velocity provides a useful indication of vibration severity and is therefore preferred in machine conditioning monitoring and preventive maintenance programmes since the energy associated with a moving body is proportional to $(\text{velocity})^2$.

Acceleration is preferred for measuring shock and high frequency vibration where the very first signs of machine wear and fatigue generally appear, since force is proportional to acceleration, thus this is the parameter which was selected for investigation in this project.

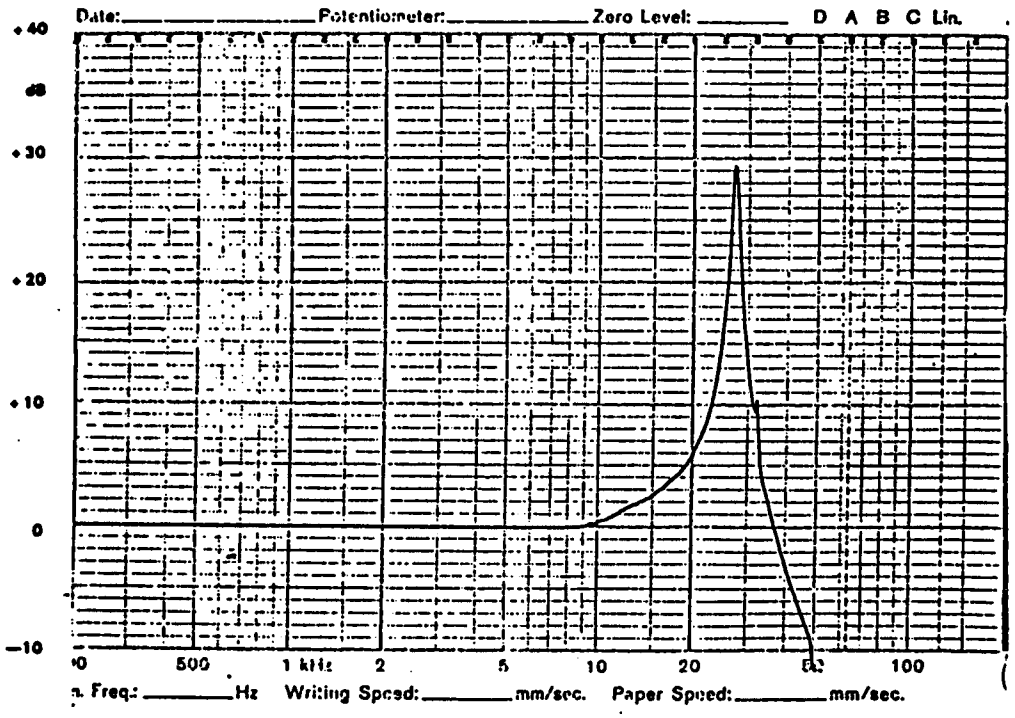

FIGURE 3.2 CALIBRATION CHART FOR ACCELEROMETER TYPE 4366

Accelerometer B & K Type		4366
*Weight (grams)		28
*Voltage Sensitivity	mV/ms^{-2}	~ 4,0
	mV/g	~ 40
*Charge Sensitivity	pC/ms^{-2}	~ 4,5
	pC/g	~ 45
*Mounted Resonance	kHz	27
*Frequency Range†	5%	0,2 – 5400
	10%	0,2 – 9000
Capacitance Incl. Cable	pF**	1200
Max. Transverse Sensitivity	%***	< 4
Piezoelectric Material		PZ23
Construction		Delta Shear
Typical Base Strain Sensitivity **** (in base plane at 250 με)	$ms^{-2}/\mu strain$	0,006
	g/μstrain	0,0006
Typical Temp Transient Sensitivity ****(3 HzLLF)	$ms^{-2}/°C$	0,1
	g/°C	0,01
Typical Magnetic Sensitivity (50 Hz–0,03 T)	ms^{-2}/T	3
	g/k Gauss	0,03
Typical Acoustic Sens. Equiv. Acc. at 154 dB SPL (2–100 Hz)	ms^{-2}	0,002
	g	0,0002
Min. Leakage Resistance at 20°C	GΩ	20
Max. Ambient Temperature	°C	250
Max. Shock (± Peak) Along main axis	kms^{-2}	50
	g	5000
Max. Cont Sinusoidal Acceleraion (Peak)	kms^{-2}	20
	g	2000
Max. Acceleration (Peak) with Mounting Magnet	kms^{-2}	1
	g	100
Base Material		Stainless Steel AISI 316

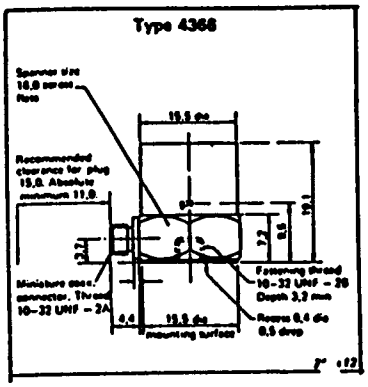

* Individual values given on the calibration chart.
** With cable supplied as standard accessory.
*** Axis of minimum transverse sensitivity indicated by red dot on the accelerometer except 4321, 8306, 8307, 8308, 8309. 8310
**** Re. ANSI S2. 11-1969 (American National Standard).

† The low frequency cut-off is determined by the preamplifier and environmental conditions.
†† Transverse resonance frequency at 11 kHz (typical) may limit the useful frequency range further

FIGURE 3.3 - SPECIFICATION OF B.&.K ACCELEROMETER

3.2 Vibration Transducer

The transducer used was an accelerometer which is an electromechanical transducer producing an electrical output proportional to the acceleration to which it is subjected.

The active element of an accelerometer consists of one or more piezoelectric discs, loaded by a seismic mass. When it is subjected to vibration the seismic mass exerts a variable force on the piezoelectric element which, due to the piezoelectric effect, produces a corresponding electric charge; the charge produced by the piezoelectric element is proportional to the acceleration to which the transducer is subjected. This charge produces a voltage due to the capacitance (electrical) of the transducer and associated cabling which can then be amplified for subsequent analysis. Special charge sensitive amplifiers are available for use with piezoelectric devices.

The transducer used was a (Bruel and Kjaer) Type 4366. It employs a Delta Shear design which makes it suitable for most vibration work. Delta shear gives a high sensitivity to mass ratio with a high resonance frequency and isolation from base strain and temperature transients. It employs three piezoelectric elements each with their own mass, which gives reduced sensitivity to extraneous environmental forces since they are arranged in the shear mode around a triangular centre post [38]

The characteristics of the accelerometer used are given in figures 3.2 and 3.3. These are for an unmounted unit and the use of a magnetic base alters the frequency response and decreases substantially the magnitude of the peak in Figure 3.2.

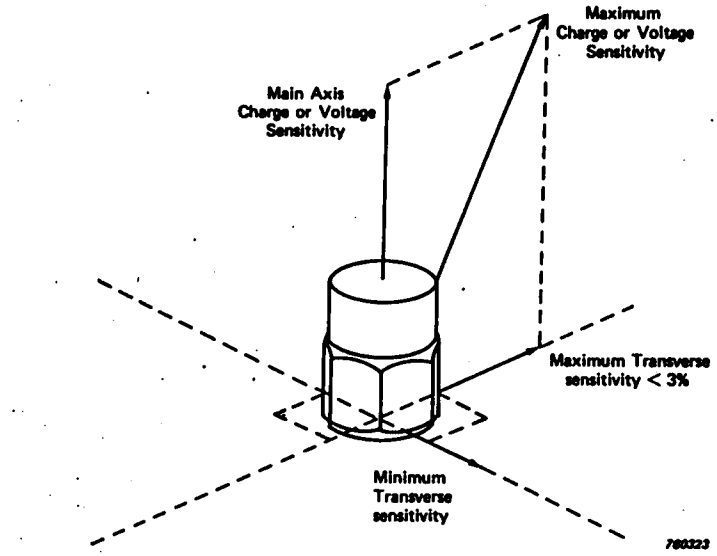

Fig. 3.4 Vectorial representation of transverse sensitivity [38]

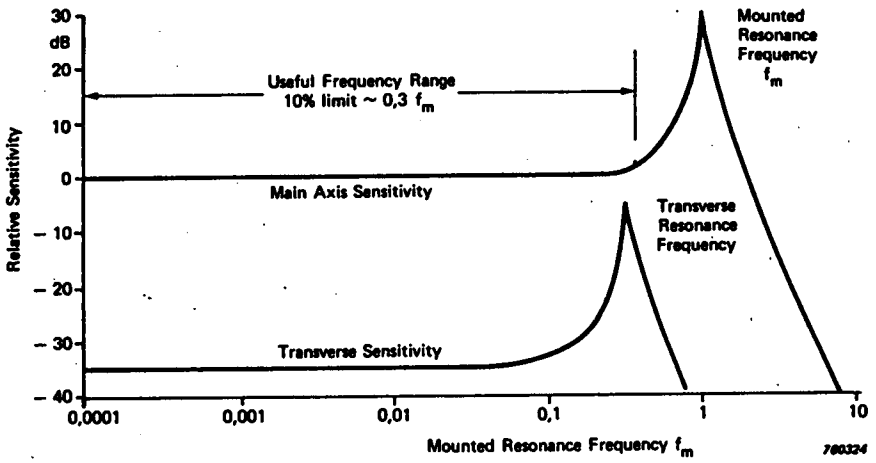

Fig. 3.5 Schematic of accelerometer main axis sensitivity and transverse sensitivity as a function of frequency (38)

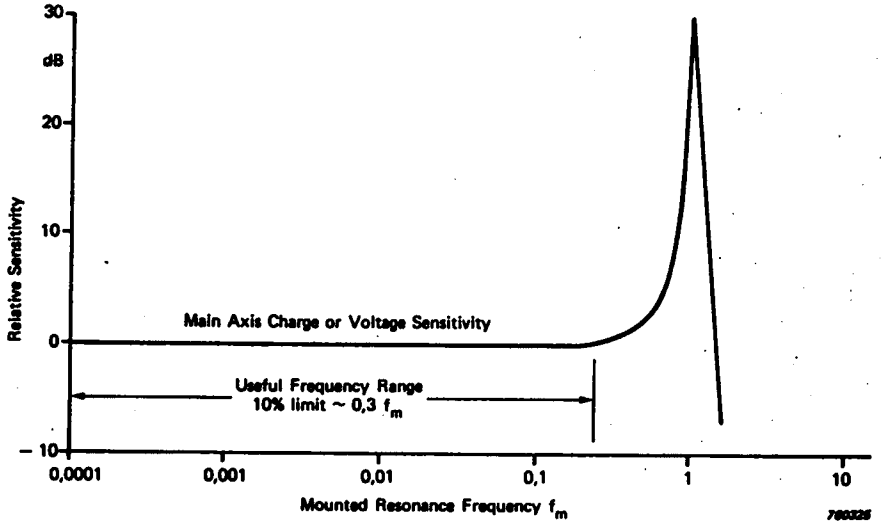

Fig. 3.6 Schematic of charge and voltage sensitivity vs frequency characteristic of an accelerometer (38)

Measurements are normally confined to the linear portion of the response curve whose high frequency limit is determined by the accelerometers natural resonant frequency (see Figure 3.6).

An accelerometer will respond to vibration in directions other than its main axis (see Figure 3.4 and 3.5). The sensitivity decreases at the angle between main axis and the direction of vibration increases. The direction of minimum transverse sensitivity was indicated by a red spot i.e. in this direction the transverse sensitivity is virtually zero.

As a general rule, the accelerometer mass should be no greater than 1/10 of the effective (dynamic) mass of the part of the structure to which the accelerometer is mounted and this requirement was met in the experiments carried out.

The method of attaching the accelerometer to the measuring point is one of the most critical factors in obtaining accurate results from practical vibration measurements. The following methods may be used.

- threaded stud

- thin layer of bees wax for sticking accelerometer.

- mica washer and isolated stud where the accelerometer is electrically isolated.

- cementing studs

- double sided adhesive tape.

- permanent magnet

- hand held probe

A permanent magnet base was used in the experiments carried out for this project.

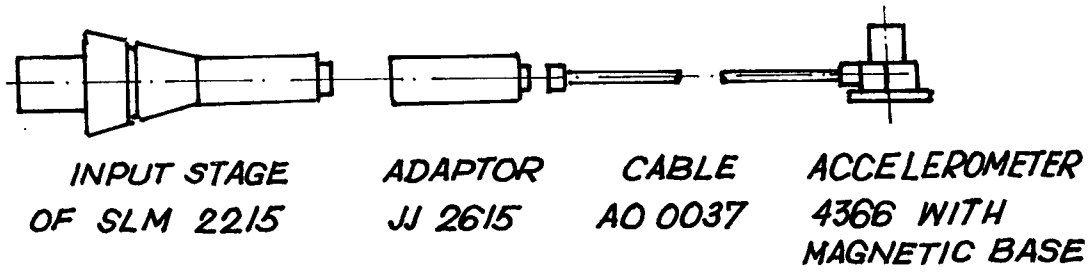

FIG. 3.7 INDICATES HOW AN ACCELEROMETER IS CONNECTED TO THE B.&.K 2215 SLM

3.3 Amplifiers

A Bruel & Kjaer Type 2215 precision sound level meter (SLM) with an adaptor was used to amplify the vibration signals to a sufficient level for recording (see Figure 3.7).

The calibration procedure employed using the built-in generator was as follows:-

- Connect the B.&.K. 4366 accelerometer to SLM

- Check adjustments and batteries as detailed in the B.&.K. Instruction Manual [39].

- Rotate the weighing selector until "Lin" appears in window of the SLM

- Switch on Power/Meter switch to "Fast"

- Rotate range selector to "Cal"

- Use small screwdriver supplied, carefully turn the sensitivity adjustment potentiometer screw until the meter needle indicates OdB with input Adaptor JJ 2615.

The sound level meter is now calibrated so that a reading of 94 dB corresponds to 9.81 m/s^2 (1 g) when using an accelerometer with sensitivity of 50 mv/g and coupled via one of the input adaptors.

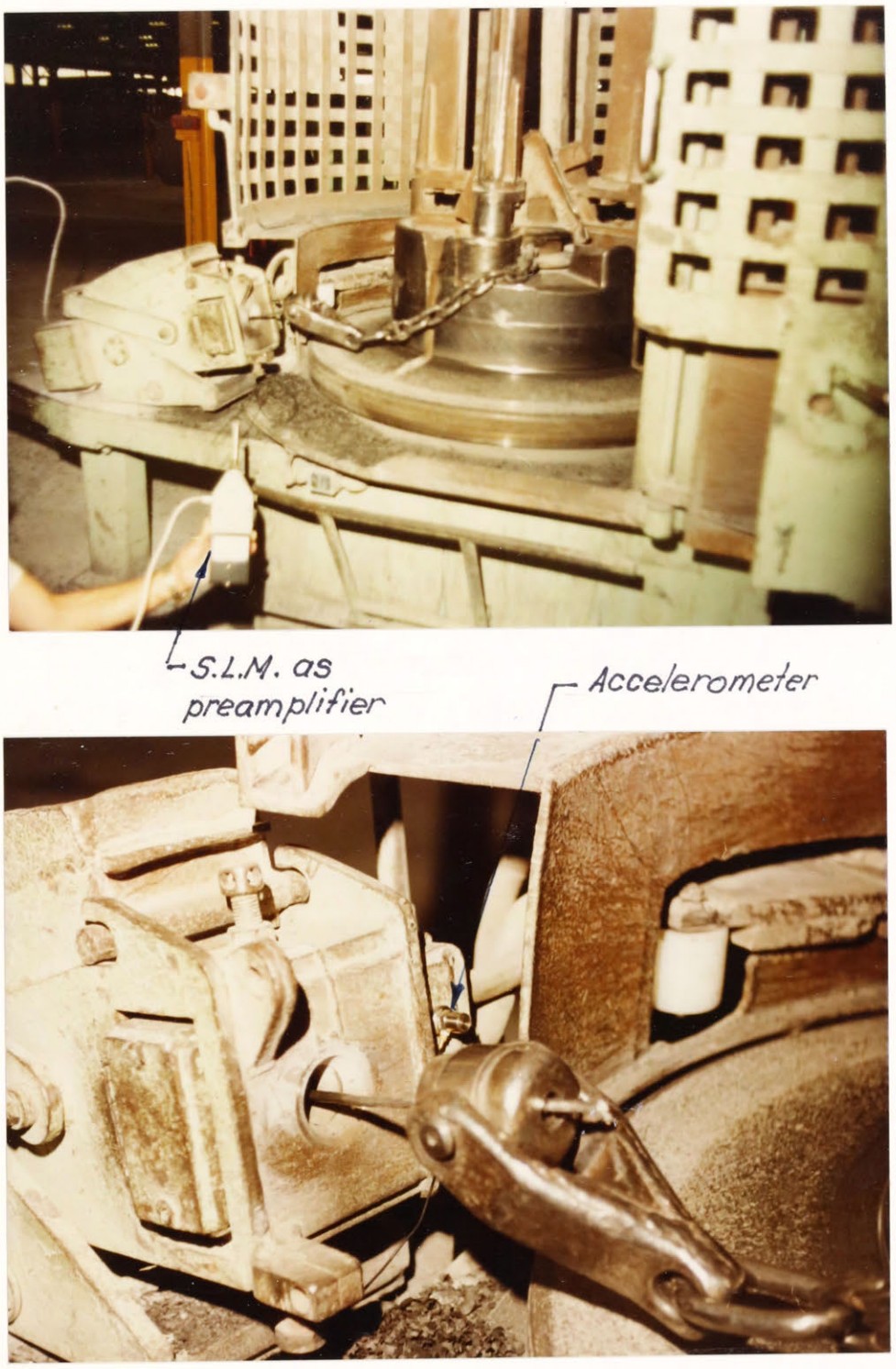

FIGURE 3.8 PHOTOGRAPHS SHOWING LOCATION OF ACCELEROMETER DURING TESTING

Figure 3.8 shows photographs of the actual disposition of the accelerometer and preamplifier.

3.4. Tape Recording

If the vibration signals are recorded this means that a permanent record is available which can be replayed later for analysis. Two recording principles are in common use:

Direct Recording (DR)
Frequency Modulation (FM)

F.M. recordings are employed to obtain good linearity and good low frequency response (down to D.C.) which is required for many vibration measurements, however, good high frequency response and good signal/noise ratio is often easier to obtain using direct recording.

The details of the tape recorder used are:

Type: Nagra Kudelski IV SJ Serial No. 7094
Direct Recording (DR)

Magnetic tape: 6.25 mm wide x 275 m long tape transport with speed and frequency response as follows:

38.1 cm/s	25 Hz to 35 k Hz
19.05 cm/s	25 Hz to 20 k Hz
9.5 cm/s	25 Hz to 10 k Hz
3.8 cm/s	25 Hz to 3.5 k Hz

A tape speed of 19.05 cm/s was chosen as no frequencies in the monitored signal were greater than 20 kHz.

Initially the length of recording was 2 minute every hour but this was later reduced to 1 minute to allow more test runs to be recorded on each tape.

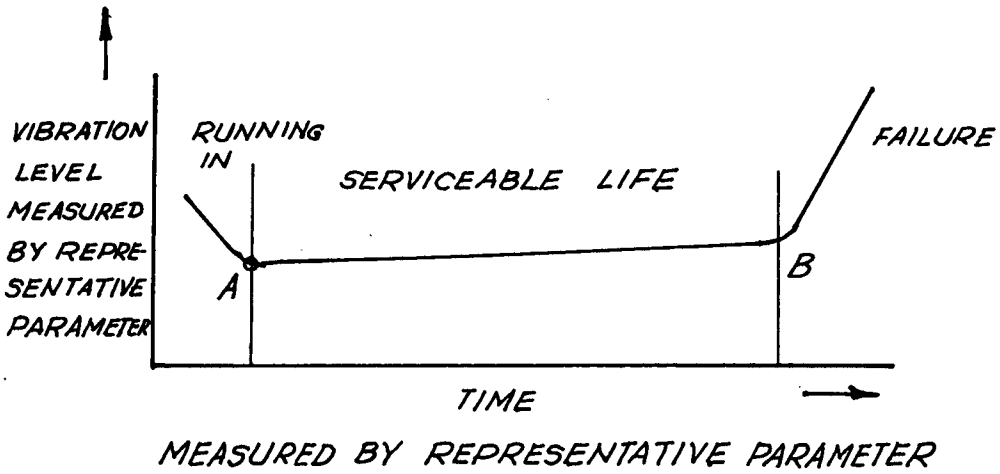

FIGURE 4.1 VIBRATION LEVEL VS TIME

4. SIGNAL ANALYSIS

4.1. Introduction

Mechanical signature analysis is a process of acquiring parameters based on vibration monitoring of operating machinery systems or their components, so as to determine their condition. It can be also used to diagnose the cause of a fault. Mechanical signature analysis is a comparative process. Vibration signatures can be compared to base line signatures on the same machine or to signatures from identical systems or machinery known to be in good condition. These signatures can then be used to establish standards for serviceability. One objective of signature analysis is to predict when the condition of a system has deteriorated to the point that some type of failure is imminent.

Figure 4.1 shows a simple vibration signature plotted against time in three regions of the total operating life of a plant. The sudden increase in the rate of change of vibration level at the point B, marks the beginning of the region of increased wear. The machinery baseline signatures for this simple analysis are from A to B. Baseline signatures imply fault - free operation [25] [24] [40].

The parameters derived from the vibration measurements may be simple ones such as the mean or variance of the amplitude or a more complicated ones such as the power spectral density.

4.2 Simple Parameters (Mean, Variance, Standard Deviation.)

The three simple statistical parameters often used to characterise a group of variables are:

mean	$- \bar{x}$
variance	$- \sigma^2$
standard deviation	$- \sigma$

The mean gives a measure of the most expected value of the variable and is defined as:

$$\bar{X} = \frac{1}{T}\int_0^T X(t)\,dt \qquad (4.1)$$

The mean square is given by:

$$\bar{X}^2 = \frac{1}{T}\int_0^T X^2(t)\,dt \qquad (4.2)$$

Which is simply the average of the squared values of the time history.

Variance is mean square value about the mean

$$\sigma^2 = \frac{1}{T}\int_0^T (X-\bar{x})^2\,dt \qquad (4.3)$$

Standard deviation gives another measure of the spread of the values about the mean.

$$\sigma = [\text{Variance}]^{1/2} \qquad (4.4)$$

Each of the equations (4.1) to (4.4) can be written in a discrete formulation for calculations using discrete data as obtained in a digital acquisition system. Thus, if the samples are x1, x2.....Xn, equation (4.1) become.

$$\bar{X} = \frac{1}{N}\sum_{i=1}^{N} X_i \qquad (4.5)$$

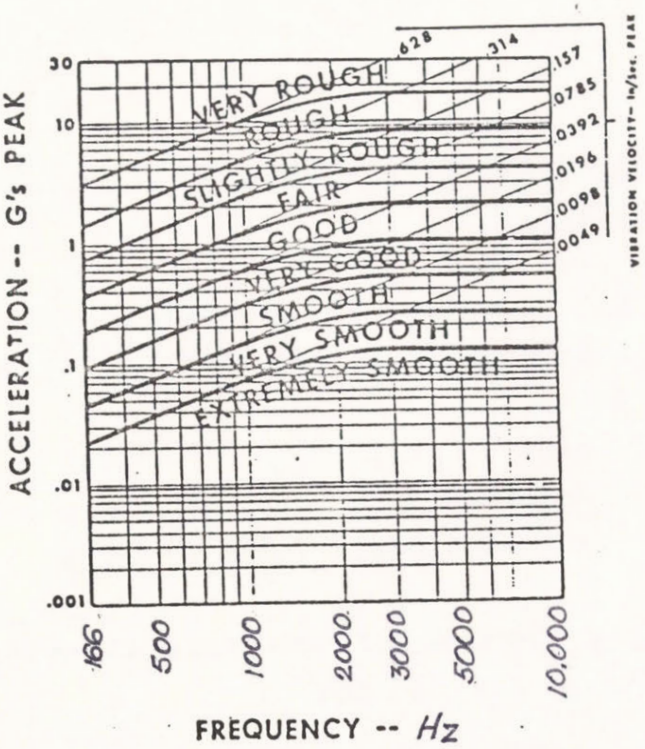

FIG. 4.2 SEVERITY CHART
REPRODUCED FROM FOX [14]

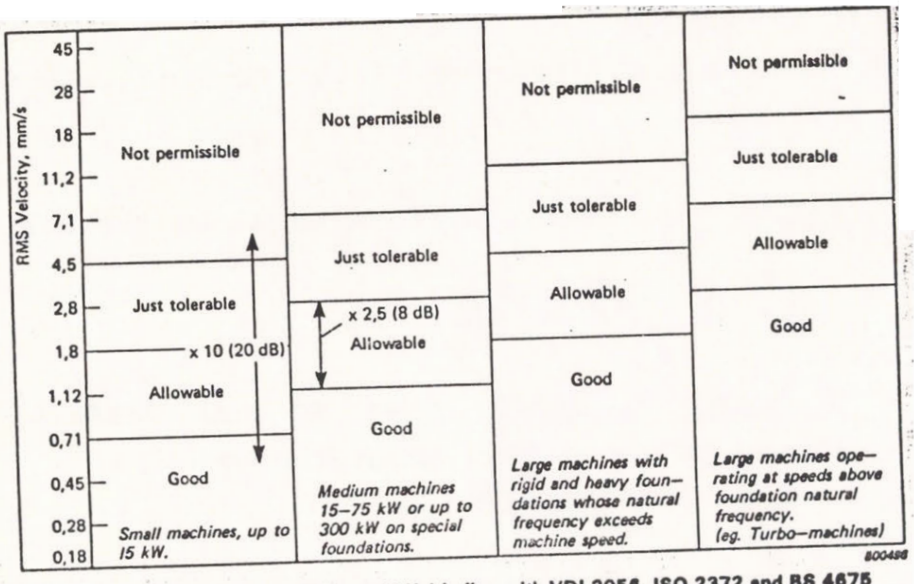

Vibration Severity Criteria (10 Hz to 1 kHz) in line with VDI 2056, ISO 2372 and BS 4675

FIG. 4.3 VIBRATION SEVERITY
CHART REPRODUCED FROM B&K [41]

The time sample should be as long as possible to ensure good statistics. The analysing equipment often has an upper limit on the length of sample that can be handled, in which case many samples have to be taken and the results averaged (ensemble averaging) which is the same as time averaging if the signal is stationary (i.e. if its statistical parameters are constant with respect to time).

The vibration level which is normally the root mean square (RMS) for the acceleration level and called a discriminant, can be an indicator of the condition of a machine. Comparison of the measured level with values on a standard vibration severity chart allows assessment of the machine [14] [41]. (See Figures 4.2 & 4.3).

4.3 Time Domain Analysis

A raw vibration signal can be simply viewed as a function of time using an oscilloscope or, sampled and digitised discrete values of the signal can be stored using a computerised data-logging system. These records are not very useful in developing a signature, as the signal is not deterministic but random in nature, so that a statistical technique must be used. Such as the calculation of the auto correlogram, Rxx (τ), defined for a signal x (t) as:

$$Rxx(\tau) = \lim_{T \to \infty} \frac{1}{2T} \int_{-T}^{T} x(t)\, x(t-\tau)\, dt \qquad (4.6)$$

The auto correlogram expresses how a signal relates to itself for different values of the time lag, τ . The auto correlation can determine whether deterministic components are present in a given signal since they will maintain a relationship for larger values of τ while random (noise) signals will not. The auto correlogram is little used in vibration analysis now but it can be used as the initial point for the calculation of the power spectral density.

4.4. Frequency Domain Analysis

The frequency domain is more popular than the time domain for processing the data because specific operating events can be correlated with specific frequency bands [17, 20, 21, 22, 27].

Normally the power spectral density (PDS) is used where the energy between two freqencies is defined as the area under the curve between those frequencies. However, some instruments determine the amplitude spectral density which is related to the PSD by the fact that power is proportional to $(\text{amplitude})^2$. It is often easier to see small differences between signals in the frequency domain using the amplitude spectral density.

The simplest type of frequency domain analysis is to pass the signals through a bank of fixed filters, such as octave band filters. This gives only very coarse frequency resolution and suffers from the disadvantage that the filters are of constant percentage bandwidth so that the absolute frequency resolution becomes worse as the centre frequency of the filter is increased. Constant narrow bandwidth filtering is preferred for signature analysis.

High resolution frequency analysis was originally carried out using a tape loop and then varying the filter centre frequency, however, it was found difficult to construct a variable filter having a constant narrow bandwidth, so a heterodyne principle was then introduced where an optimised fixed filter was constructed and the incoming signal mixed with a local oscillator to produce a

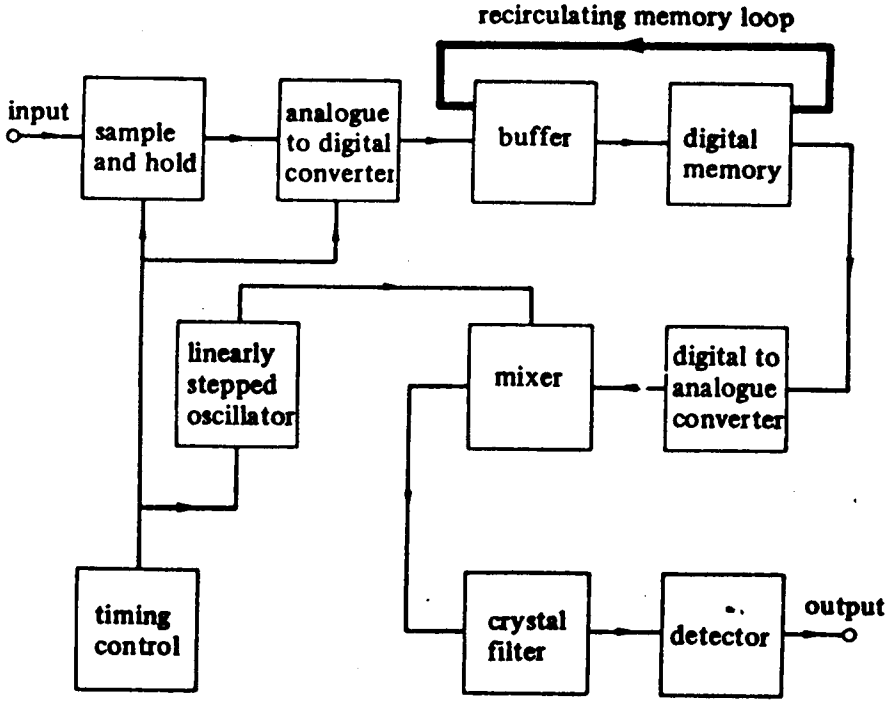

FIGURE 4.4 SCHEMATIC OF HYBRID ANALOG DIGITAL REAL TIME ANALYER
(From R. Harris [43])

sum/difference frequency which is then within the range of the fixed filter. To minimize the analysis time the signal is compressed in time and this is carried out digitally in modern analysers using the heterodyne approach. A schematic of such a unit is given in figure 4.4 [43]. The output of such a unit is the amplitude spectral density.

Certain precautions have to be observed when digitising the signal for the analyser. A most important one is that the sampling frequency be at least twice the highest frequency component present in the signal, or aliasing may take place where higher frequencies are folded back to occur apparently in the range being analysed.

The length of signal that an analyser can handle is limited and to meet requirements of good statistics many samples of the signal are taken and the results of the analyses averaged (ensemble averaging). Provided a signal is stationary (statistical properties do not change with time) then ensemble and time averaging will both give the same results.

The quantity computed is the power spectral density (loosely referred to as a spectrum) and the energy in a band specified by two cut-off frequencies is found by computing the area under the curve. The calculation of the power spectral density allows discrete frequencies in the signal to be identified. Using the power spectral density as raw input for subsequent analyses, it is possible to compute a group of other parameters to identify the spectrum of a signal, such as its average

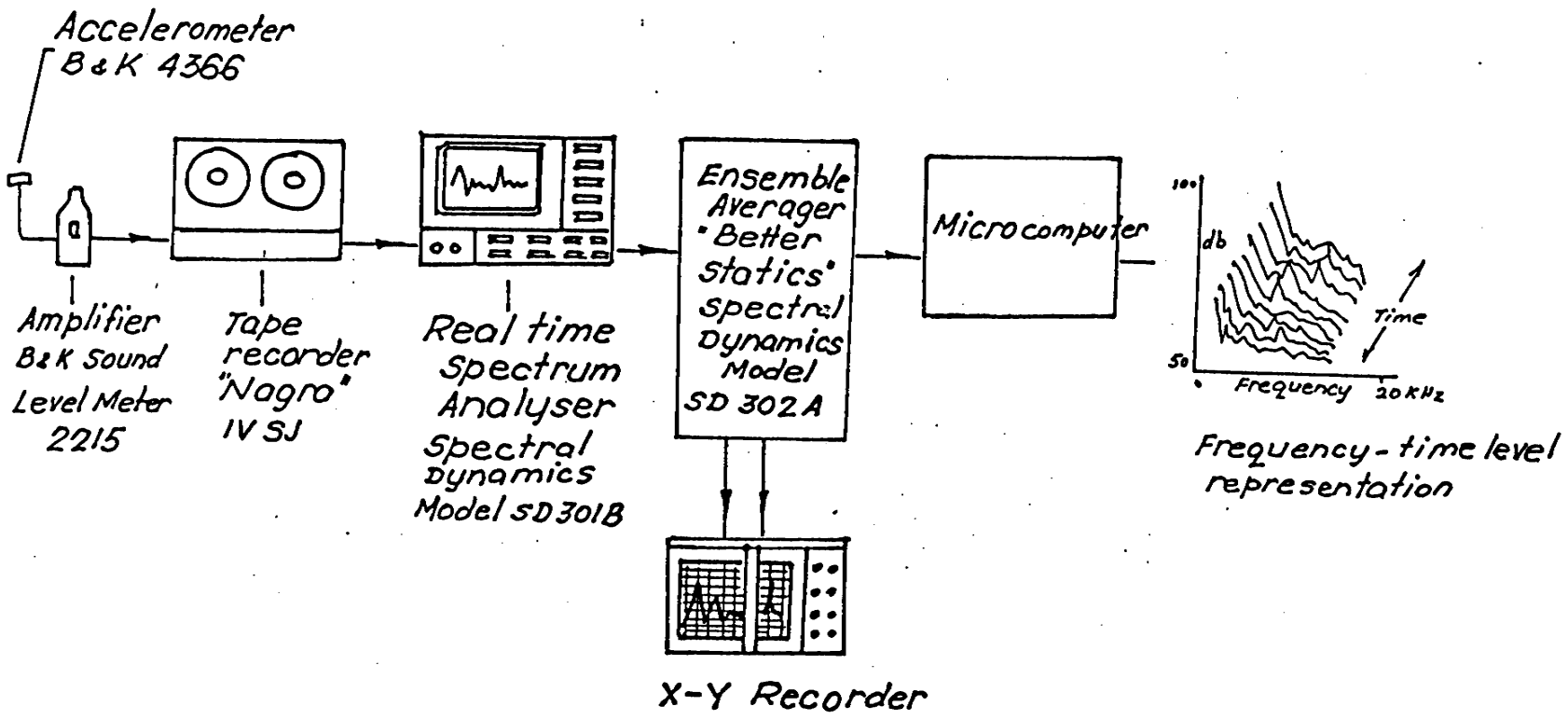

FIGURE 4.5 INSTRUMENTS FOR OVERALL MEASUREMENTS INCLUDING ANALYSIS EQUIPMENT

value; the variation about this average value expressed as the standard deviation; the frequency which divides the curve into two equal areas (median frequency); and the position and magnitude of the most dominant peak.

The real time analyser used in this project was a Spectral Dynamics Model SD301B which gave a frequency resolution of 60 Hz when the upper frequency setting was 20 kHz. A schematic of the experimental arrangement is given in figure 4.5.

4.5 - Some Other Analysis Tools

Cepstrum analysis is a data processing method that can be used to separate the periodic effects from random ones in a vibration spectrum. The mathematical definition of the cepstrum is the power spectrum of the logarithm of the power spectrum [18] [44]. An important feature of the cepstrum is in studying a periodic structure in the PSD due to a series of harmonics. The cepstrum can detect and give a measure for phenomena which produce periodicities in the spectrum such as harmonics and sidebands. The cepstrum is useful in analysing complex signals containing a mixture of both several groups of different harmonics and/or sidebands [18].

Further information on a signal can be obtained using statistics of the amplitude. Simple parameters such as mean and standard deviation can be computed, as well as more sophisticated functions such as the probability density function and the peak probability function. These techniques require that many samples of data be acquired.

The kurtosis method uses the fourth moment of the signal about the mean as defined by the following:

1st moment mean $$\bar{x} = \frac{1}{T}\int_0^T x(t)\,dt \qquad [4.7]$$

2nd moment variance $$\sigma^2 = \frac{1}{T}\int_0^T (x-\bar{x})^2\,dt \qquad [4.8]$$

4th moment $$k^4 = \frac{1}{T}\int_0^T (x-\bar{x})^4\,dt \qquad [4.9]$$

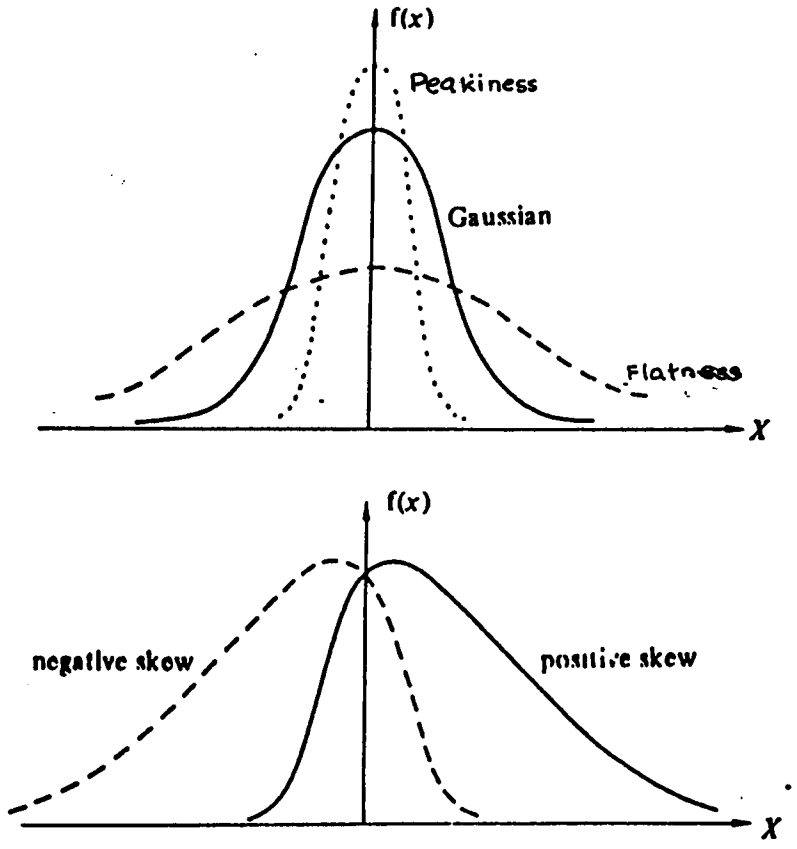

FIGURE 4.6 COMPRESSION OF KURTOSIS AND SKEWNESS IN PROBABILITY DISTRIBUTION
From Harris [43]

The nature of the probability density function gives information about the source of a vibration signal. Two important aspects of a probability density function are the "peakiness" and the "skew" which are depicted in Figure 4.6. The "peakiness" of the probability density function is an important factor in machine integrity assessment since it depends on the amount of wear in moving machinery. A quantitive assessment of this "peakiness" can be expressed by the kurtosis, which is the fourth moment about the mean value normalised by dividing by the second moment about the mean squared, namely $k^4/(\sigma^2)^2$ as defined in equations [4.8] and [4.9]. A gaussian curve has a kurtosis value of 3. As the mechanical condition deteriorates and causes increased material contact, the density curve will flatten resulting in a larger value for the kurtosis.

Vibrations measurements were taken in situ on three single hole machines Nos. 26, 27 & 30.

- No. 26 Single hole machine has a stationary die. The block is driven by 100 h.p. motor via a two speed gearbox.

- No. 27 Single hole machine has a rotating die; the block is driven by a 100 h.p. motor via a two speed gearbox.

- No. 30 Single hole machine also has a rotating die. The block is driven by 150 h.p. motor via a two speed gearbox.

Wire Products - H.D. Low Carbon AS 1303

- No. 26 Machine was drawing two sizes of wire dia. at different time.
  10 mm to 7.90 mm as finished size (39% reduction).
  8 mm to 6.23 mm as finished size (38% reduction).

- No. 27 Machine was drawing only one size of wire diameter.
  9 mm to 7.02 mm as finished size (39% reduction).

- No. 30 Machine was drawing only one size of wire diameter.
  10 mm to 7.90 mm as finished size (39% reduction).

TABLE 5.1 ACCELEROMETER SITUATIONS AND WIRE SPECIFICATIONS

VIBRATION LEVEL SURVEY

Sound level Meter : B&K 2215
Accelerometer : B&K 4366
Cable : B&K AO 0037

LOCATION	POSITION	OCTAVE BAND CENTRE FREQUENCY										REMARKS
		31.5	63	125	250	500	1K	2K	4K	8K	16K	
FIXED	DIE											WIRE REDUCTION
26 m/c	FRONT	57	67	65	70	81	83	83	99	97	83	FROM 10mm TO 7.9mm
"	SIDE	65	69	71	68	70	74	84	95	94	80	
26 m/c	FRONT	66	67	70	75	78	87	91	93	86	85	FROM 8mm TO 6.23 mm

TABLE 5.2 OCTAVE BAND VIBRATION LEVEL
(dB re m/s^2) RESULTS FOR NO. 26 MACHINE

LOCATION	POSIT.	OCTAVE BAND CENTRE FREQUENCY										REMARKS
		31.5	63	125	250	500	1K	2K	4K	8K	16K	
WITH ROTATING DIE												WIRE REDUCTION
												FROM
27 m/c	FRONT	55	55	68	65	73	80	85	93	78	74	9mm TO 7.02 mm
"	SIDE	55	63	71	68	71	77	85	95	80	73	

TABLE 5.3 OCTAVE BAND VIBRATION LEVEL
(dB re m/s^2) RESULTS FOR NO. 27 MACHINE

LOCATION	POSIT.	OCTAVE BAND CENTRE FREQUENCY										REMARKS
		31.5	63	125	250	500	1K	2K	4K	8K	16K	
WITH ROTATING DIE												WIRE REDUCTION
												FROM
30 m/c	FRONT	60	63	71	72	70	75	82	87	97	76	10mm TO 7.9mm
"	SIDE	59	65	65	65	66	73	80	93	78	60	

TABLE 5.4 OCTAVE BAND VIBRATION LEVEL
(dB re m/s^2) RESULTS FOR NO. 30 MACHINE

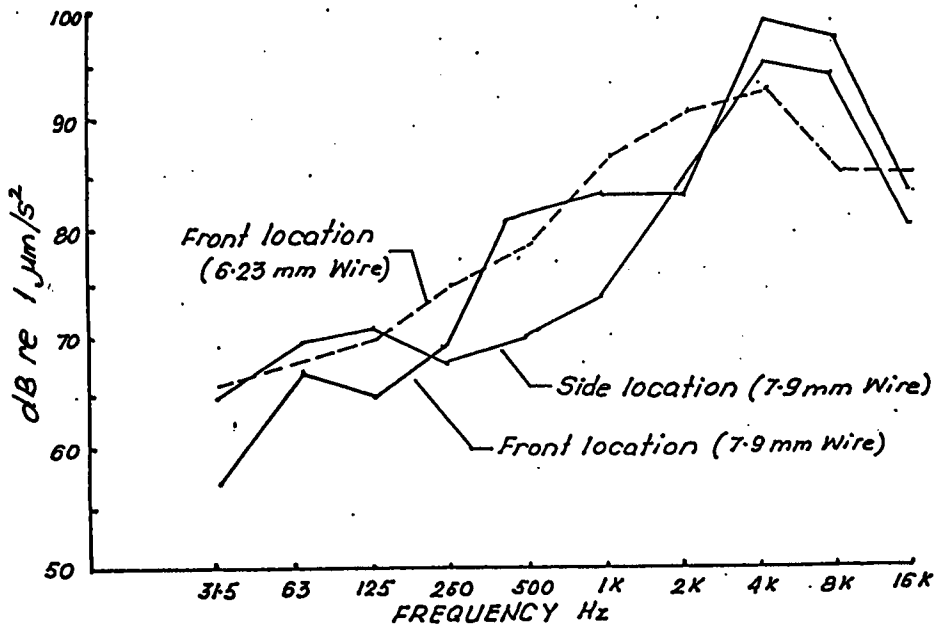

FIGURE 5.1 PLOT OF OCTAVE BAND VIBRATION ANALYSIS FOR NO. 26 MACHINE

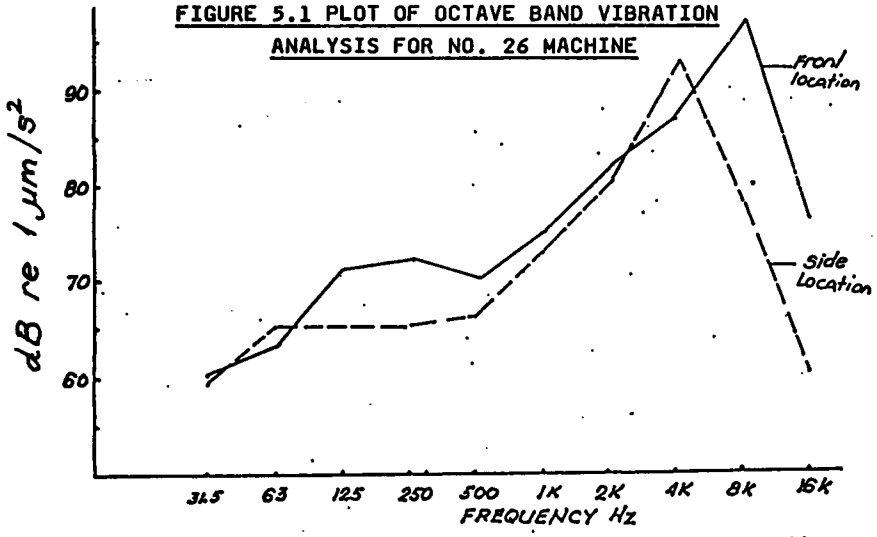

FIGURE 5.2 PLOT OF OCTAVE BAND VIBRATION ANALYSIS FOR NO. 27 MACHINE

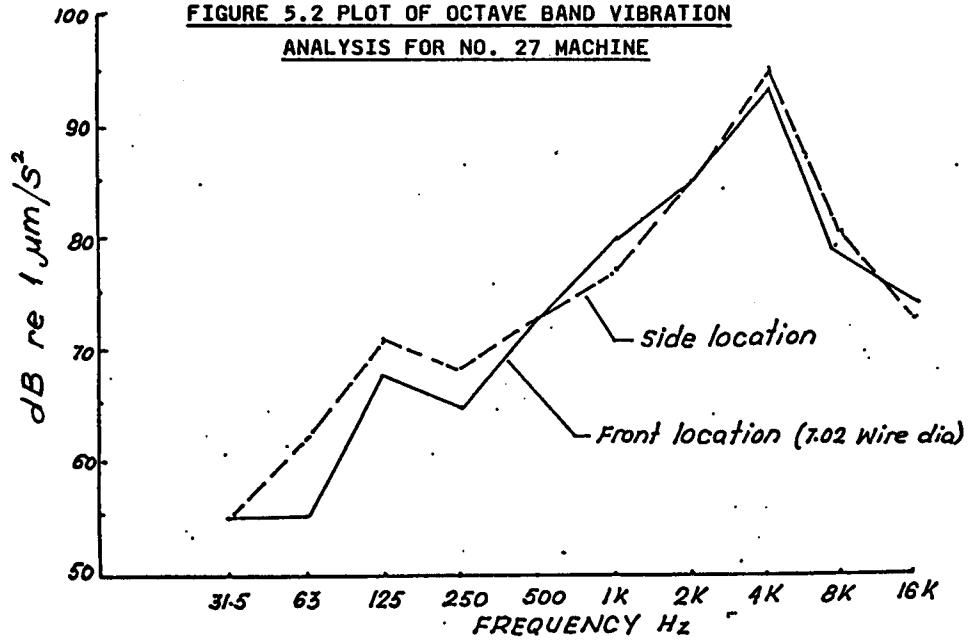

FIGURE 5.3 PLOT OF OCTAVE BAND VIBRATION ANALYSIS FOR NO. 30 MACHINE

5. RESULTS AND DISCUSSION

5.1. Overall Vibration Levels

To gain some idea of the overall vibration, the signals from the accelerometer were examined using an octave analyser attached to a sound level meter. The positions for the accelerometer and the nature of the wire being drawn are given in Table 5.1.

The following results were obtained from a series of preliminary tests prior to the main monitoring tests. The vibration signals were sensed at the front and the side location of the die holder, for both fixed and rotating dies. Tables 5.2, 5.3 and 5.4 show the experimental results which are graphed in Figures 5.1, 5.2 and 5.3 for different machines. There is slightly less vibration for the rotating dies, most probably due to the poorer mechanial coupling from the die to the casting.

After the preliminary tests proper monitoring commenced with new die No. 6149 with nominal diameter 6.23 hole and die 9104 with diameter 7 mm hole as a back up unit. Die No. 6149 was in use over 20 hours when a crack was detected and the die was withdrawn from further use.

Test Run	Wire Dia. mm	Wire Speed M/Min.	Breaking Stress MPa	Time	Date
1	6.230	264		9.35	22.7.82
2		264		9.45	"
3		324		10.40	"
4		324		11.30	"
5	6.238	324	615	9.00	30.8.82
6	6.246	324	654	9.30	"
7	6.253	324	654	10.30	"
8	6.254	221	666	11.30	"
9	6.252	264		12.30	"
10	6.240	274	673	13.30	"
11	6.246	287	668	14.20	"
12	6.268	223	650	15.00	"
13	6.268	370	650	15.00	"
14	6.267	341	644	15.40	"
15	6.267	357		16.40	"
16	6.268	357	647	17.35	"
17	6.259	218	654	18.10	"
18	6.268	309		19.50	"
19	6.270	262	616	9.10	31.8.82
20	6.264	280	636	10.40	"
21	6.265	252	636	11.40	"
22	2.269	299		12.30	"
23	6.272	365	653	14.35	"
24	6.262	373	647	15.20	"
25	6.262	373	650	16.00	"
26	6.279	375	637	16.30	"

Visual inspection showed a fracture in the die after 26th run.

TABLE 5.5 RELEVANT PHYSICAL DATA FOR DIE 6149 DURING VIBRATION MONITORING

Test Run	Wire Dia. mm	Wire Speed M/Min.	Breaking Stress MPa	Time	Date
1	7.020	296	746	12.45	22.7.82
2	7.015	296	543	13.45	"
3	7.030	300	680	8.00	23.7.82
4	7.037	312	643	9.00	"
5	7.000	331	738	9.50	"
6	7.035	331	618	10.45	"
7		326		11.50	"
8	7.934	327	695	12.30	"
9	7.039	324	720	13.30	"
10	7.036	263	608	8.00	10.9.82
11	7.032	266	639	9.00	"
12	7.035	304	624	10.40	"
13	7.034	309	642	11.35	"
14	7.037	309	663	12.45	"
15	7.037	309	552	13.50	"
16	7.040	309	611	14.20	"
17	7.025	210	615	8.00	13.9.82
18	7.030	240	607	8.40	"
19	7.020	268	746	9.30	"

TABLE 5.6 RELEVANT PHYSICAL DATA FOR DIE 9104 DURING VIBRATION MONITORING

5.2 Raw Amplitude Spectral Density

The vibration at the die was sampled and recorded on magnetic tape at specific times and subsequently the amplitude spectral densities were determined. Table 5.5 gives the relevant physical data for die 6149; namely test run, wire diameter, breaking stress of wire in MPa, time of sample, date and wire speed. Table 5.6 gives the relevant physical data for die 9104. The amplitude spectral densities are included as Appendix I. An examination of these graphs shows that it is difficult to conclude much from a simple examination so various parameters computed from the spectral densities were used to see if any simple relations between single parameters was possible. Since the aim of the investigation was to compare the analyses of the vibration signals at different times, no absolute calibration of the spectrum analyser was carried out, however, the effect of all the gains in the system were allowed for and any graphs were plotted using the same scaling factor.

TABLE 5.7 COMPUTED PARAMETERS FROM SPECTRAL DATA FOR DIE 6149

RUN NUMBER	DATE	TIME	SPEED	POWER	MEDIAN FREQUENCIES		DEVIATIONS	
					AMPLITUDE	POWER	AMPLITUDE	POWER
1	22.7	935	264	22.08	6840	5440	0.12286	0.10972
2	22.7	945	264	11.59	6840	6160	0.09305	0.04759
3	22.7	1040	324	14.84	8840	8440	0.08427	0.03585
4	22.7	1130	324	11.41	7840	7240	0.07886	0.03302
5	30.8	900	324	18.61	8720	8400	0.08579	0.04042
6	30.8	930	324	4.77	8160	6080	0.05020	0.02390
7	30.8	1030	324	9.45	7760	7040	0.06602	0.02928
8	30.8	1130	228	11.36	7880	7200	0.07090	0.03155
9	30.8	1230	264	11.52	7320	6680	0.07869	0.03543
10	30.8	1330	274	9.91	8200	7240	0.06242	0.02969
11	30.8	1420	287	14.19	7520	6960	0.08630	0.03967
12	30.8	1510	223	13.58	5240	4640	0.11708	0.07780
13	30.8	1540	370	12.81	7200	5440	0.10034	0.07495
14	30.8	1540	341	13.02	8040	7440	0.07659	0.03611
15	30.8	1640	357	13.80	7520	7160	0.09222	0.04839
16	30.8	1735	357	11.39	7840	7240	0.07788	0.03696
17	30.8	1810	218	11.72	7280	6720	0.08034	0.03875
18	31.8	750	309	6.50	7080	5920	0.06182	0.03060
19	31.8	910	262	13.64	7120	6320	0.09425	0.04840
20	31.8	1040	280	11.36	8240	7600	0.06876	0.03263
21	31.8	1140	252	15.28	7840	7400	0.08875	0.04254
22	31.8	1230	299	9.85	6520	5800	0.08364	0.04352
23	31.8	1335	365	8.23	7160	6120	0.07042	0.03285
24	31.8	1520	373	9.04	7480	6680	0.07218	0.03422
25	31.8	1600	373	11.98	8640	8320	0.07821	0.03800
26	31.8	1630	375	12.35	8080	7440	0.07953	0.03872

TABLE 5.8 COMPUTED PARAMETERS FROM SPECTRAL DATA FOR DIE 9104

RUN NUMBER	DATE	TIME	SPEED	POWER	MEDIAN FREQUENCIES		DEVIATIONS	
					AMPLITUDE	POWER	AMPLITUDE	POWER
1	22.7	1245	296	1097.23	5440	5240	1.19769	7.64229
2	22.7	1345	296	141.58	6640	6080	0.34313	0.73874
3	23.7	800	300	146.42	6600	6040	0.32831	0.63186
4	23.7	900	312	61.78	7680	5200	0.20319	0.42123
5	23.7	950	331	518.74	8160	7960	0.50549	1.27939
6	23.7	1045	331	373.06	8440	8280	0.43387	0.96680
7	23.7	1150	326	265.92	6640	6000	0.43561	0.87736
8	23.7	1230	327	246.39	6280	5880	0.44944	0.99124
9	23.7	1330	324	948.57	8080	8000	0.83723	2.98623
10	10.9	800	263	350.45	7480	7120	0.50962	1.14025
11	10.9	900	266	342.91	7760	7360	0.46013	1.17950
12	10.9	1040	304	1716.50	7640	7360	1.15143	6.27673
13	10.9	1135	309	215.93	7760	7400	0.34659	0.66135
14	10.9	1245	309	197.16	9000	7480	0.30338	0.90025
15	10.9	1350	309	202.09	10200	9960	0.26649	0.48465
16	10.9	1420	309	712.88	5920	5840	0.91199	4.16875
17	13.9	800	210	350.47	8680	9440	0.50479	1.53036
18	13.9	840	240	214.76	9040	9320	0.33282	0.63045
19	13.9	930	268	354.98	5440	5280	0.63459	2.41947

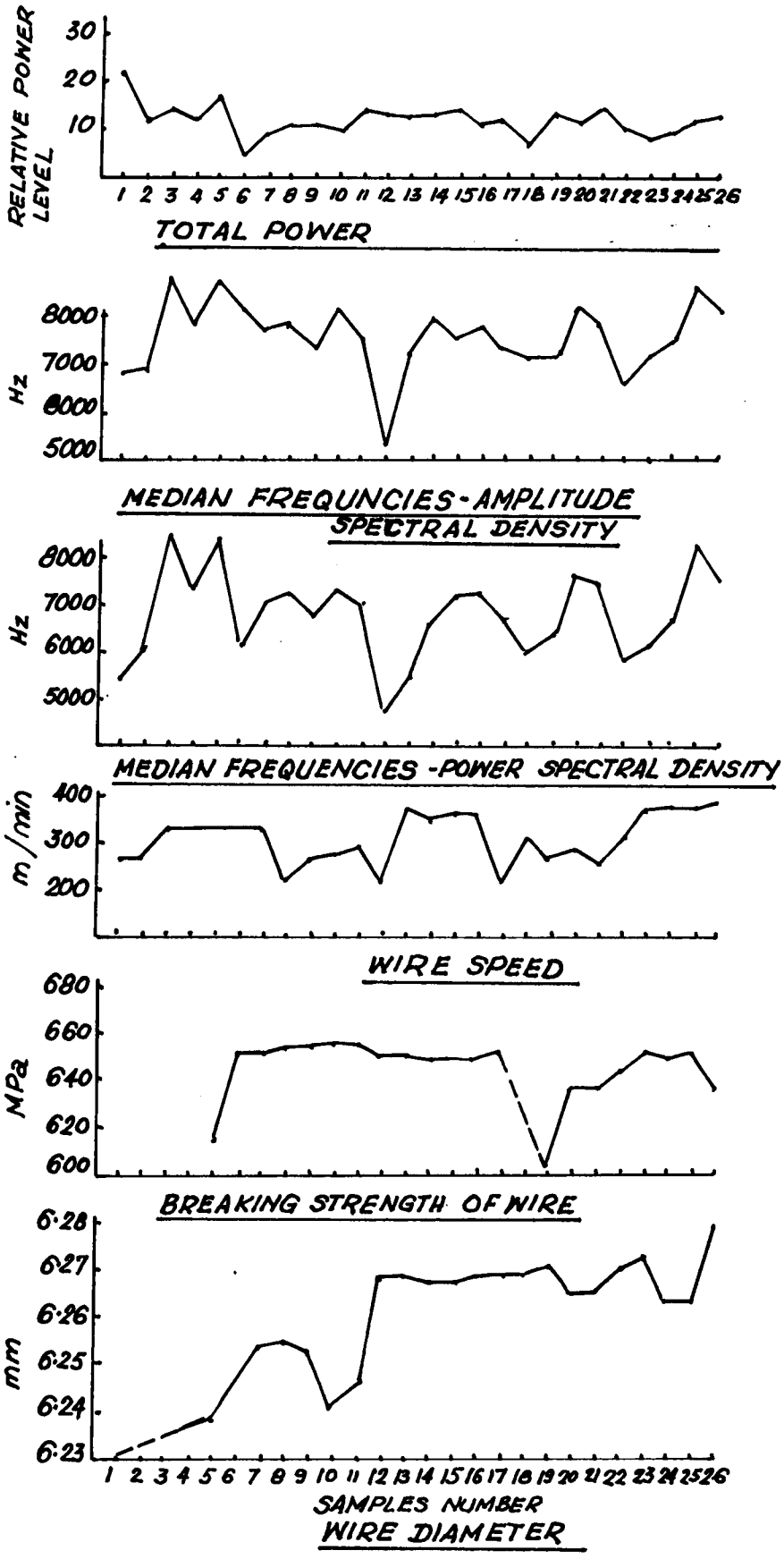

FIGURE 5.4 PARAMETER PLOT FOR DIE 6149

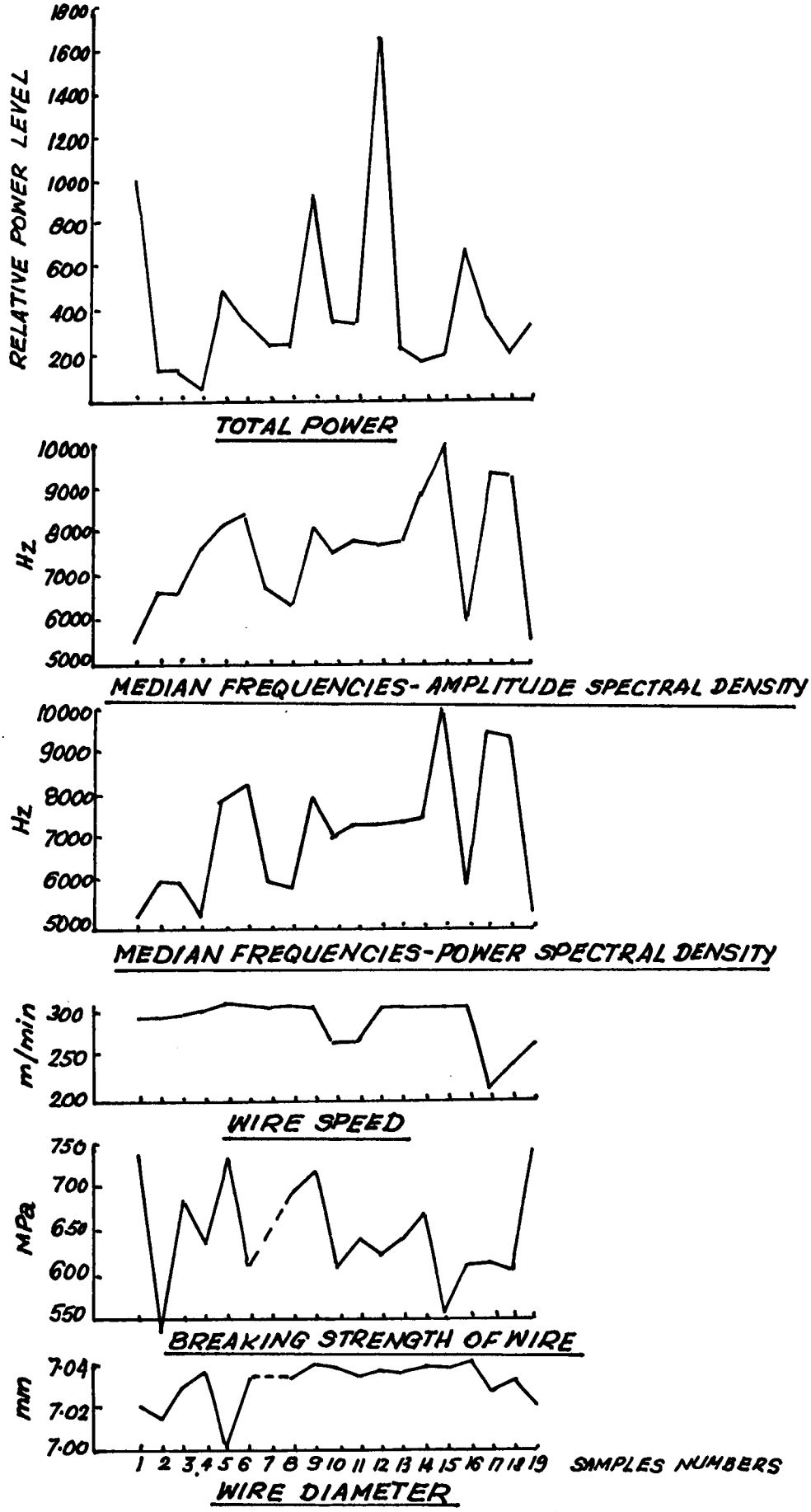

FIGURE 5.5 PARAMETER PLOT FOR DIE 9104

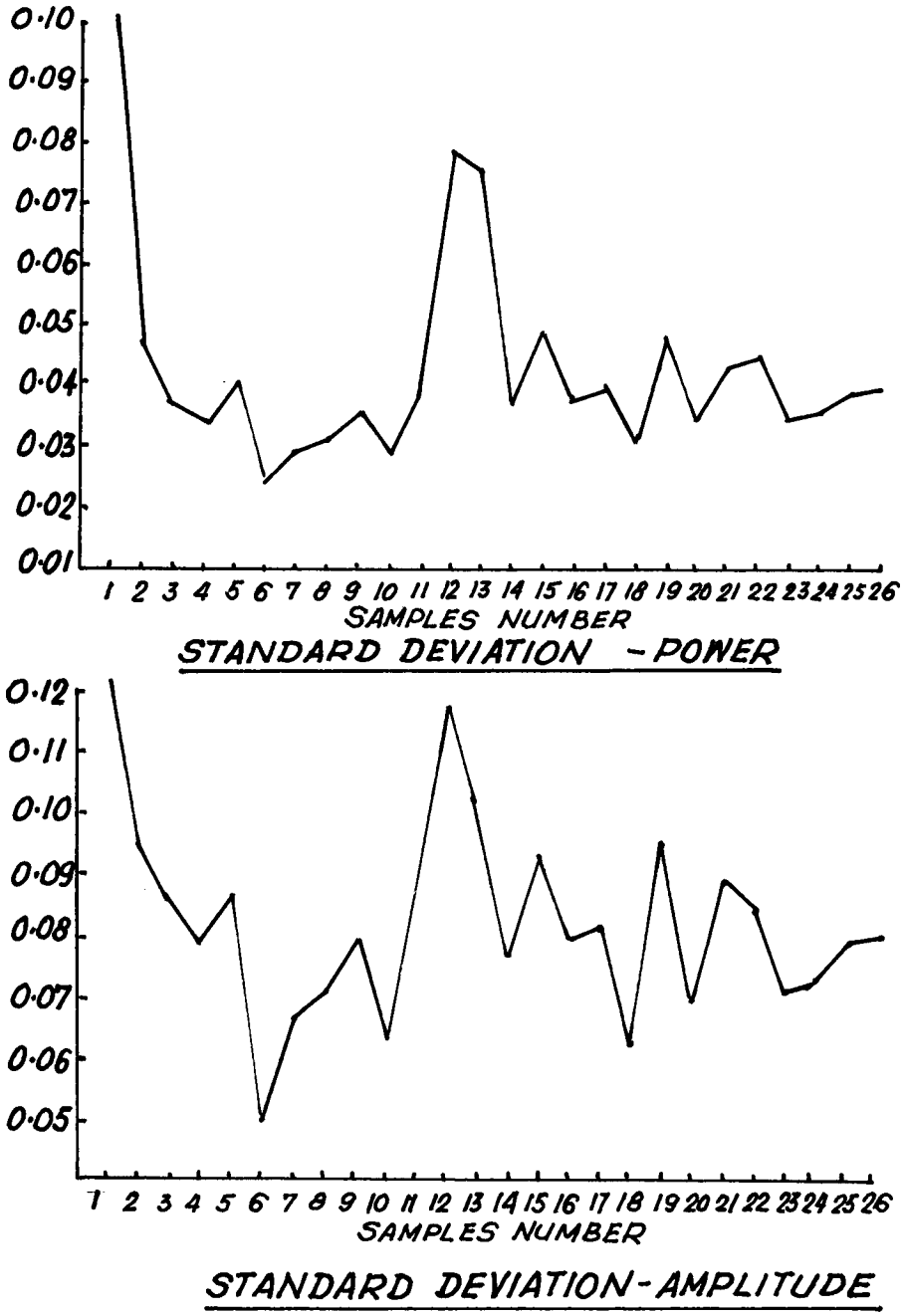

FIGURE 5.6 PLOT OF STANDARD DEVIATIONS OF VIBRATION SPECTRA FOR DIE 6149

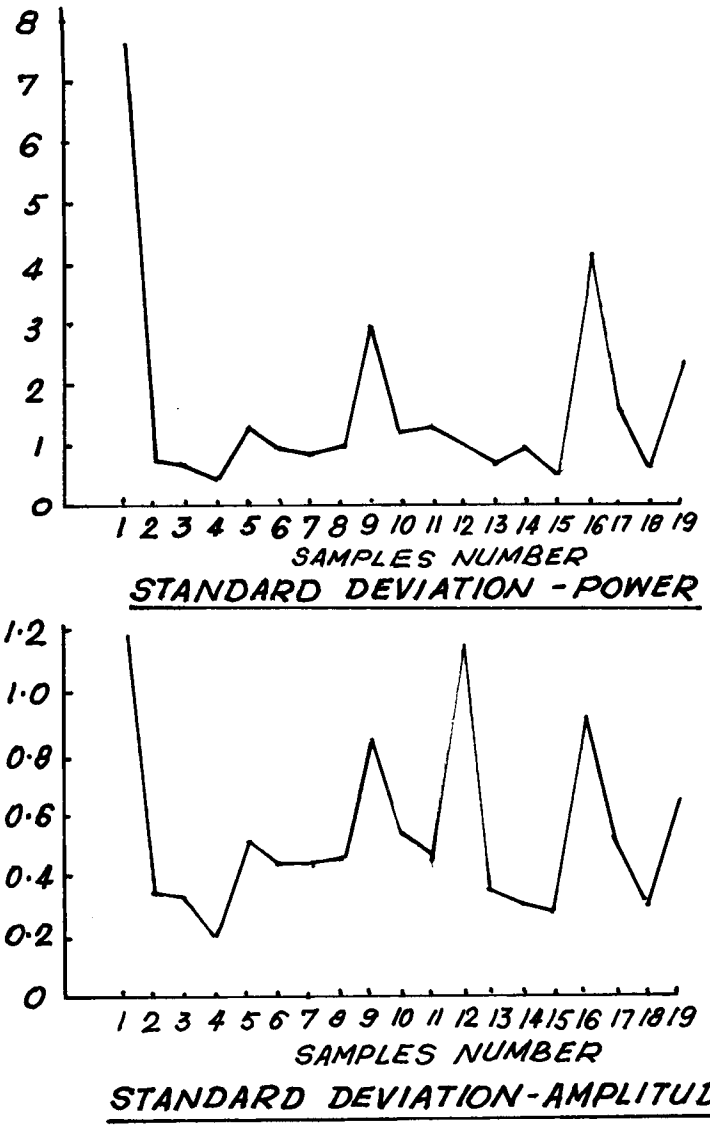

FIGURE 5.7 PLOT OF STANDARD DEVIATIONS OF VIBRATION SPECTRA FOR DIE 9104

5.3 Parameters Using Spectral Data

Using the raw amplitude spectral densities several single parameters can be computed. The ones chosen were:

- total relative power (computed by squaring ordinates of amplitude spectral density)
- median frequency for amplitude spectral density (median divides the graph into two halves of equal area).
- median frequency for power spectral density (power obtained by squaring amplitude value).
- standard deviation for amplitude spectral density (a measure of how spread out the graph is).
- standard deviation of power spectral density.

These parameters were computed from the raw spectral data using the computer programs in Appendix II. The computer program is written in FORTRAN language.

The computed parameters are listed in Table 5.7 for die 6149 and in Table 5.8 for die 9104. The results for power and median frequencies together with wire speed, breaking stress and wire diameter are plotted in Figure 5.4 for die 9104 and in Figure 5.5 for die 6149.

Figure 5.6 is a plot of the standard deviations of power amplitude for die 6149 and Figure 5.7 for die 9104.

An examination of the graphed data shows some general relationships, however, since the observed vibration signals depend to some degree on such parameters as wire speed, wire diameter, tensile strength, die wear (which one wants to know), lubrication, surface finish of both die and wire, cooling and logistics of the process (stop-start operation), no specific deductions can be arrived at. The general trends observed are as follows:

(i) wire speed is a dominating factor. As the speed is increased so the load on the die increases which increases the contact area accelerating the wear. An increasing load also reduces the lubrication thickness which means more asperity contact and a further increase in wear rate. Figure 5.4 shows that associated with a drop in wire speed at sample run 12 is also a drop in median frequencies as expected, however, the spectrum becomes more spread out as shown in Figure 5.6 while there is a slight drop in the total power.

(ii) a new die gives a higher vibration level at lower frequencies but with a large spread in the spectrum which can be seen by comparing sample runs 1 and 2 in figures 5.5 and 5.6.

Sample 1 was taken just after a new die was inserted and Sample 2 was taken at a later time in the history of this die.

(iii) a shock load start occurred when sample 18 was taken for Figure 5.4 and associated with this was a low value for the power of the vibration signal and some decrease in the standard deviations for the spectra.

(iv) An examination of Figure 5.5 for sample 15 where the wire speed was constant and the breaking strength of the wire decreased, showed an increase in the median frequency.

(v) In some instances a decrease in median frequency was associated with an increase in standard deviation (see Figures 5.4, 5.5, 5.6).

6. CONCLUSIONS

There are many factors that affect the vibration detected due to a wire being drawn through a die assembly and thus it was not possible to provide a parameter which would give some strong indication of the mechanical integrity of the die. The examination of raw frequency spectra was tedious and proved difficult to use in determining trends. Various parameters were computed from the spectra including the total power, median frequency and standard deviation. The median frequency gave an indication of the dominant frequency band and the standard deviation the extent of the spread of the spectrum.

The wire speed was an important parameter and generally a decrease in wire speed resulted in decrease in median frequency and an increase in the standard deviation. A decrease in the breaking strength showed in some cases an increase in median frequency but no simple trend was apparent.

To definitely determine whether die condition can be deduced from the analysis of vibration signals, the following approaches are recommended.

(i) Continuously monitor vibration signals and other plant variables such as wire speed and wire diameter;

(ii) Examine die wear as frequently as possible;

(iii) Use several accelerometers to determine the optimal placing of the sensors;

(iv) Attempt to maintain a constant wire speed to make the initial evaluation of the technique easier.

REFERENCES

1. DOVE, A.
STEEL WIRE HANDBOOK

Volume 1, 2, 3 - The Wire Association Branford CT 1969.
Chapter 4 - Theory of Wire Drawing
Chapter 5 - Wire Drawing Dies - General
Chapter 6 - Lubrication for Wire Drawing
Chapter 9 - The Cooling of Wire During Drawing

2. FELDER E.

Testing of various materials for the production of dies for steel wire drawing.
Wire Industry 46.551 November, 1979 pp 817-820

3. EDER, K

History of and new trends in wire drawing dies.
Wire Industry 48.576 - November, 1981 pp 797-803

4. WRIGHT R.N.

Mechanical Analysis and Die Design.
Wire Journal 12.10 October, 1979 - pp 60-61

5. VERDUZCO M.A. - DALLY J.W.

Photoelastic analysis of stresses in drawing dies and their reaction to failure.
Journal of the Iron and Steel Institute
July, 1970 pp 675-679

6. SMITH, B. F. - COOPER, A.

The theory of lubrication
Wire Journal 12.1 - January, 1979 pp 76-80

7. SHATYNSKI S.R. - WRIGHT R.N.

Die wear during wire drawing operations
Wire Technology 7/8 - 1979 pp 59-69

8. REID, C. G.

Analysis of wiredrawing using a computer program and load cell system.
Wire Journal International 16.3 - March, 1983
pp 52-56

9. AVITZUR B.

Study of flow through conical converging dies.
Part I - Wire Industry 49.582 June, 1982
- pp 449-454
Part II - Wire Industry 49.583 July, 1982
- pp 503-509
Part III - Wire Industry 49.584 August, 1982
- pp 613-619

10. GLEN K.E.

Die Design - Wire Journal 13.12 Dec, 1980 pp 68-69

11. NAKAMURA Y. KAWAKAMI H

An evaluation of lubrication in wire industry.
Wire Journal 13.6 June, 1980 pp 54-58.

12. DEORA, P.V.

Power productivity of a wiredrawing machine.
Wire Industry 50.592 - April, 1983 pp 206-211

13. HARPER S

Lubrication aspects of drawing Non-Ferrous wire.
Wire Industry 43.512 August, 1976 pp 623-626

14. FOX, R.

Preventive maintenance of rotating machinery using vibration detection.
Iron and Steel Engineer - April, 1977 pp 52-60

15. ESCHLEMAN, R.

Identification and correction of machinery vibration problems.
Sound and Vibration 15.4 - April, 1981 pp 12-18

16. ALLISON, H.

Noise data recording and computer controlled analysis.
Sound and Vibration 7.4 - April, 1973 pp 43-45

17. ESHLEMAN, R.

The roll of sum and difference frequencies in rotating machinery fault diagnosis.

18. TAYLOR, J.

Fault diagnosis of gears using spectrum analysis
Inst. Mech. Eng. 1980 Conference Publications

19. BABKIN, A.

Mechanical Signature Analysis Sound and Vibration 7.4 April, 1973 pp 35-42

20. MITCHELL, J.S.

Bearing diagnostics - An overview
The winter annual meeting of
The American Society of Mechanical Engineers
San. Fran. Calif.
December 10-15, 1978 pp 15-24

21. CORBEN, R

Vibration Monitoring
Noise Control Vibration and Insulation
August, September, 1976 pp 258-267
Presented at Symposium of the Society of Environment Engineers, Imperial College, London. September, 1975.

22. HOUSER, D.

Signal analysis techniques for vibration diagnostics.
MFPG Proceed Anaheim Cal. - April, 1975 pp 3-15

23. BRUNN P

Machine Condition Monitoring
Noise and Vibration Control Worldwide
September, 1981 pp 249-251

24. SWANSON, N.

Application of vibration signal analysis techniques to condition monitoring.
Friction and Wear - Eng. 1980 pp 262-267
Conference on Lubrication Friction and Wear in Engineering, 1980. Melbourne, 1-5 December. By the National Committee on Applied Mechanics of the Institution of Engineers, Australia.

25. NORMAN, C.

Identification and control of machinery and noise.
Conference on Machinery Noise and Vibration
Adelaide, 1978 29-30 May pp 21-27
Organised by the Committee on Applied Mechanics of the Institution of Engineers, Australia and the South Australian Division of the Australian Acoustical Society.

26. LEES, A. PANDEY, P.

Vibration specta from gear drives.
Institute of Mechanical Engineers, 1980 Conference Publication.

27. BHATTACHARAYYAA PATKIG

Frequency response characteristics of meshing gears for transmission errors and dynamic loading.
Noise, Shock and Vibration Conference 1974.
Monash University - Melbourne pp 426-433
Sponsored by Monash University, Department of Mechanical Engineering and Australian Acoustical Society, Victoria Division.

28. RANDALL, R.

Vibration signature analysis - Techniques and instrument systems. Noise, Shock and Vibration Conference 1974. Monash University Melbourne pp 445-455

29. FRANCE D. & GRAINER, H.

Investigation of a D.C. motor vibration problem. Inst. Mech. Eng. 1980 - 2nd Inter. Conf. Cambridge pp 83-90

30. SHATTOF, J.

Using vibration analysis to determine the dynamic health of turbine/generators.
Power 119.5 - May, 1976 pp 23-28

31. SMITH, D.M.

Recognition of the causes of rotor vibration in turbo machinery. Inst. Mech. Eng. 1980 2nd Inter. Conference, Cambridge pp 1-4

32. MITCHELL, J.S.

Monitoring Machinery Health I
Designing a surveillance system
Power 120.3 - March, 1977 pp 46-50

Monitoring Machinery Health II
Putting vibration and other operating variables to work in a monitoring system.
Power 120.5 - May, 1977 pp 87-89

33. BROCH, J.T.

On the damaging effects of vibration.
Bruel and Kjaer Technical Review No. 21975
pp 148-153

34. ROOT, L.W.

Random sine fatigue data correlation.
Shock and Vibration Bulletin No. 33 Pt. II
March, 1964 pp 279-285

35. TAIT, J.N.

Analysis of sinoosoidal and random vibration energies. Shock and Vibration Bulletin No. 40. Pt II - December, 1969 pp 135-161

36. LAMBERT, R.

Analysis of fatigue under random vibration.
Shock and Vibration Bulletin No. 47 Sept. 1977
pp 43-54

37. LAMBERT, R.

Probability of failure prediction for step-stress fatigue under sine or random stress Shock and Vibration Bulletin 47 - September, 1977 pp 31-41

38.

Piezelectric accelerometer and vibration preamplifier handbook.
Bruel and Kjaer Theory and Application Handbook.
Revision March, 1978.

39.

Bruel & Kjaer Instruction Manual for B & K 2215 Sound Level Meter.

40. MITCHELL, J.

Mechanical signature analysis as a first step in quantifying the characteristics of operating machinery MFPG (Detect. Dig and Prog.). Proceed. Chicago Ill. - May, 1977 pp 77-78

41. RANDALL

Frequency analysis.
Bruel & Kjaer Publication 1977.

42. BEAUCHAMP, K. PITTEN, S. WILLIAMSON, M.

Analysis vibration and shock data.
Pt. I - Data acquisition and preprocessing pp 17-22
Ot. II - Processing and presentation of results pp 25-32
Journal of the Society of Environmental Engineer
December, 1972

43. HARRIS, R. W. LEDWIDGE, T.

Introduction to Noise Analysis.
Pion Limited 1974 - London by Arrowsmith.

44. RANDALL, R.B.

Advances in the application of Cepstrum analysis to gearbox diagnosis. Inst. Mech. Eng. 1980.
Conference Publication.

45. HARBAJER, W. G.

Vibration signature survellience of axial flow compressors. Sound and Vibration 10.3 March 1976 pp 38-43

46.

New engine maintenance strategy: Throw it out just before it breaks.
Machine Design 55.5 - March 10, 1983 pp 25-30

47. DALY, B. B.

Woods Practical Guide to Fan Engineering - Woods of Colchester Ltd. 1978

48. KARASSIKI, KRUTZSCH W, FRASER W, MESSINA, J.

Pump Handbook. McGraw-Hill Co. 1976 New York

BIBLIOGRAPHY

B.1. DIETER G.

Rod and Wire Drawing
Mechanical Metallurgy 2nd Edition 1976.
McGraw-Hill Book Company - New York

B.2. ZUCKER L

A die maker looks at quarter century of change and offers a few predictions - Wire Journal 13.3 March, 1980.
pp 78-80.

B.3. NAKAMURA Y. FUJITA T. KAWAKAMI H.

New cooling system for high speed wire drawing

Wire Journal 9.6 July, 1976 pp 59-66

B.4. WRIGHT R.

Control of Heating During Wire Drawing

Wire Journal 6.9 September, 1973 pp 135-140

B.5. SMITH B.

Factors affecting the strength and power required for drawing steel wire.

Part I - Wire Journal 10.10 - Oct. 1977 pp 56-59
Part II - Wire Journal 10.11 - Nov. 1977 pp 68-72

B.6. DOELAND O.M. MACKEN A.C.

Optimisation of tungsten - wire drawing process based on certain theory of wire drawing.

Wire 26.5 - Sept/Oct. 1976 pp 187-192

B.7. HAEMERS, G.

The importance of the surface in wire making and wire quality.

Wire Journal 6.9 September, 1978 pp 134-140

B.8. GLIA, H.

Wire Breaks - Wire Journal 9.2 - Feb. 1976 pp 70-75

B.9. JONES, A. E.

Friction and lubrication in wiredrawing
The BHP Technical Bulletin pp 13-20

B.10. HENDERSON, P.

Machine Health Monitoring
Noise and Vibration Control Worldwide
August, September, 1980 pp 279-280

B.11. KNIGHT, A.

A brief review of the monitoring of vibration in rotating machines.
Noise Control Vibration and Insulation.
May, 1977 pp 168-170

B.12. ESHLEMAN, R.

Vibration of rotating machinery
Sound and Vibration 15.4 - April, 1981 pp 12-18

B.13. MUSTAIN, R.W.

Vibration measurements. Shock and Vibration Bulletin No. 34 pt 1 - February, 1965 pp 15-43

B.14. TUSIN, W.

Measurement and analysis of machinery. Chemical Engineering Progress (Vol. 67 N-6)
June, 1971 pp 62-69

B.15. LANG, G.

Understanding vibration measurements. Sound and Vibration. 10.13 March, 1976 pp 26-37

B.16. CHALLIS, L.

The quest of improved precision in vibration measurements.
Conference on Machinery Noise and Vibration
Adelaide, 1978 pp 66-69
By the National Committee on Applied Mechanics of the Institution of Engineers, Australia and the South Australian Division of the Australian Acoustical Society.

B.17. BOARD, D.

Rotating machinery diagnosis through shock pulse monitoring.
Winter Annual Meeting of The American Society of Mechanical Engineers - San Francisco
Cal. December, 1978 pp 25-40

B.18. FRAREY, J.

Comparison of vibration signature analysis techniques.
MFPG Proceed Chicago Ill. - May, 1977 pp 82-92

B.19. BUCHMAN, E. TUCKERMAN R.G.

Vibration data analysis. Procedure for the analysis and presentation of vibration data.
Shock and Vibration Bulletin No. 33 Pt II
March, 1964 pp 243-258

B.20. VOLIN R.

Techniques and applications of mechanical signature analysis. Shock and Vibration Digest. 11.9
September, 1979 pp 17-32

B.21. WELARATNA, S.

A signal processing system for vibration, shock and noise. Noise Control Vibration and Insulation
May, 1977 pp 156-158

B.22. HAMILTON, J.

The role of signal processing in machinery vibration analysis. MFPG. Proceed Chicago Ill.
May, 1977 pp 93-96

B.23. KROEGER, R. HASSLACHER, G.J.

The relationship of measured vibration data to specification criteria.
Shock and Vibration Bulletin No. 31 Pt II
March, 1963 pp 49-63

B.24. PHILLIPS, G.J. HIRSCHFELD, F.

Rotating machinery bearing analysis. Mechanical Engineering - July, 1980 pp 28-33

B.25. IGARASHI, T. HANADA, H.

Studies on the vibration and sound of defective rolling bearings.
Journal of the Acoustical Society of Japan - Vol.25 No. 204
June, 1982 pp 994-1001

B.26. WILSON, D.S.

Machinery protection through automated diagnosis.
The Winter Annual Meeting of The American Society of Mechanical Engineers San. Fran. Calif.
December, 1978 pp 1-14

B.27. BADGLEY, R. GILBERT, J.S.

Computerised assessment of machinery performance and health.
The Winter Annual Meeting of The American Society of Mechanical Engineers San. Fran. Calif.
December, 1978 pp 41-52

B.28. LANG G.

Spectrum analysis and machinery monitoring.
MFPG Proceed. Chicago Ill. - May, 1977 pp 79-81

B.29. CATLIN, J. B.

Another look at time wave form analysis ----------

B.30. UNGAR, E.

Analysis of vibration distributions in complex structures. Shock and Vibration Bulletin No. 36 Pt V - January, 1967 pp 41-52

B.31. KESSLER, M.

Noise data recording and computer controlled analysis. Sound and Vibration 7.4 - April, 1973 pp 43-45

B.32. KELLER, A.

Real time spectrum analysis of machinery dynamics.
Sound and Vibration 9.4 April, 1975 pp 40-48

B.33. RAMSEY, K.

Effective measurements for structural dynamic testing.
Pt I - Sound & Vibration 9.11 - Nov. 1975 pp 24-35
Pt II - Sound & Vibration 10.4 - April, 1976
pp 18-31

B.34. SMITH, T.C. CUSAK, P.L.

Determination of vibration mode shapes for large machinery using cross power spectral analysis techniques.
Conf. on Machinery Noise & Vibration Adelaide 1978
pp 48-52
The National Committee on Applied Mechanics of the Institution of Engineers, Australia and the South Australian Division of the Australian Acoustical Society.

B.35. PULLEN, C.

The development of digital techniques for the statistical analysis of random information.
Shock and Vibration Bulletin No. 33 Pt II
March, 1964 pp 286-290

B.36. HAWKES, P.

Response of a single degree of freedom system to exponential sweep rates.
Shock and Vibration Bulletin No. 33 Pt. II
March, 1964 pp 296-303

B.37. WOODHOUSE, J.

Statistical energy analysis of structural vibration. Applied Acoustics - 14.6 (1981) pp 455-469

B.38. OSGOOD, C.

Analysis of random responses for calculation of fatigue damage.
Shock and Vibration Bulletin No. 36 Pt. V
January, 1967 pp 1-8

B.39. KACENA, W. JONES P.

Fatigue prediction for structures subjected to random vibration.
Shock and Vibration Bulletin 46 (3) 1976
pp 87-96

B.40. LEIS, B. BROCK, D.

The roll of similtude in fatigue and fatigue crack growth analysis.
Wear, 54 (1979) pp 321-330

B.41. HILLS, D. ASHELBY, D.

On the application of fracture mechanics to wear.
Wear, 54.2 - June, 1979 pp 321-330

B.42. FORELIFER, W.

The effects of filter bandwidth in spectrum analysis of random vibration. Shock and Vibration Bulletin No. 33 Pt. II - March, 1964 pp 273-278

B.43. SWEENEY G.

Vibration of Machine Tools.
McGraw Hill 1961.

B.44. HARRIS AND CREDE

Shock and Vibration Handbook 2nd edition.
McGraw Hill 1976

B.45. BROCH, J.T.

Mechanical Vibration and Shock Measurements
Bruel & Kjaer publication 1980.

B.46.

Frequency Analysis and Power Spectral Density Measurements.
Bruel and Kjaer publication 1972.

B.47. MCFARLANE, G.

On-Condition Maintenance in the Run.
Australian Corrosion Engineering - March, 1982
pp 9-15

APPENDIX I

AMPLITUDE SPECTRAL DENSITY PLOTS

IDENTICAL SCALING FOR ALL GRAPHS

(NO CORRECTIONS APPLIED FOR ACCELEROMETER RESPONSE)

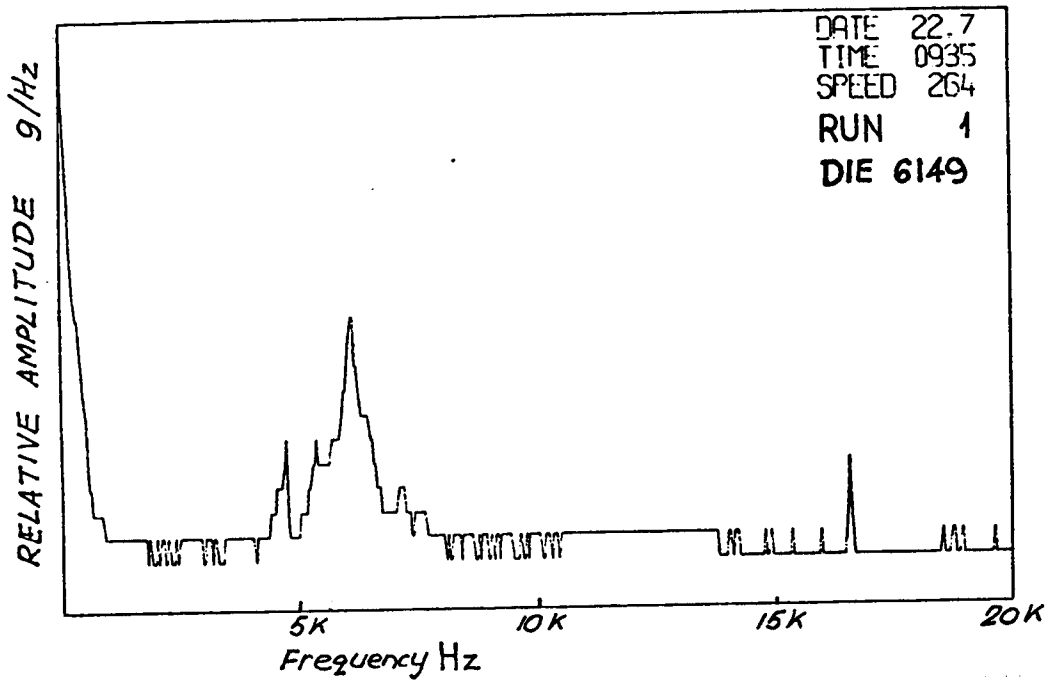
DATE 22.7
TIME 0935
SPEED 264
RUN 1
DIE 6149
RELATIVE AMPLITUDE g/Hz
5K
10K
15K
20K
Frequency Hz

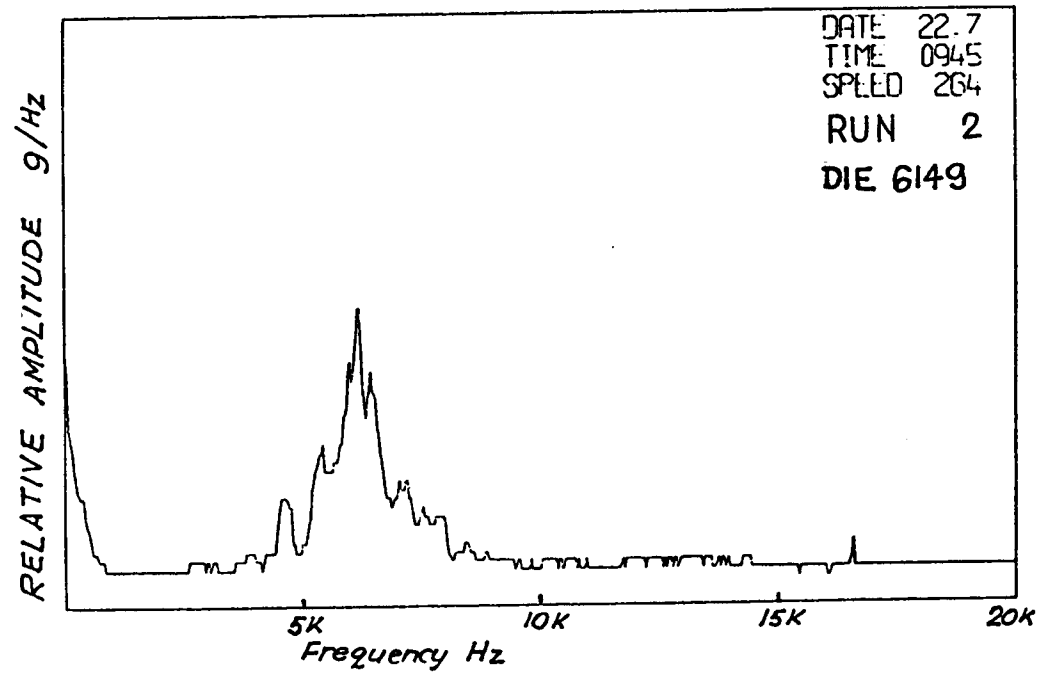
DATE 22.7
TIME 0945
SPEED 264
RUN 2
DIE 6149
RELATIVE AMPLITUDE g/Hz
5K
10K
15K
20K
Frequency Hz

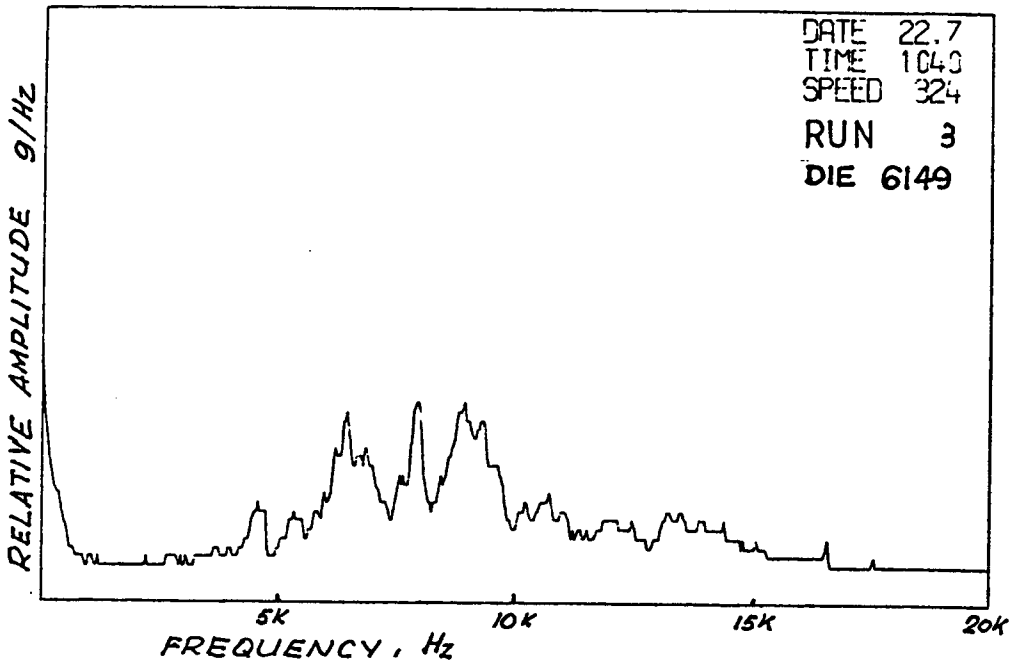
DATE 22.7
TIME 1040
SPEED 324
RUN 3
DIE 6149
RELATIVE AMPLITUDE g/Hz
5K
10K
15K
20K
FREQUENCY, Hz

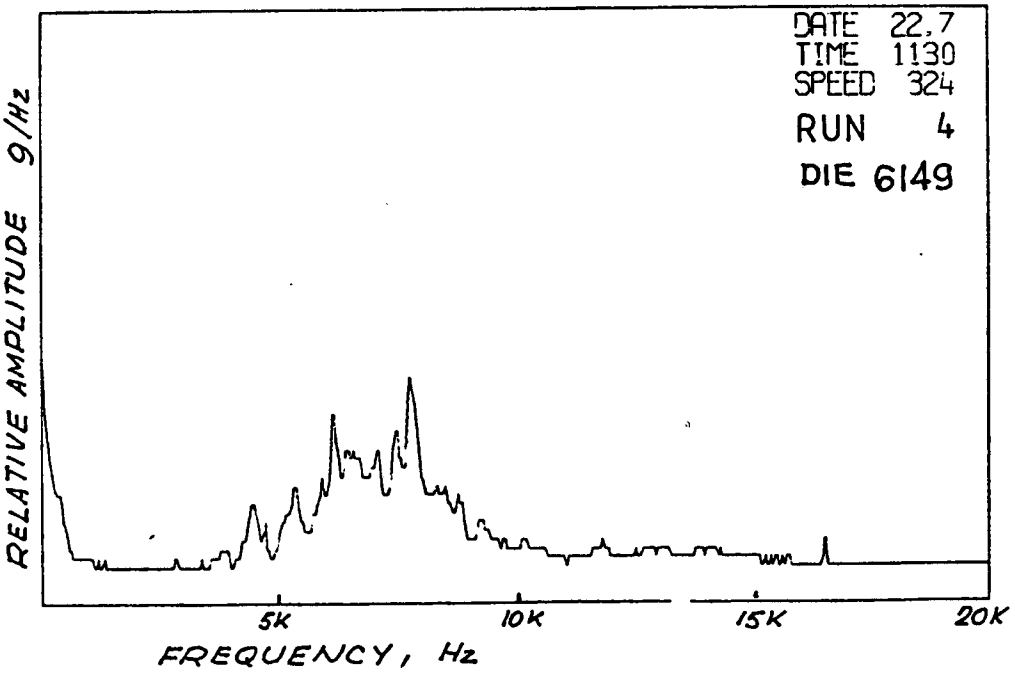
DATE 22.7
TIME 1130
SPEED 324
RUN 4
DIE 6149
RELATIVE AMPLITUDE g/Hz
5K
10K
15K
20K
FREQUENCY, Hz

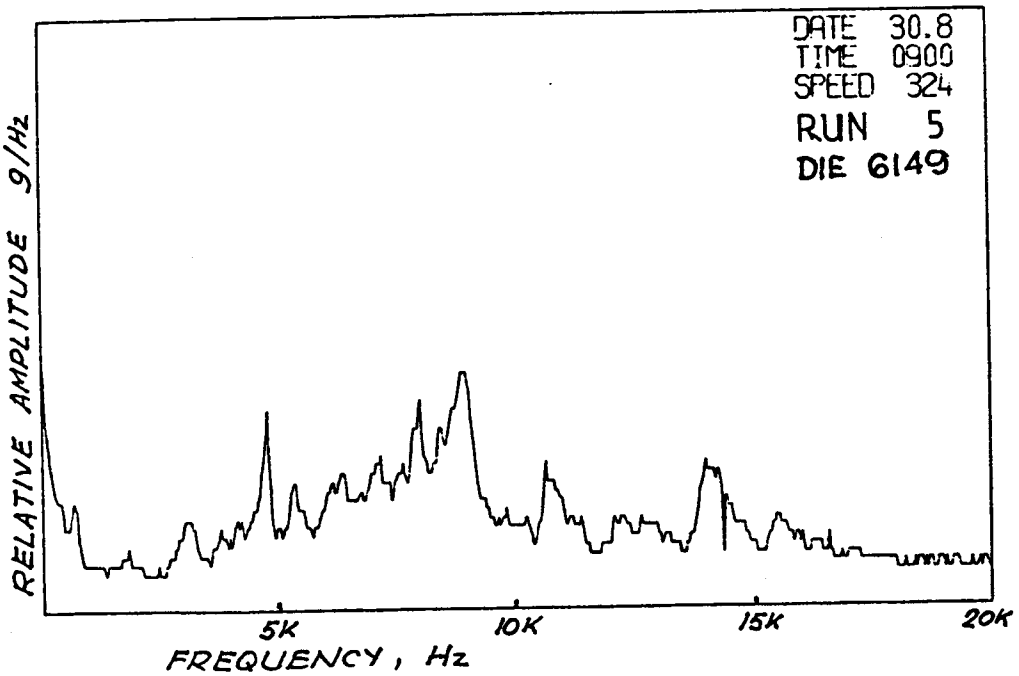
DATE 30.8
TIME 0900
SPEED 324
RUN 5
DIE 6149
RELATIVE AMPLITUDE 9/Hz
5K
10K
15K
20K
FREQUENCY, Hz

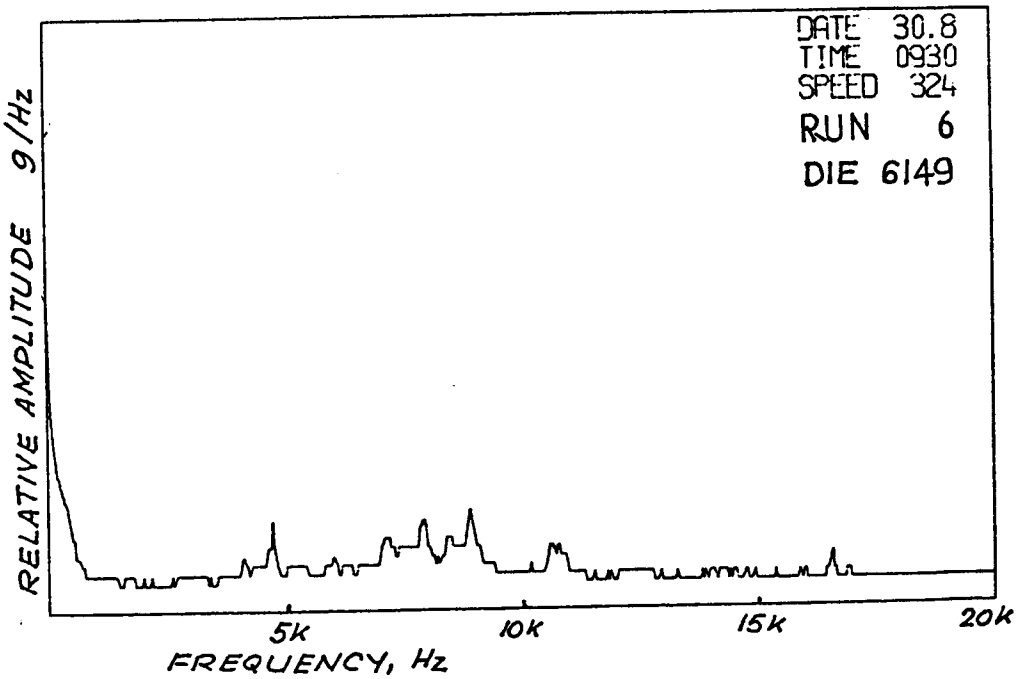
DATE 30.8
TIME 0930
SPEED 324
RUN 6
DIE 6149
RELATIVE AMPLITUDE 9/Hz
5K
10K
15K
20K
FREQUENCY, Hz

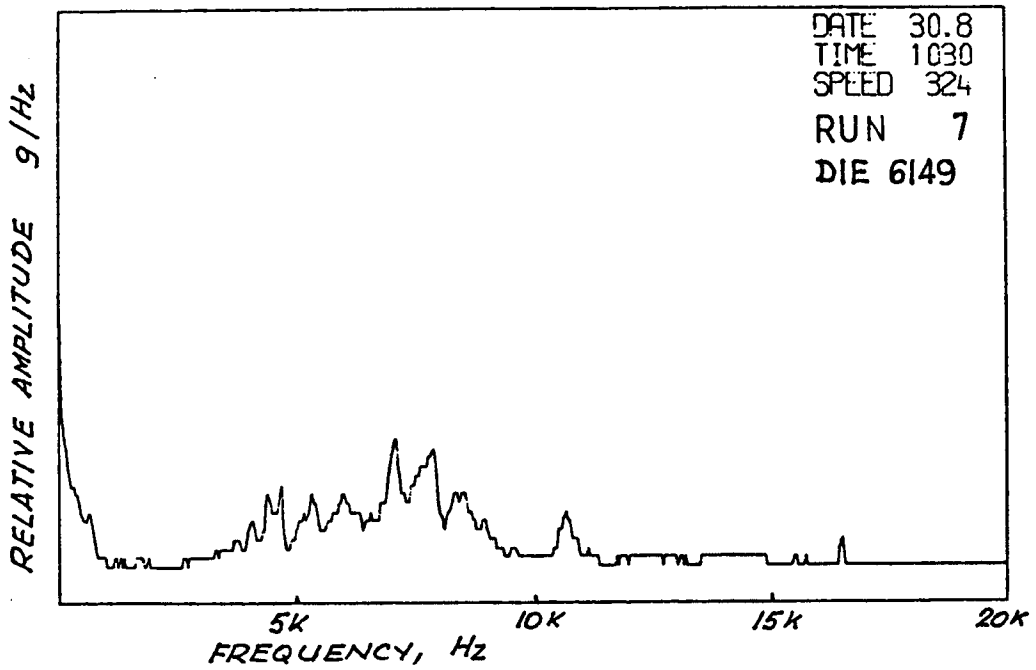
DATE 30.8
TIME 1030
SPEED 324
RUN 7
DIE 6149
RELATIVE AMPLITUDE g/Hz
5K
10K
15K
20K
FREQUENCY, Hz

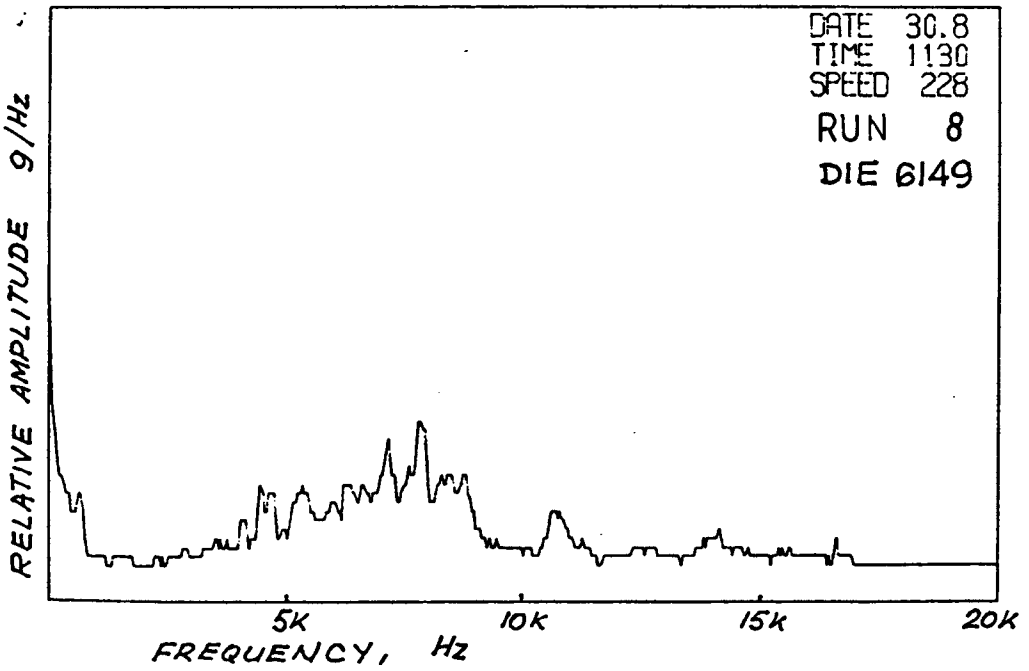
DATE 30.8
TIME 1130
SPEED 228
RUN 8
DIE 6149
RELATIVE AMPLITUDE g/Hz
5K
10K
15K
20K
FREQUENCY, Hz

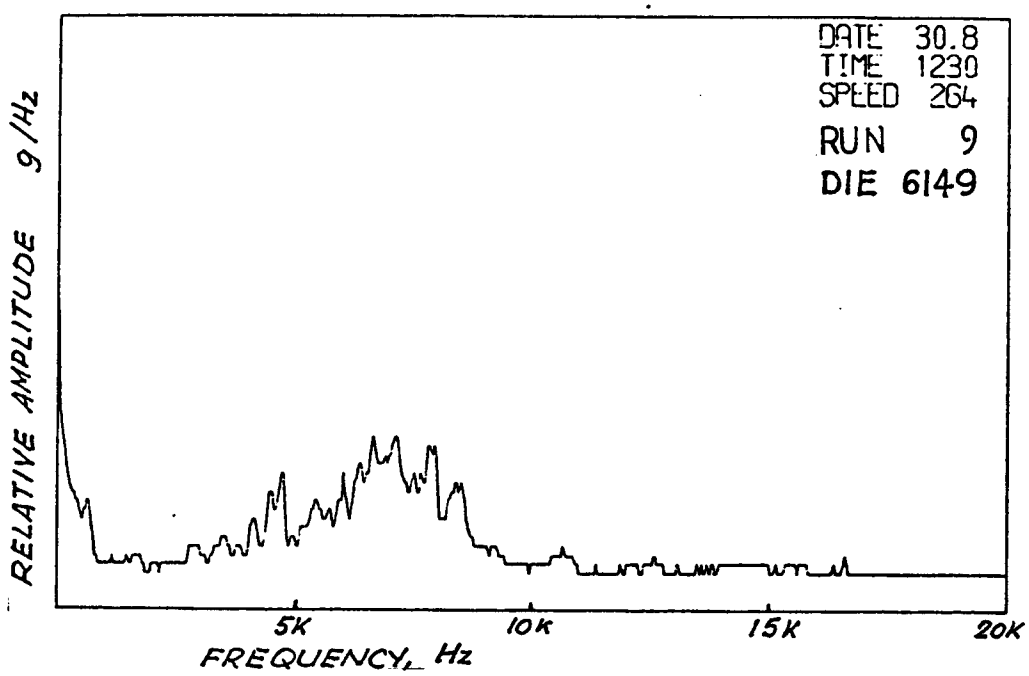
DATE 30.8
TIME 1230
SPEED 264
RUN 9
DIE 6149
RELATIVE AMPLITUDE g/Hz
5K
10K
15K
20K
FREQUENCY, Hz

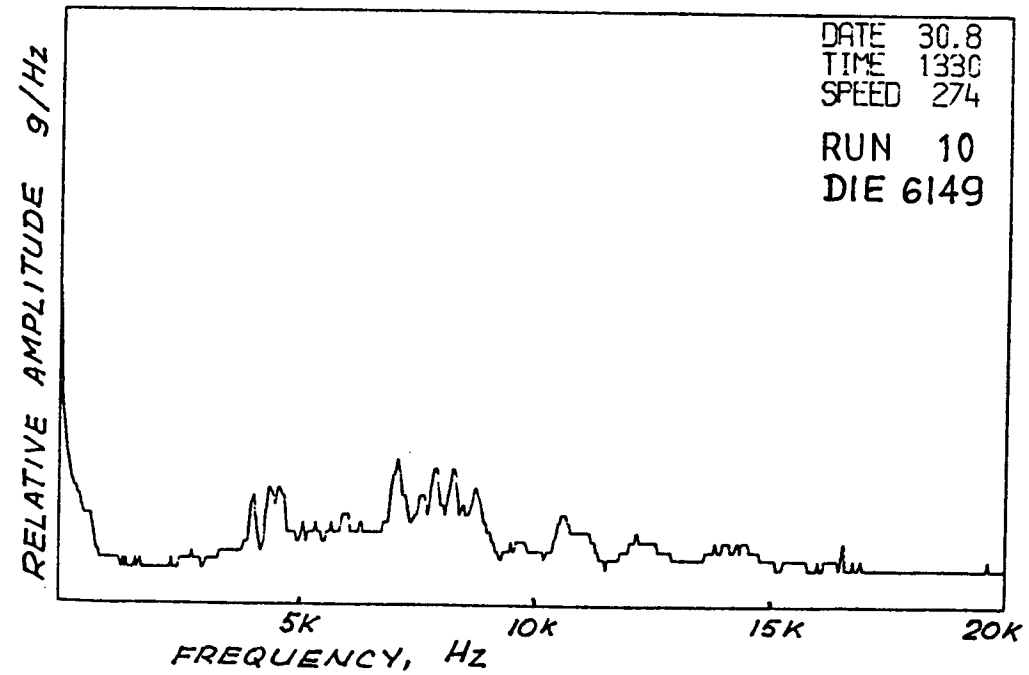
DATE 30.8
TIME 1330
SPEED 274
RUN 10
DIE 6149
RELATIVE AMPLITUDE g/Hz
5K
10K
15K
20K
FREQUENCY, Hz

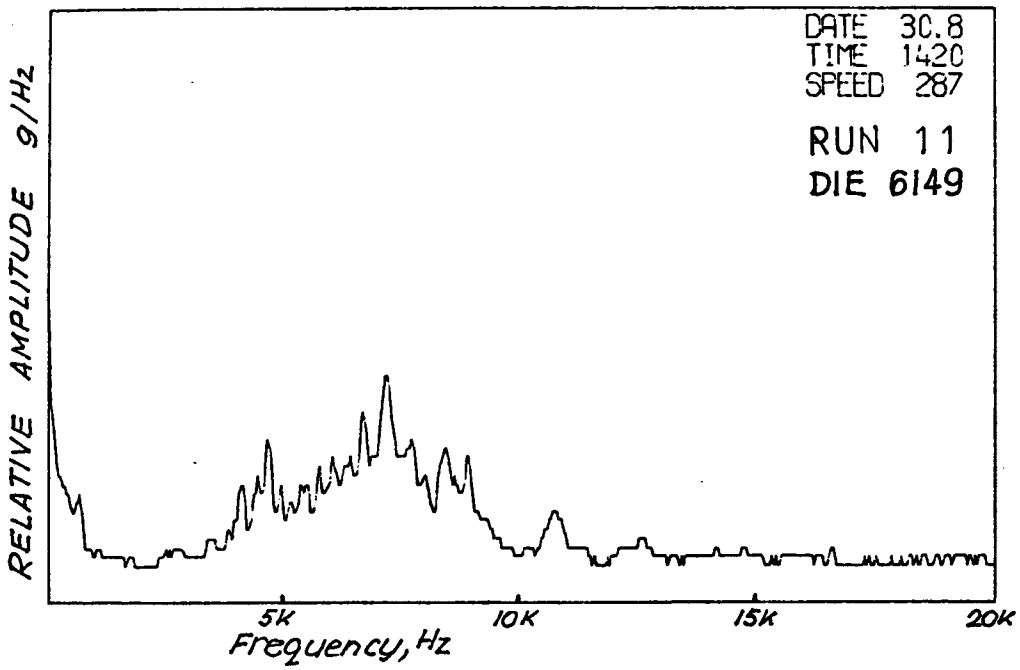
DATE 30.8
TIME 1420
SPEED 287
RUN 11
DIE 6149
RELATIVE AMPLITUDE g/Hz
5K
10K
15K
20K
Frequency, Hz

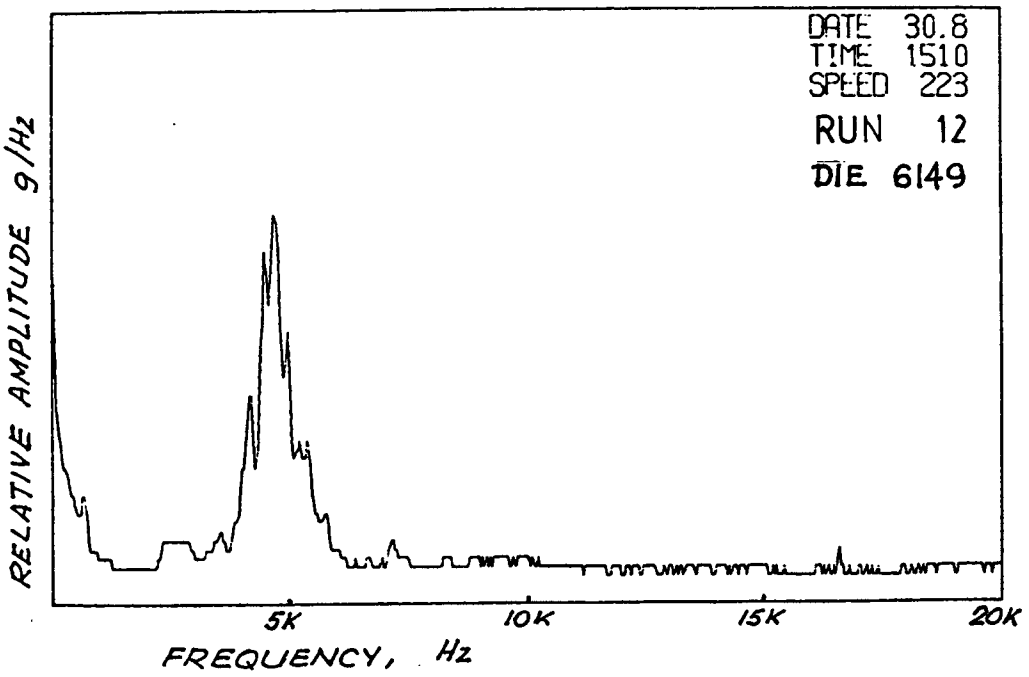
DATE 30.8
TIME 1510
SPEED 223
RUN 12
DIE 6149
RELATIVE AMPLITUDE g/Hz
5K
10K
15K
20K
FREQUENCY, Hz

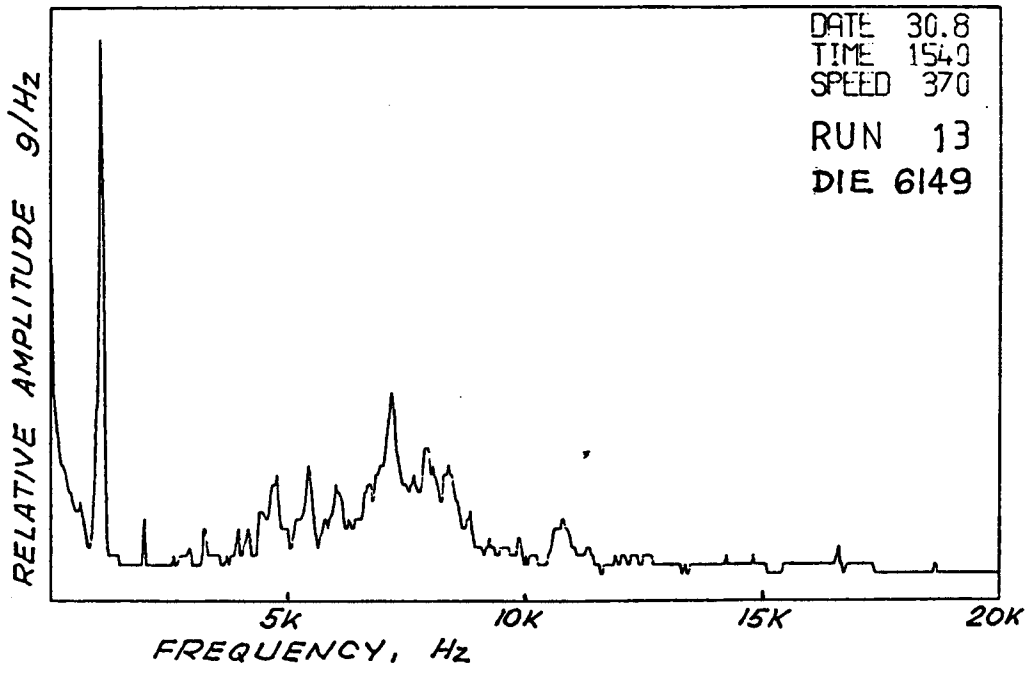
DATE 30.8
TIME 1549
SPEED 370
RUN 13
DIE 6149
RELATIVE AMPLITUDE g/Hz
5K
10K
15K
20K
FREQUENCY, Hz

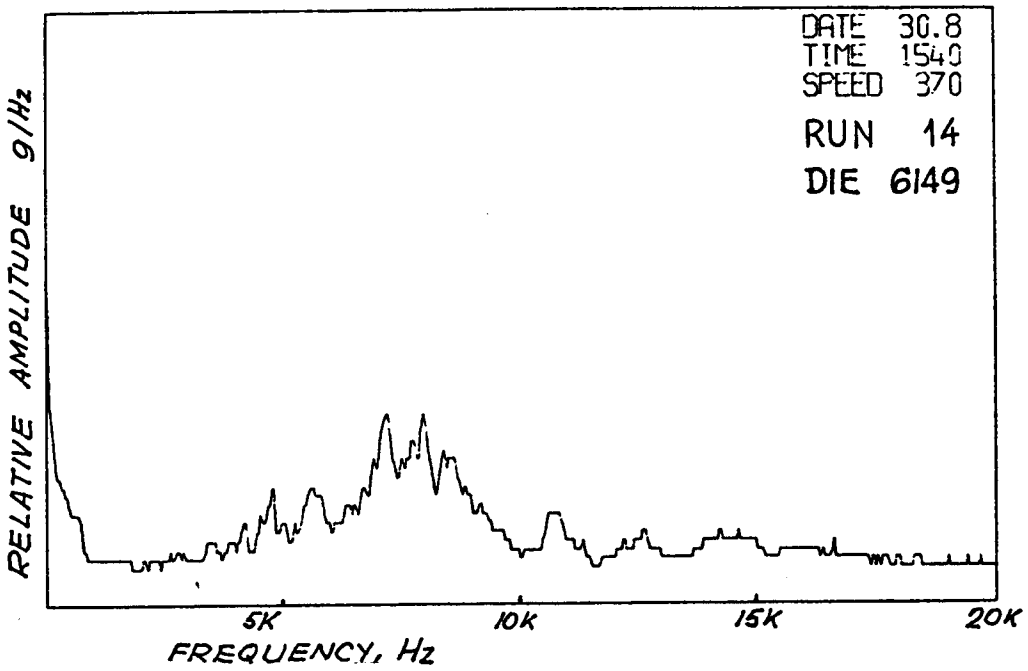
DATE 30.8
TIME 1540
SPEED 370
RUN 14
DIE 6149
RELATIVE AMPLITUDE g/Hz
5K
10K
15K
20K
FREQUENCY, Hz

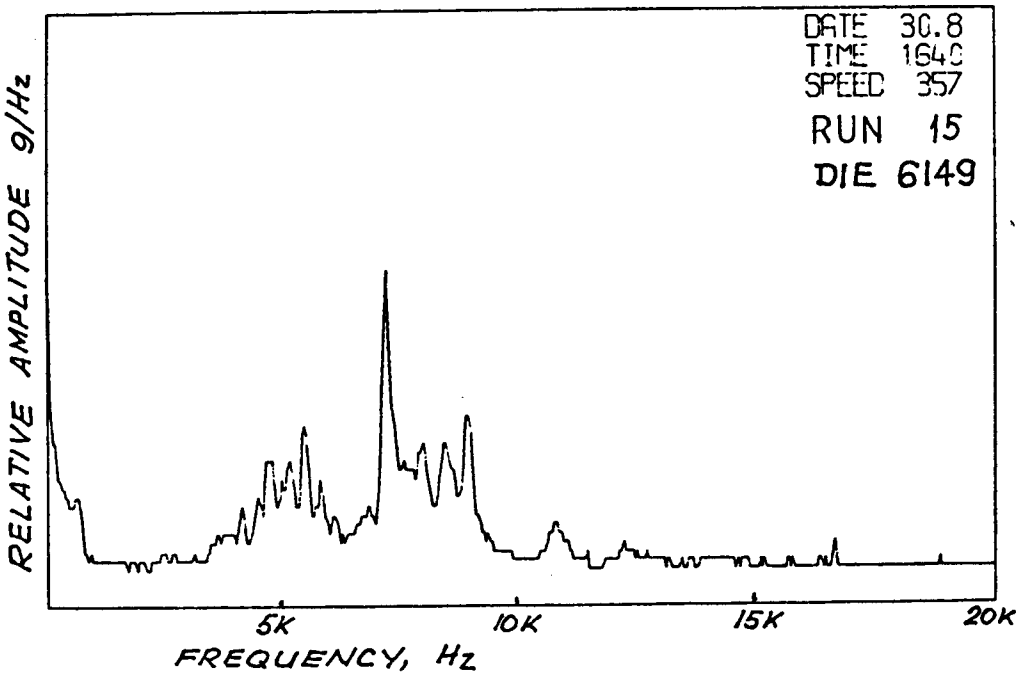
DATE 30.8
TIME 1640
SPEED 357
RUN 15
DIE 6149
RELATIVE AMPLITUDE g/Hz
5K
10K
15K
20K
FREQUENCY, Hz

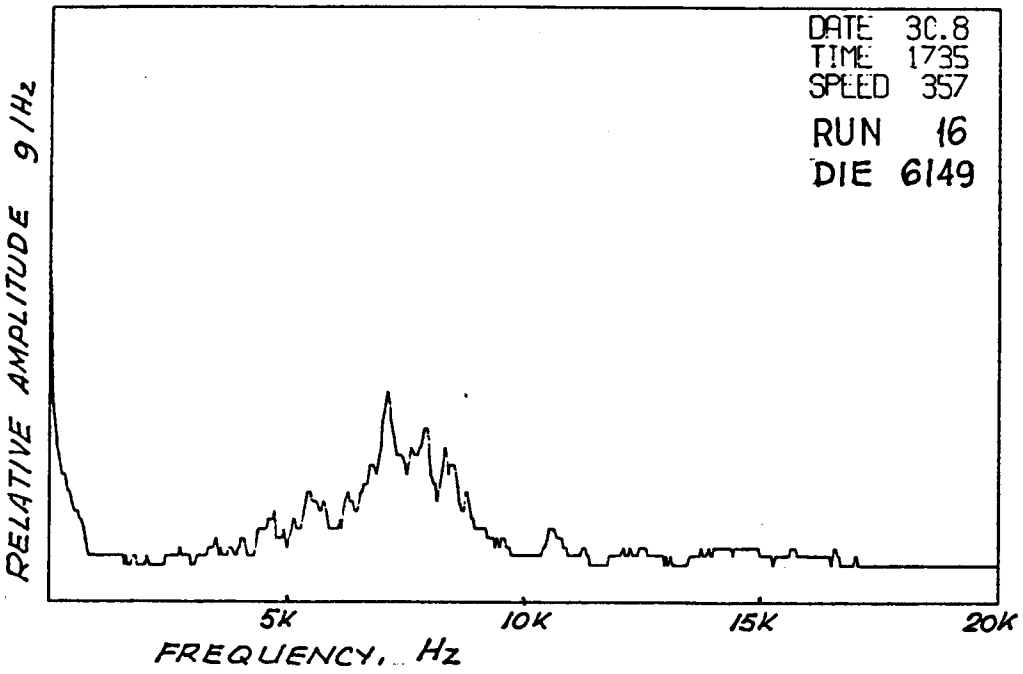
DATE 30.8
TIME 1735
SPEED 357
RUN 16
DIE 6149
RELATIVE AMPLITUDE g/Hz
5K
10K
15K
20K
FREQUENCY, Hz

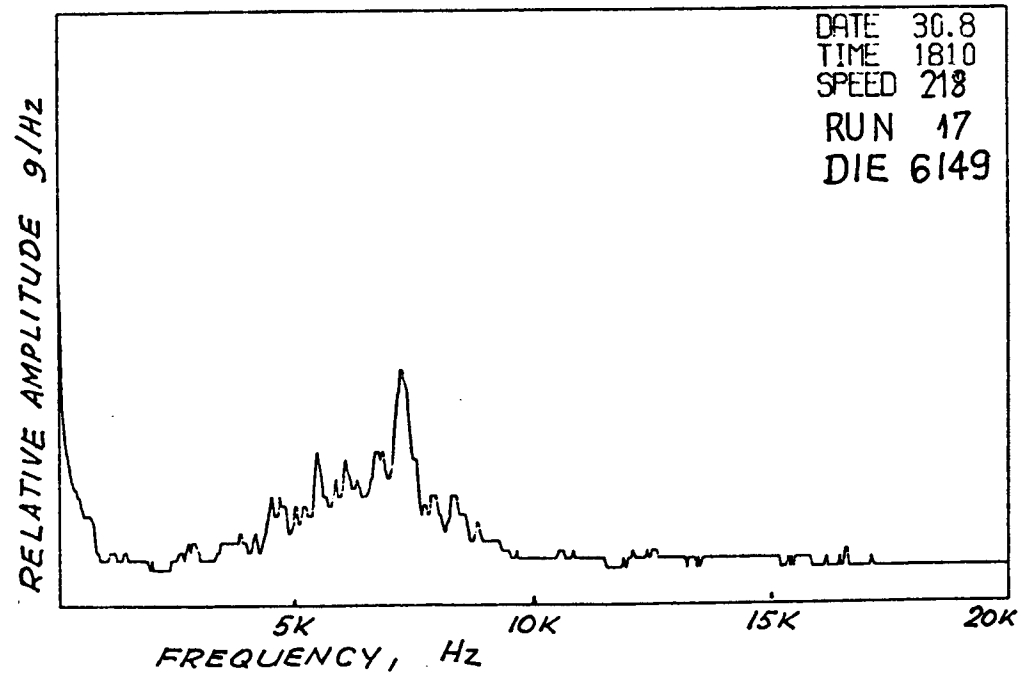
DATE 30.8
TIME 1810
SPEED 218
RUN 17
DIE 6149
RELATIVE AMPLITUDE g/Hz
5K
10K
15K
20K
FREQUENCY, Hz

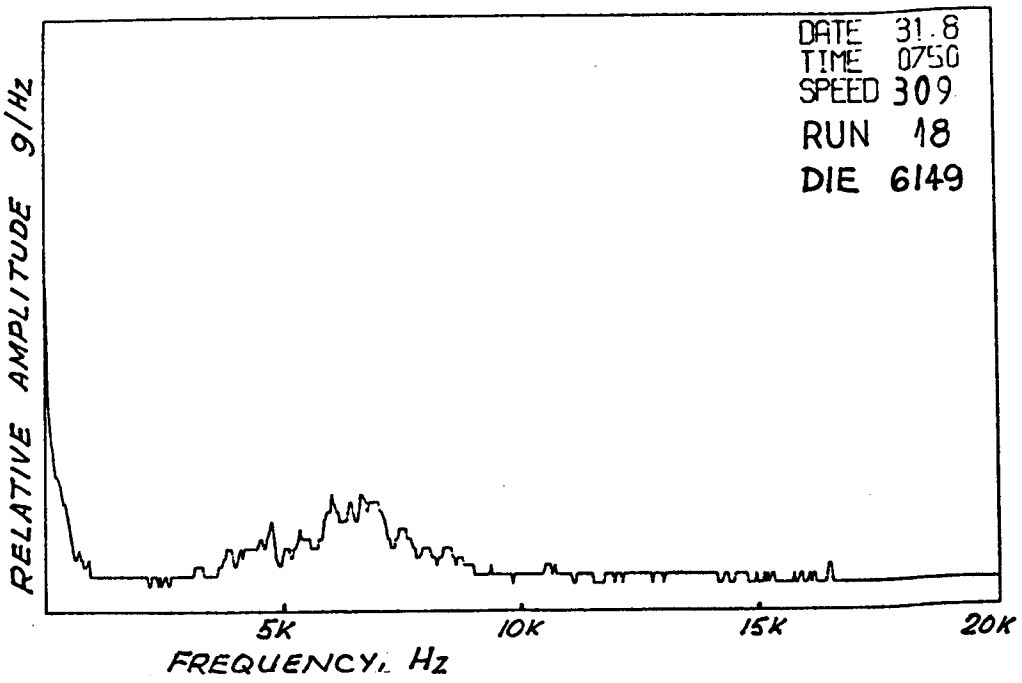
DATE 31.8
TIME 0750
SPEED 309
RUN 18
DIE 6149
RELATIVE AMPLITUDE g/Hz
5K
10K
15K
20K
FREQUENCY, Hz

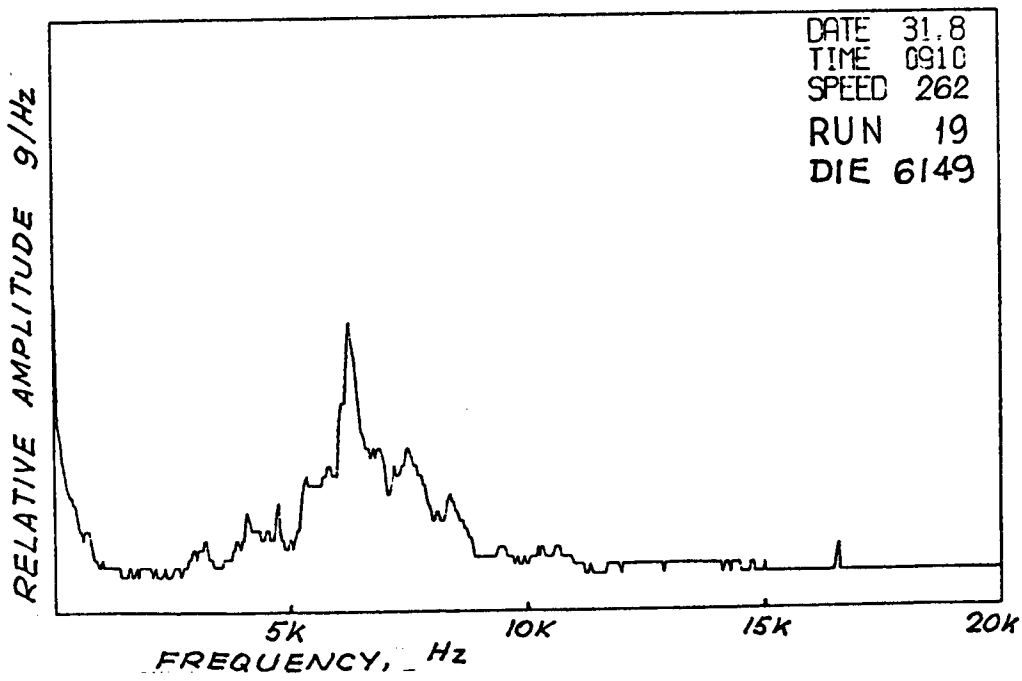
DATE 31.8
TIME 0910
SPEED 262
RUN 19
DIE 6149
RELATIVE AMPLITUDE g/Hz
5K
10K
15K
20K
FREQUENCY, Hz

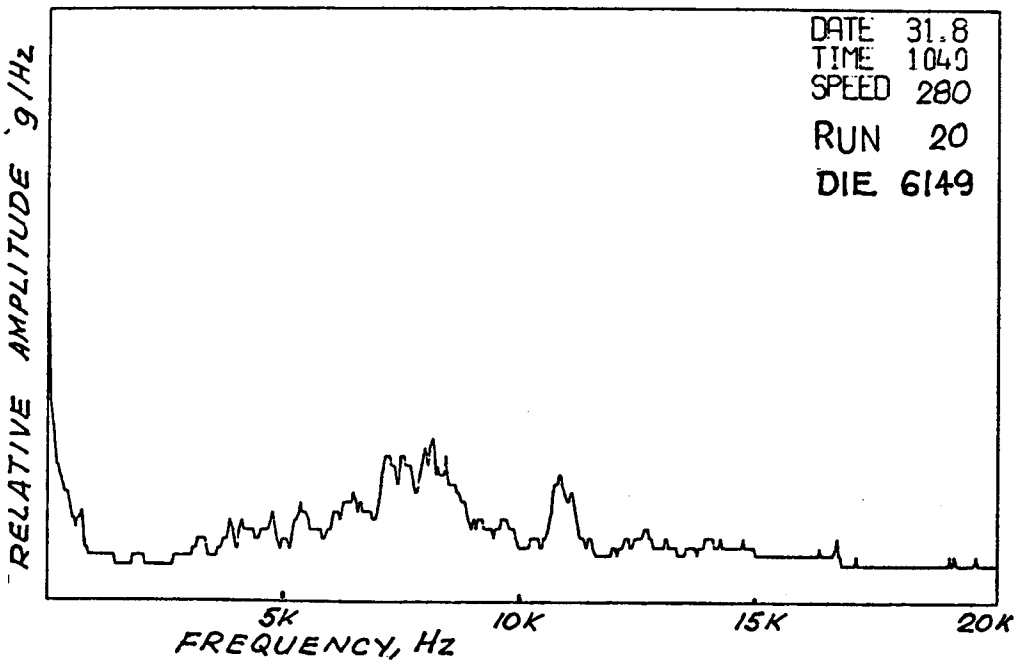
DATE 31.8
TIME 1040
SPEED 280
RUN 20
DIE 6149
RELATIVE AMPLITUDE g/Hz
5K
10K
15K
20K
FREQUENCY, Hz

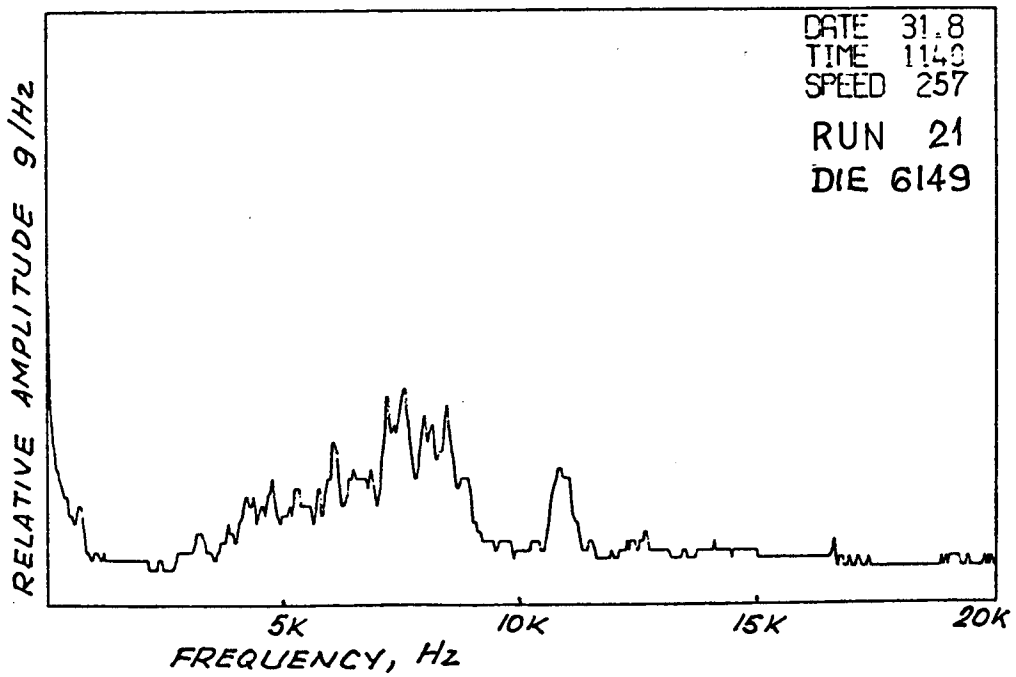
DATE 31.8
TIME 1140
SPEED 257
RUN 21
DIE 6149
RELATIVE AMPLITUDE g/Hz
5K
10K
15K
20K
FREQUENCY, Hz

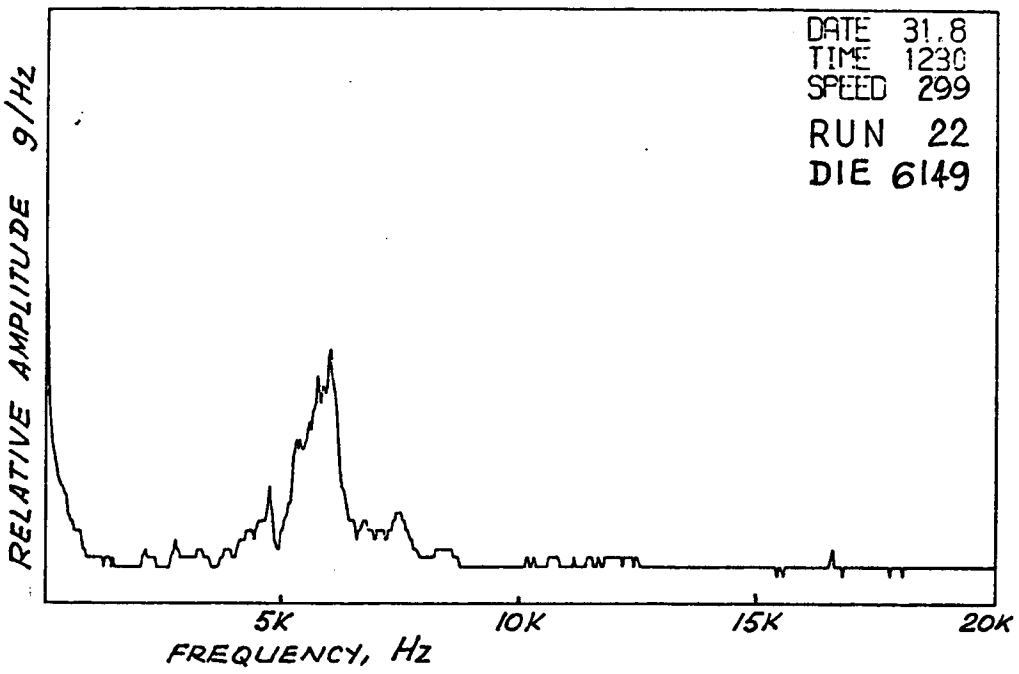
DATE 31.8
TIME 1230
SPEED 299
RUN 22
DIE 6149
RELATIVE AMPLITUDE g/Hz
5K
10K
15K
20K
FREQUENCY, Hz

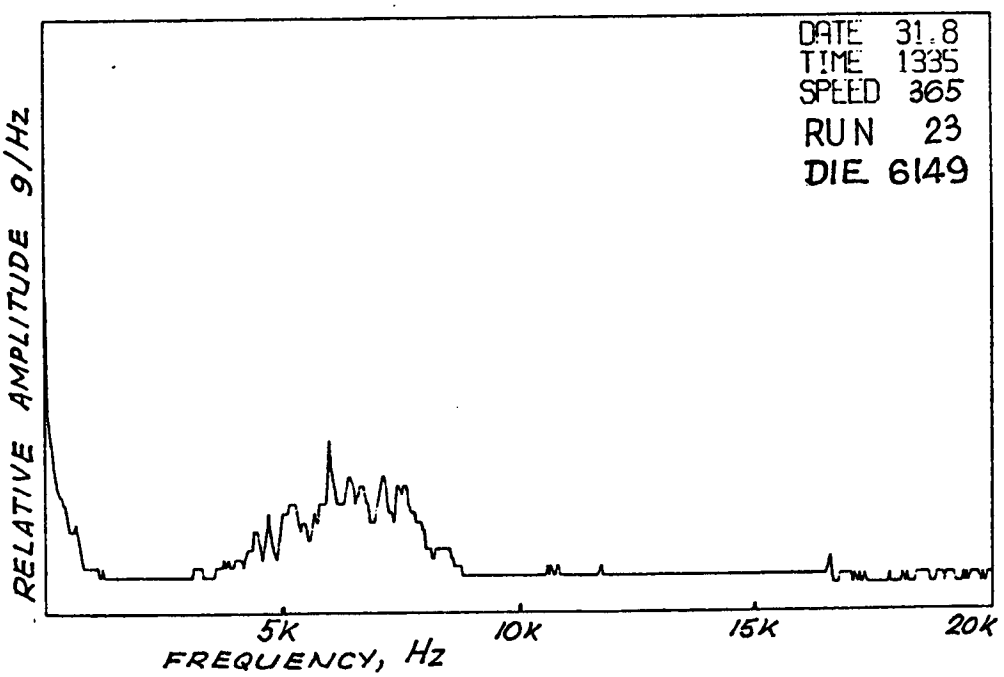
DATE 31.8
TIME 1335
SPEED 365
RUN 23
DIE 6149
RELATIVE AMPLITUDE g/Hz
5K
10K
15K
20K
FREQUENCY, Hz

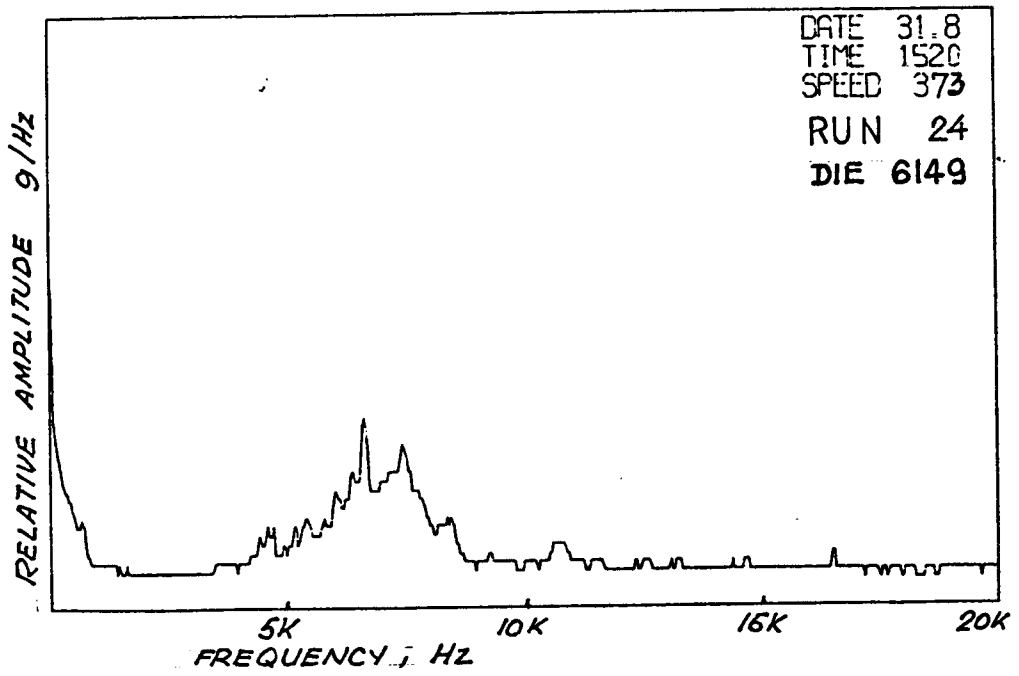
DATE 31.8
TIME 1520
SPEED 373
RUN 24
DIE 6149
RELATIVE AMPLITUDE g/Hz
5K
10K
15K
20K
FREQUENCY, Hz

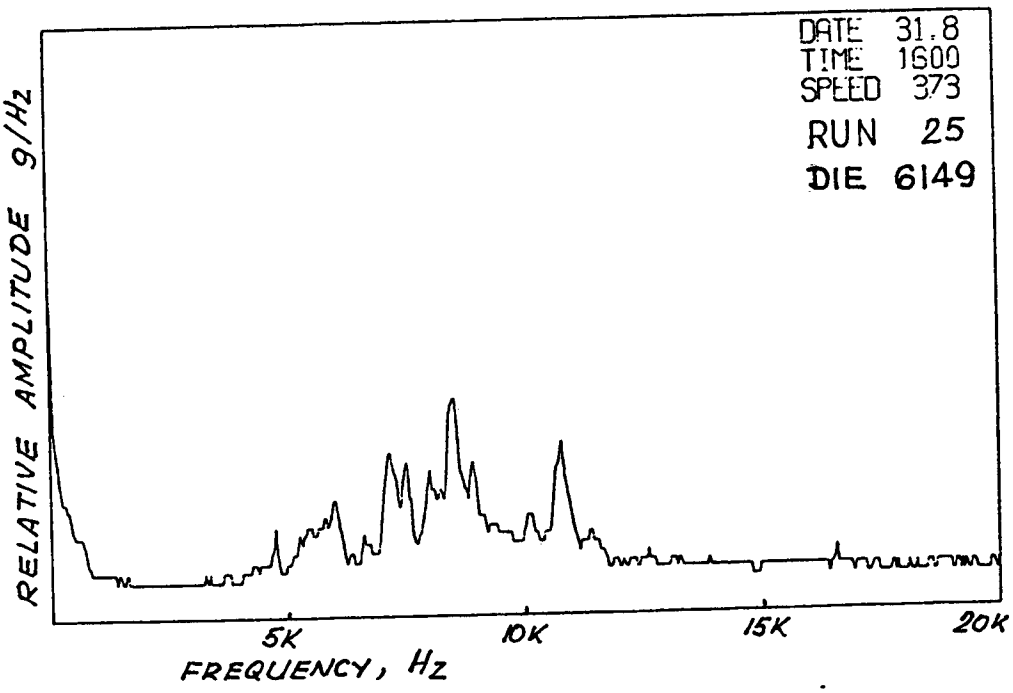
DATE 31.8
TIME 1600
SPEED 373
RUN 25
DIE 6149
RELATIVE AMPLITUDE g/Hz
5K
10K
15K
20K
FREQUENCY, Hz

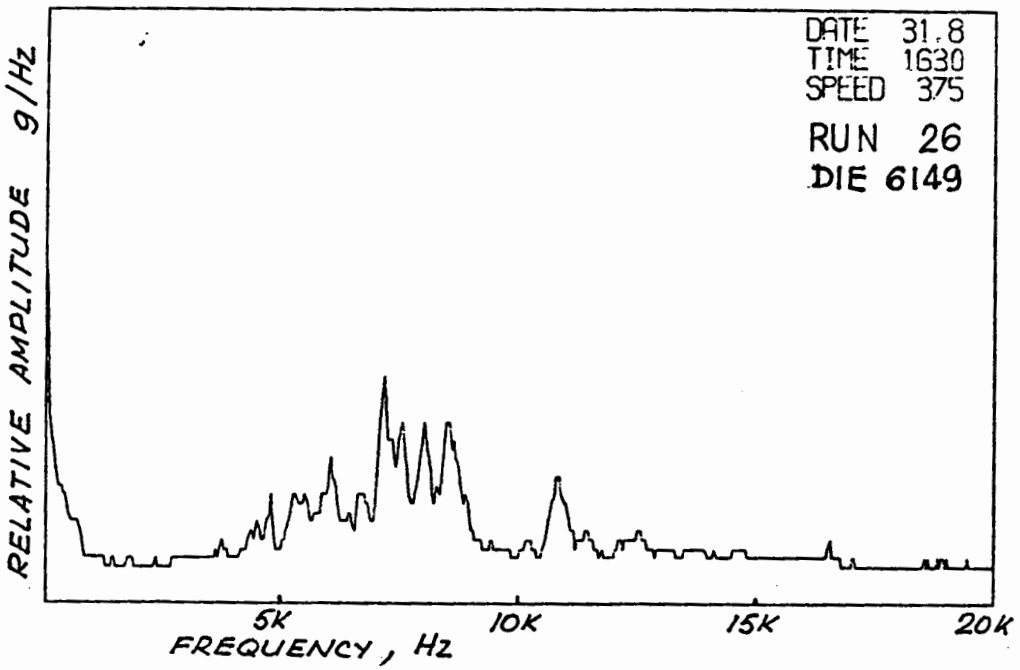
DATE 31.8
TIME 1630
SPEED 375
RUN 26
DIE 6149
RELATIVE AMPLITUDE g/Hz
5K
10K
15K
20K
FREQUENCY, Hz

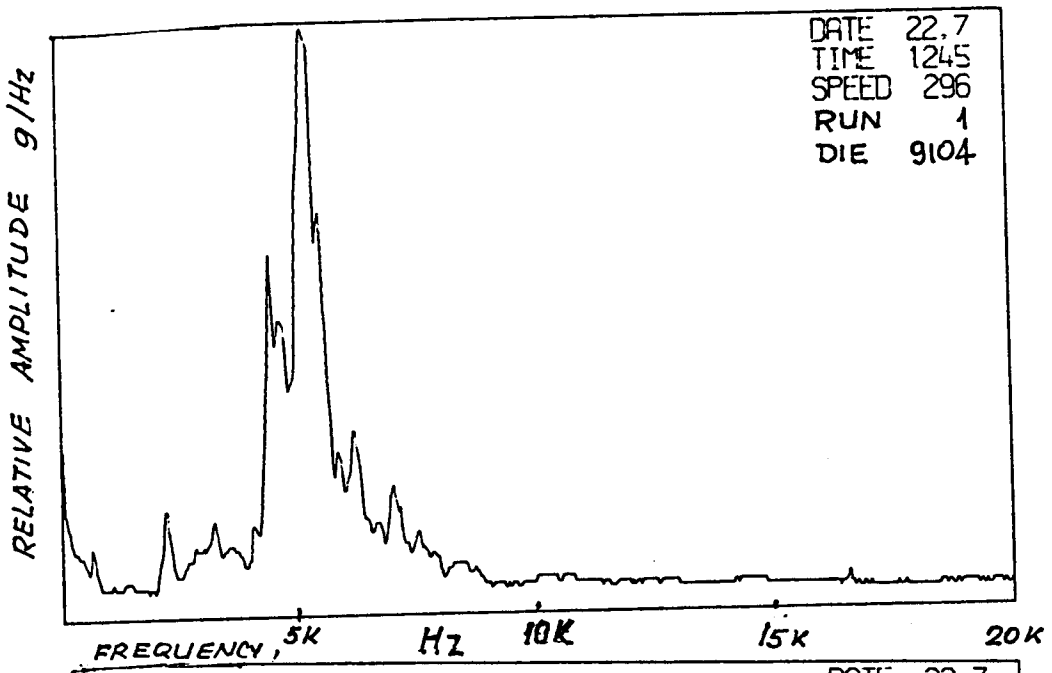
DATE 22.7
TIME 1245
SPEED 296
RUN 1
DIE 9104
RELATIVE AMPLITUDE g/Hz
FREQUENCY, 5K Hz 10K 15K 20K

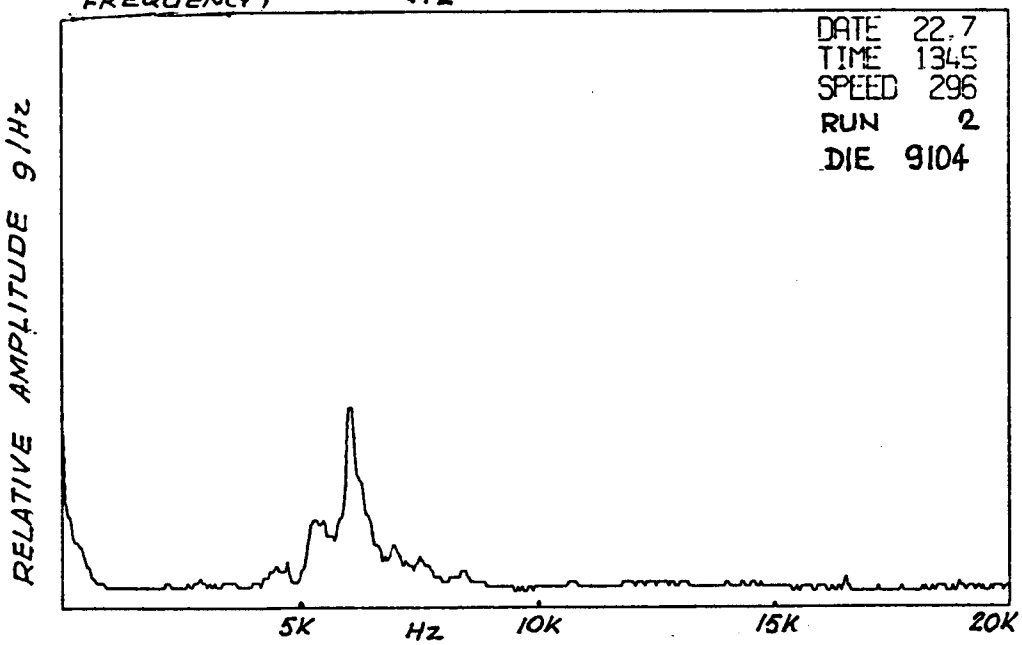
DATE 22.7
TIME 1345
SPEED 296
RUN 2
DIE 9104
RELATIVE AMPLITUDE g/Hz
5K Hz 10K 15K 20K

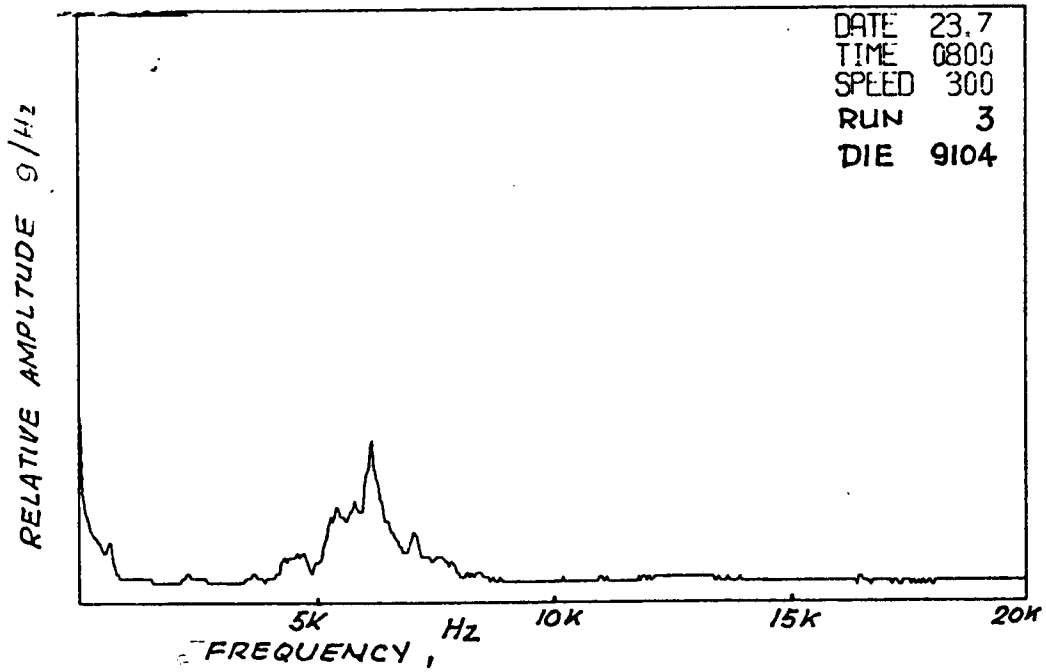
DATE 23.7
TIME 0800
SPEED 300
RUN 3
DIE 9104
RELATIVE AMPLTUDE g/Hz
5K Hz 10K 15K 20K
FREQUENCY,

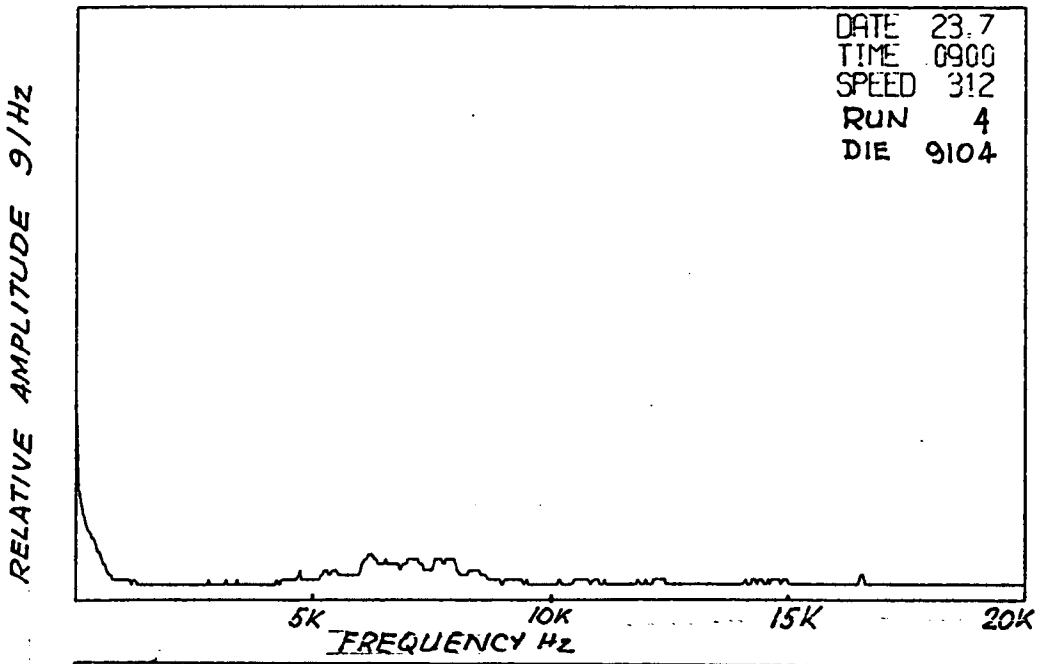
DATE 23.7
TIME 0900
SPEED 312
RUN 4
DIE 9104
RELATIVE AMPLITUDE g/Hz
5K
10K
15K
20K
FREQUENCY Hz

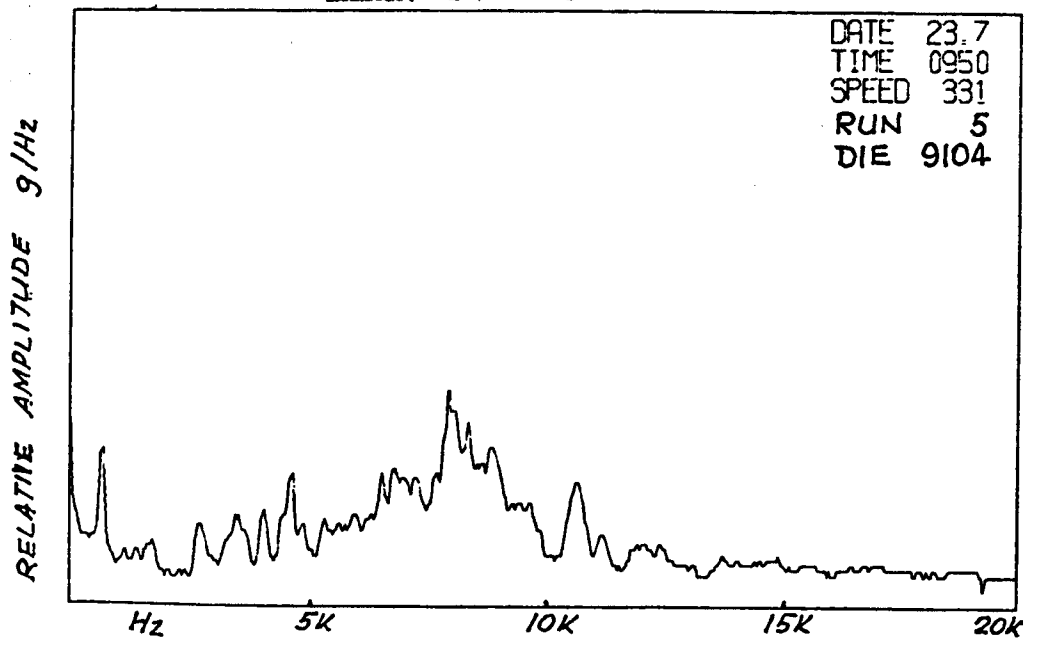
DATE 23.7
TIME 0950
SPEED 331
RUN 5
DIE 9104
RELATIVE AMPLITUDE g/Hz
Hz
5K
10K
15K
20K

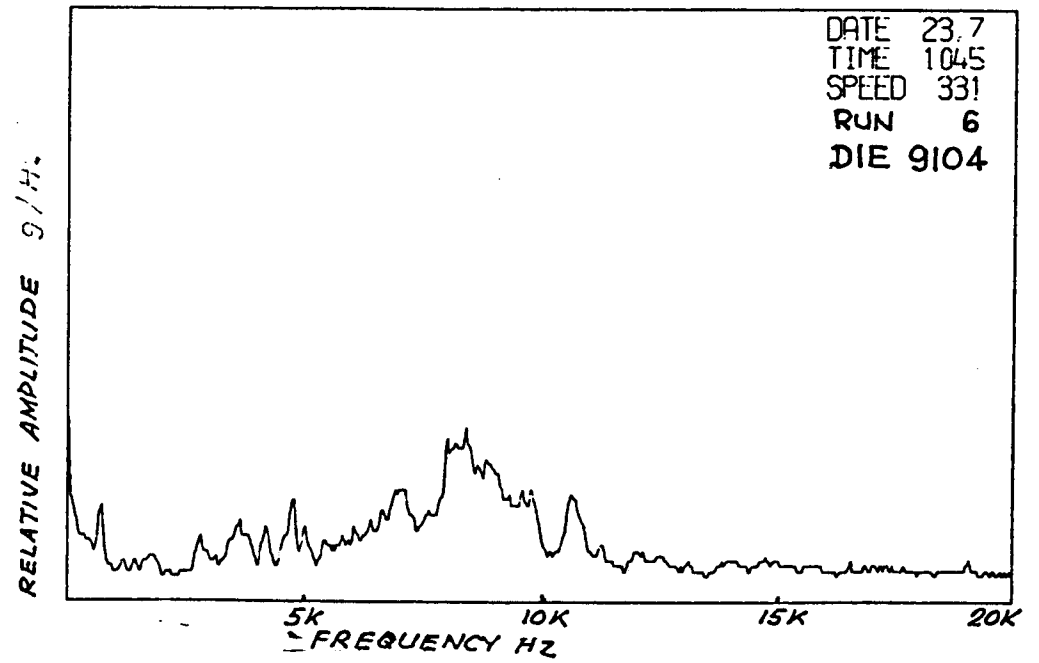
DATE 23.7
TIME 1045
SPEED 331
RUN 6
DIE 9104
RELATIVE AMPLITUDE g/Hz
5K
10K
15K
20K
FREQUENCY Hz

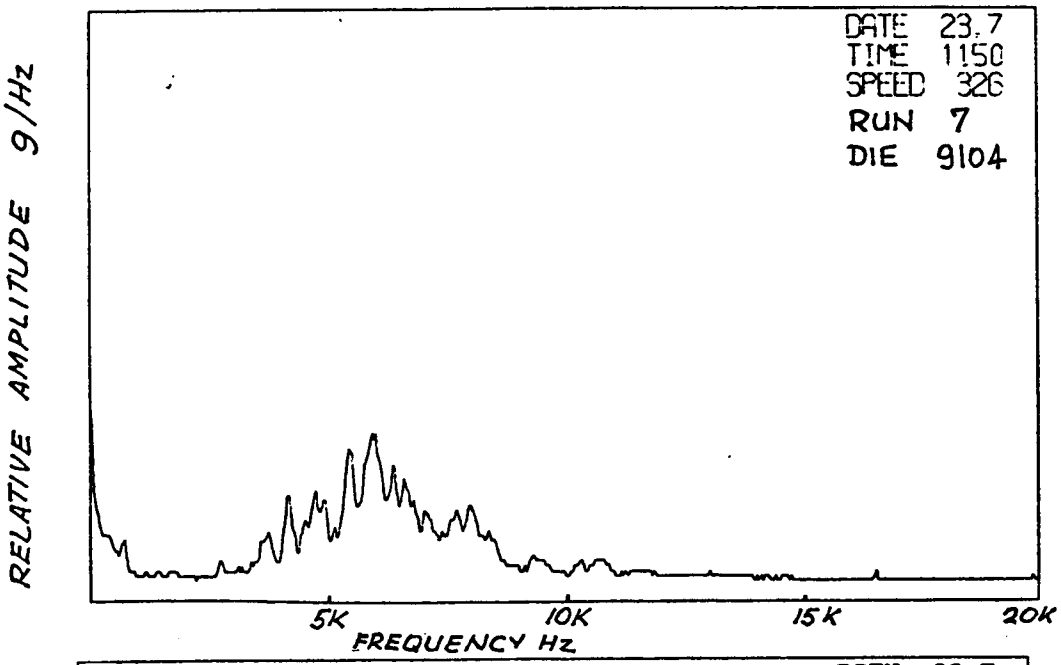
RELATIVE AMPLITUDE g/Hz
DATE 23.7
TIME 1150
SPEED 326
RUN 7
DIE 9104
5K
10K
15K
20K
FREQUENCY Hz

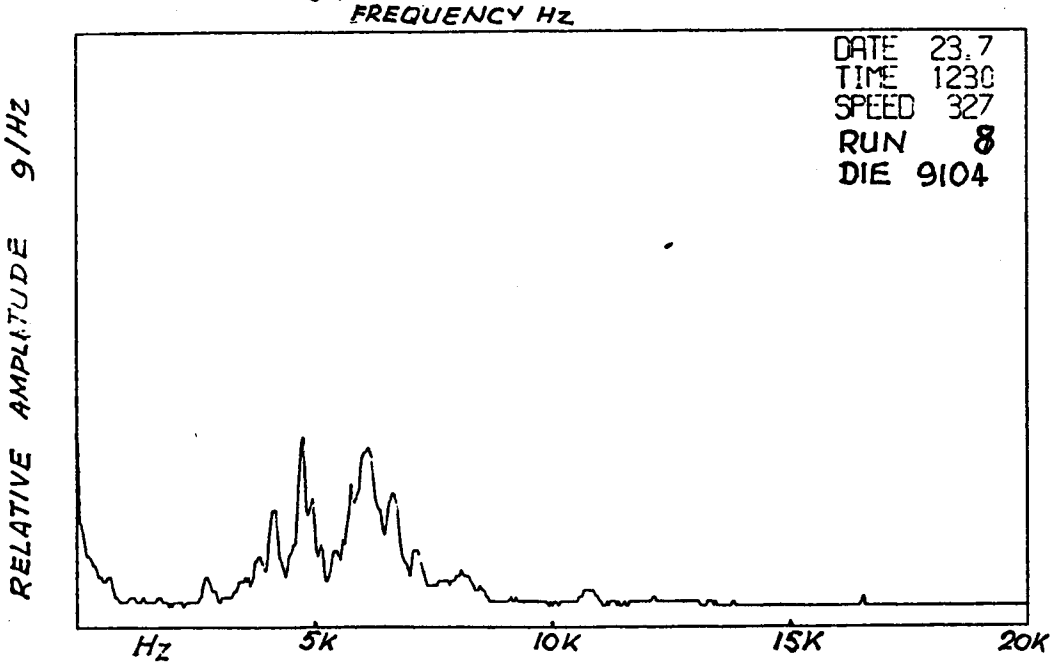
RELATIVE AMPLITUDE g/Hz
DATE 23.7
TIME 1230
SPEED 327
RUN 8
DIE 9104
Hz
5K
10K
15K
20K

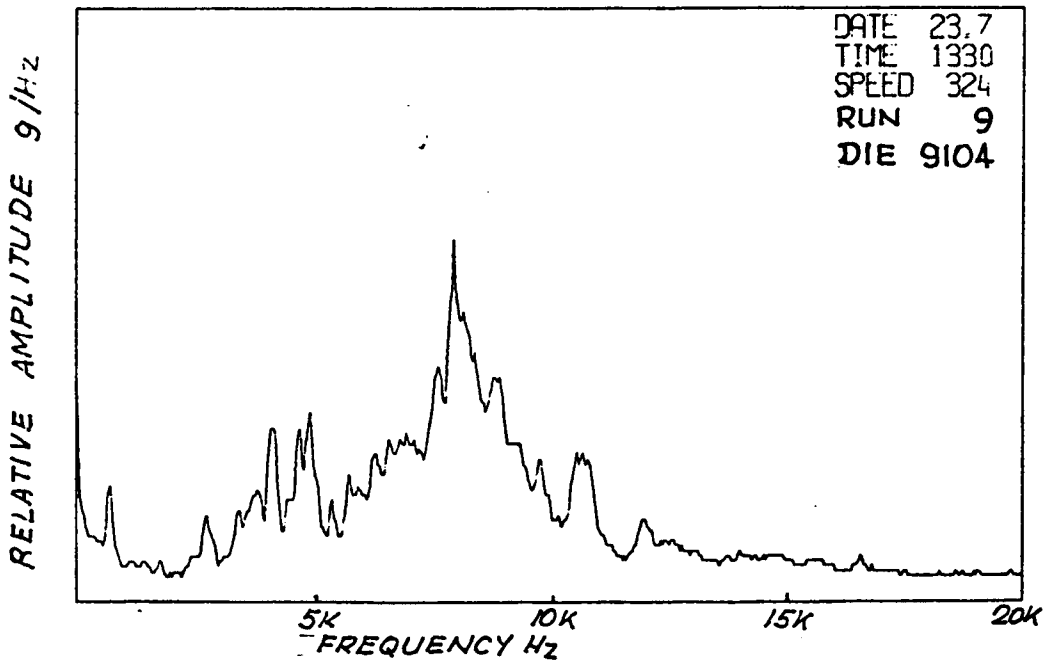
RELATIVE AMPLITUDE g/Hz
DATE 23.7
TIME 1330
SPEED 324
RUN 9
DIE 9104
5K
10K
15K
20K
FREQUENCY Hz

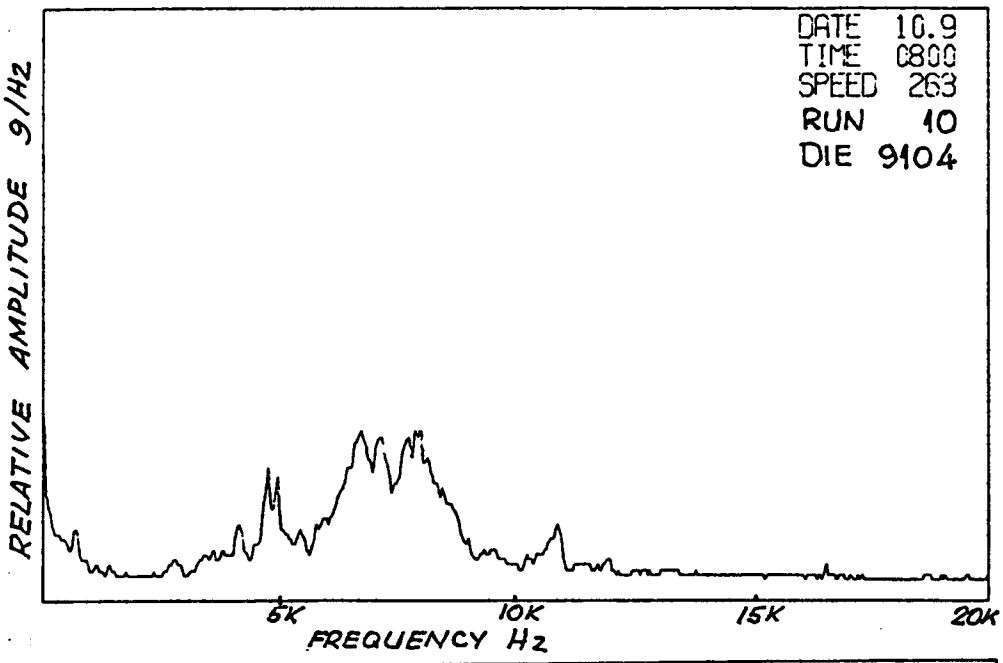
DATE 10.9
TIME 0800
SPEED 263
RUN 10
DIE 9104
RELATIVE AMPLITUDE g/Hz
5K
10K
15K
20K
FREQUENCY Hz

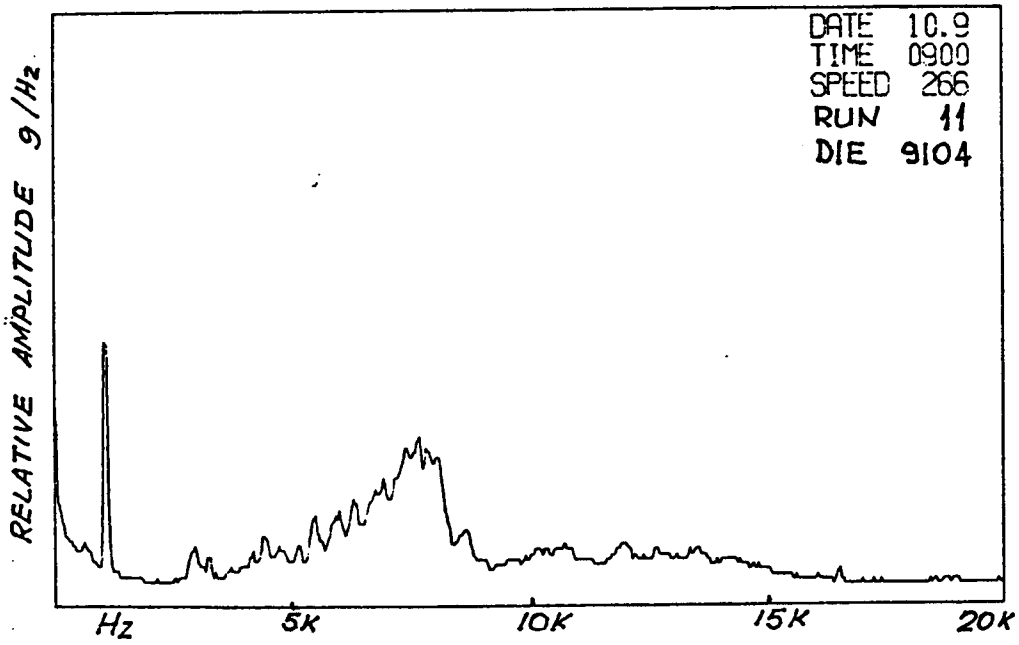
DATE 10.9
TIME 0900
SPEED 266
RUN 11
DIE 9104
RELATIVE AMPLITUDE g/Hz
Hz
5K
10K
15K
20K

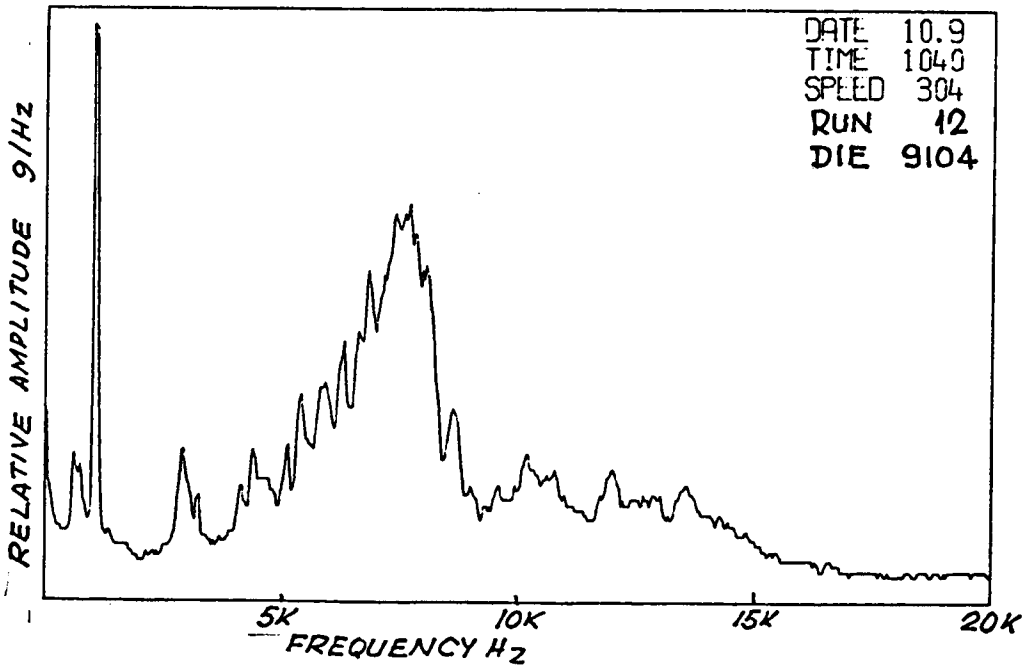
DATE 10.9
TIME 1040
SPEED 304
RUN 12
DIE 9104
RELATIVE AMPLITUDE g/Hz
5K
10K
15K
20K
FREQUENCY Hz

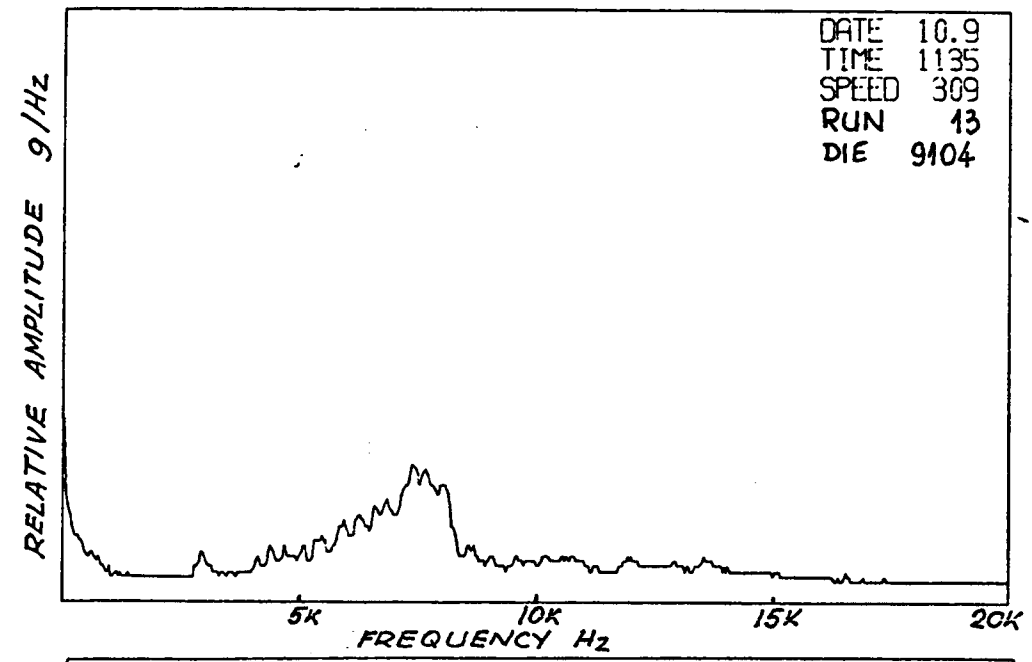
DATE 10.9
TIME 1135
SPEED 309
RUN 13
DIE 9104
RELATIVE AMPLITUDE g/Hz
5K
10K
15K
20K
FREQUENCY Hz

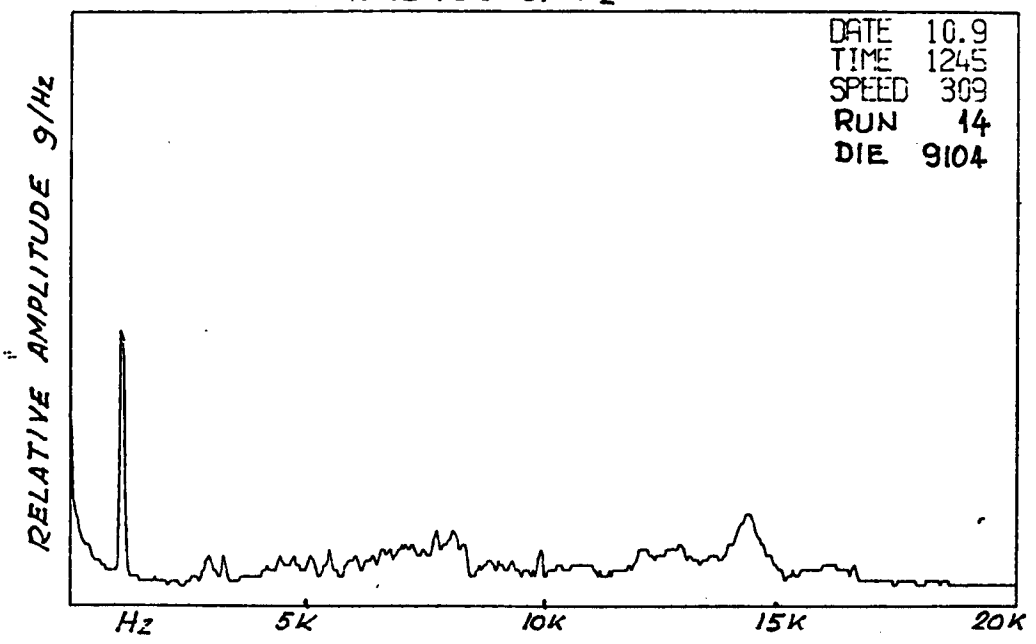
DATE 10.9
TIME 1245
SPEED 309
RUN 14
DIE 9104
RELATIVE AMPLITUDE g/Hz
Hz
5K
10K
15K
20K

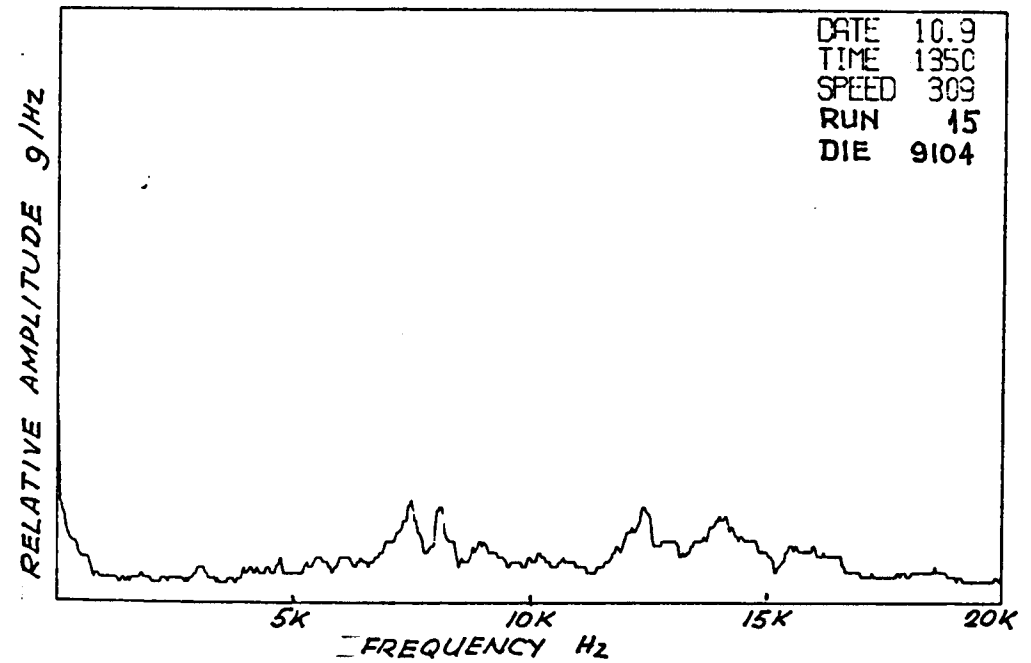
DATE 10.9
TIME 1350
SPEED 309
RUN 15
DIE 9104
RELATIVE AMPLITUDE g/Hz
5K
10K
15K
20K
FREQUENCY Hz

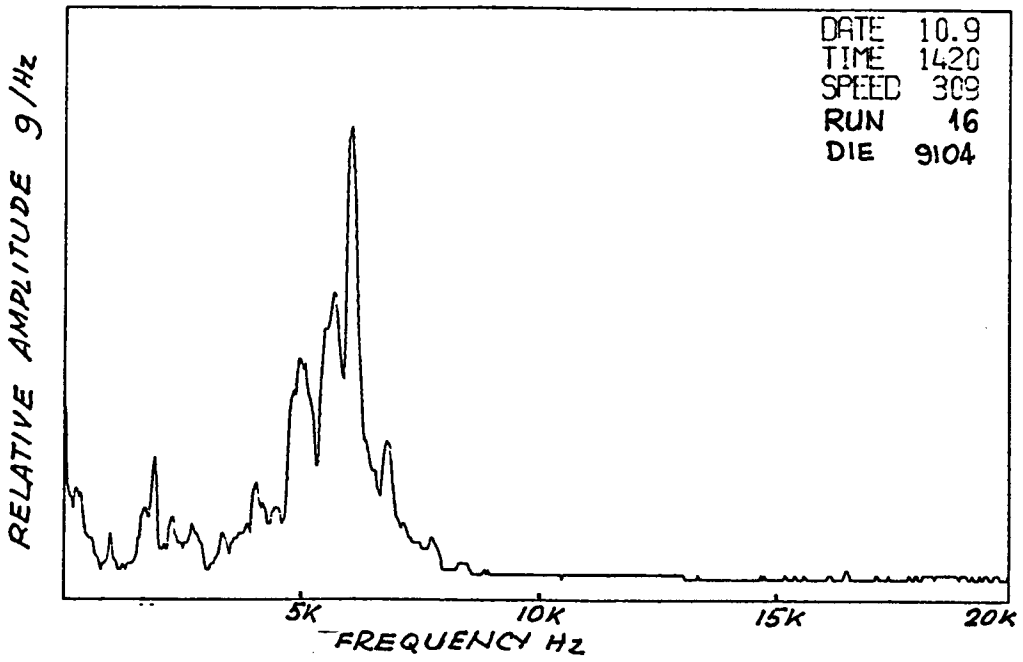
RELATIVE AMPLITUDE g/Hz
DATE 10.9
TIME 1420
SPEED 309
RUN 16
DIE 9104
5K
10K
15K
20K
FREQUENCY Hz

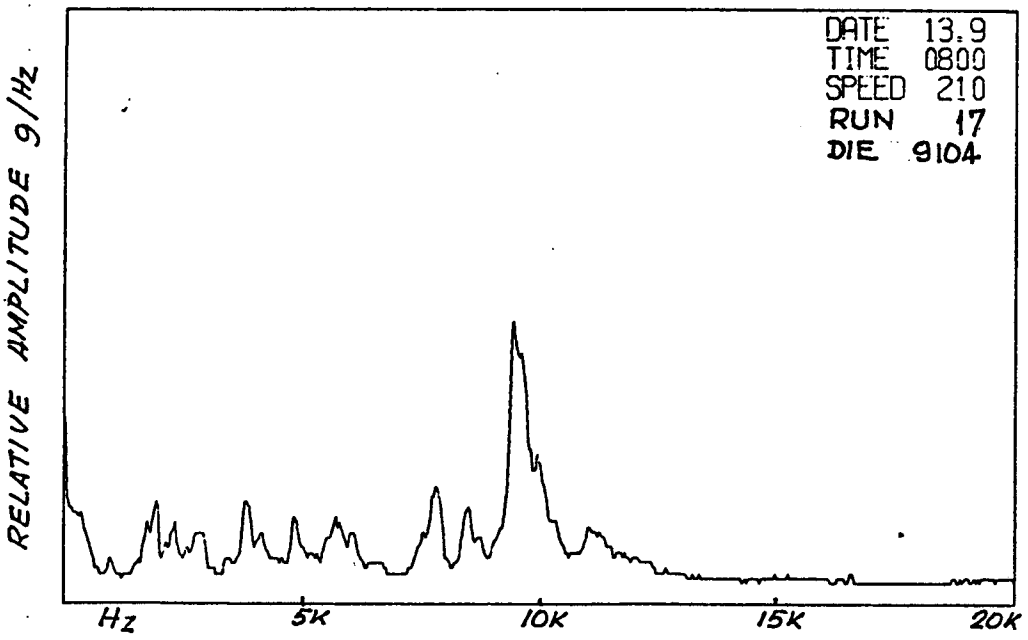
RELATIVE AMPLITUDE g/Hz
DATE 13.9
TIME 0800
SPEED 210
RUN 17
DIE 9104
Hz
5K
10K
15K
20K

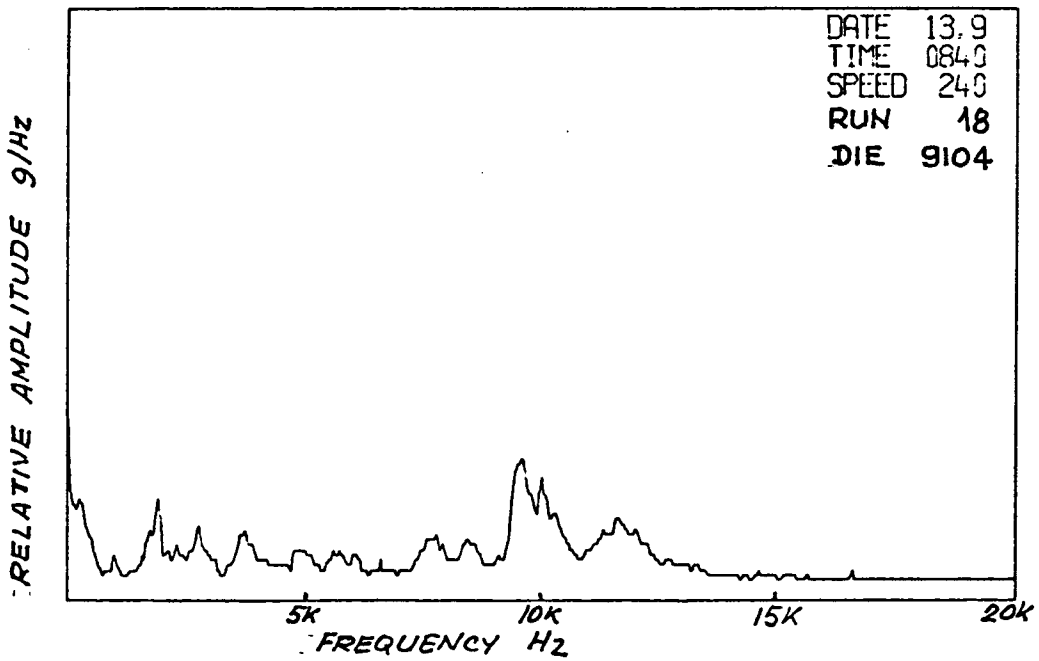
RELATIVE AMPLITUDE g/Hz
DATE 13.9
TIME 0840
SPEED 240
RUN 18
DIE 9104
5K
10K
15K
20K
FREQUENCY Hz

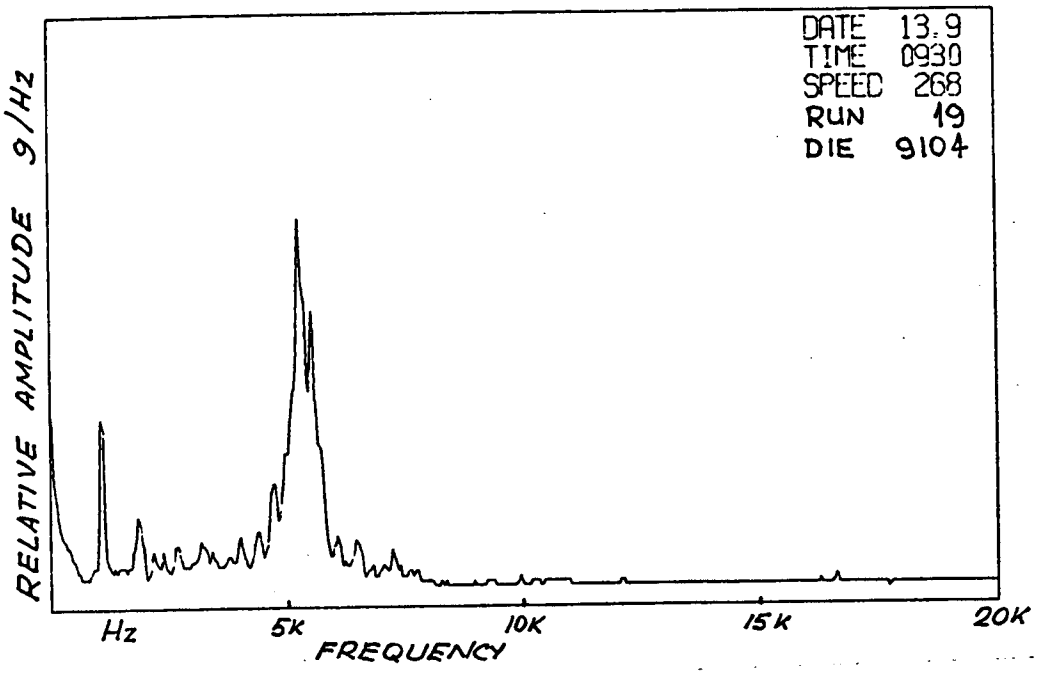
DATE 13.9
TIME 0930
SPEED 268
RUN 19
DIE 9104
RELATIVE AMPLITUDE g/Hz
Hz
5K
10K
15K
20K
FREQUENCY

APPENDIX II

COMPUTER PROGRAMS TO ANALYSE STORED AMPLITUDE SPECTRAL DENSITY DATA

PLOT PROGRAM

```
FORTRAN IV G LEVEL  21                  MAIN                DATE = 83332

 0001                   DIMENSION A(20000),AMP(500),PEAK(500),TELL(50,3)
 0002                   READ(9)N
 0003                   NJ=N/500
 0004                   WRITE(3,1)NJ
 0005              1     FORMAT('1',' NUMBER OF SETS  ',I4)
 0006                   READ(9)(A(I),I=1,N)
 0007                   DO 30 I=1,NJ
 0008                   READ(10)TELL(I,1),TELL(I,2),TELL(I,3)
 0009             30    CONTINUE
 0010                   WRITE(3,33)
 0011             33     FORMAT('1',61X,'MEDIAN FREQUENCIES',6X,
                     1 'DEVIATIONS')
 0012                   WRITE(3,34)
 0013             34     FORMAT(' ','NUMBER',6X,'DATE',8X,'TIME',8X,
                     1'SPEED',7X,'POWER',7X,'AMPLITUDE',3X,'POWER',
                     14X,'AMPLITUDE',3X,'POWER')
 0014                   DO 10 I=1,NJ
 0015                   P=0.
 0016                   V=0.
 0017                   QP=0.
 0018                   DO 11 J=1,500
 0019                   Z=A(500*(I-1)+J)
 0020                   V=V+Z
 0021                   P=P+Z*Z
 0022                   QP=QP+Z**4
 0023                   AMP(J)=V
 0024                   PEAK(J)=P
 0025             11    CONTINUE
 0026                   HP=0.
 0027                   HV=0.
 0028                   TV=V/2.
 0029                   TP=P/2.
 0030                   QP=QP/500.-(P/500.)**2
 0031                   QV=P/500.-(V/500.)**2
 0032                   QP=SQRT(QP)
 0033                   QV=SQRT(QV)
 0034                   DO 12 J=1,500
 0035                   IF(PEAK(J).GT.TP)GO TO 20
 0036                   LP=J
 0037             20    IF(AMP(J).GT.TV)GO TO 12
 0038                   LV=J
 0039             12    CONTINUE
 0040                   LP=40*LP
 0041                   LV=40*LV
 0042                   WRITE(3,2)I,TELL(I,1),TELL(I,2),TELL(I,3),P,LV,LP,QV,QP
 0043             2      FORMAT(' ',I4,F12.1,I12,I12,5X,F7.2,2(6X,I6),2(4X,F8.5))
 0044             10    CONTINUE
 0045                   STOP
 0046                   END
```

```
//RwHHLA   JOB ('********/7130CCCO',M2),R.W.HARRIS,                    
//             CLASS=1,TIME=1                                          LCG00010
/*ROUTE  PRINT VIEW                                                    LCG00020
/*JOBPARM  L=1                                                         LCG00030
//   EXEC  FORTGCLG                                                    LCG00040
//FORT.SYSIN  DD  *                                                    LCG00050
        DIMENSION A(20000),AMP(500),PEAK(500),TELL(50,3)               LCG00060
        READ(5)N                                                       LCG00070
        NJ=N/500                                                       LCG00080
        WRITE(3,1)NJ                                                   LCG00090
   1     FORMAT('1',' NUMBER OF SETS  ',I4)                            LCG00100
        READ(5)(A(I),I=1,N)                                            LCG00110
        DO 30 I=1,NJ                                                   LCG00112
        READ(10)TELL(I,1),TELL(I,2),TELL(I,3)                          LCG00113
  30    CONTINUE                                                       LCG00114
        WRITE(3,33)                                                    LCG00116
  33     FORMAT('1',61X,'MEDIAN FREQUENCIES',6X,                       LCG00117
     1 'DEVIATIONS')                                                   LCG00118
        WRITE(3,34)                                                    LCG00119
  34     FORMAT(' ','NUMBER',6X,'DATE',8X,'TIME',8X,                   LCG00120
     1'SPEED',7X,'POWER',7X,'AMPLITUDE',3X,'POWER',                    LCG00121
     1 4X,'AMPLITUDE',3X,'POWER')                                      LCG00122
        DO 10 I=1,NJ                                                   LCG00123
        P=0.                                                           LCG00130
        V=0.                                                           LCG00140
        QP=0.                                                          LCG00145
        DO 11 J=1,500                                                  LCG00150
        Z=A(500*(I-1)+J)                                               LCG00160
        V=V+Z                                                          LCG00170
        P=P+Z*Z                                                        LCG00180
        QP=QP+Z**4                                                     LCG00181
        AMP(J)=V                                                       LCG00182
        PEAK(J)=P                                                      LCG00183
  11    CONTINUE                                                       LCG00190
        HP=0.                                                          LCG00200
        HV=0.                                                          LCG00210
        TV=V/2.                                                        LCG00220
        TP=P/2.                                                        LCG00230
        QP=QP/500.-(P/500.)**2                                         LCG00232
        QV=P/500.-(V/500.)**2                                          LCG00233
        QP=SQRT(QP)                                                    LCG00235
        QV=SQRT(QV)                                                    LCG00236
        DO 12 J=1,500                                                  LCG00240
        IF(PEAK(J).GT.TP)GO TO 20                                      LCG00260
        LP=J                                                           LCG00290
  20    IF(AMP(J).GT.TV)GO TO 12                                       LCG00300
        LV=J                                                           LCG00310
  12    CONTINUE                                                       LCG00320
        LP=40*LP                                                       LCG00325
        LV=40*LV                                                       LCG00326
        WRITE(3,2)I,TELL(I,1),TELL(I,2),TELL(I,3),P,LV,LP,QV,QP        LCG00330
  2      FORMAT(' ',I4,F12.1,I12,I12,5X,F7.2,2(6X,I6),2(4X,F8.5))      LCG00340
  10    CONTINUE                                                       LCG00370
        STOP                                                           LCG00380
        END                                                            LCG00390
/*                                                                     LCG00400
//GO.FT09F001 DD  DSN=RWH.SITC27.SPECS,DISP=SHR                        LCG00410
//GO.FT10F001 DD  DSN=RWH.HLV.ANN1,DISP=SHR                            LCG00420
12345678901234567890                                                   LCG00430
```

SPECTRUM PARAMETER CALCULATIONS

```
//RWHHL1   JOB ('********/71300000',T2),R.W.HARRIS,                    LOG00100
//             CLASS=2,TIME=2                                          LOG00140
/*ROUTE PUNCH VIEW                                                     LOG00145
/*ROUTE PRINT VIEW                                                     LOG00150
/*JOBPARM L=3                                                          LOG00300
//     EXEC  FORTGCLG                                                  LOG00400
//FORT.SYSIN     DD    *                                               LOG00500
C PLOT OF TRANSFERRED DATA                                            LOG00550
C AUTOMATIC X AND Y SCALING                                           LOG00560
C         PLOT SIZE FACTORS (XF,YF) READ IN (2F4.0)                   LOG00580
          IMPLICIT REAL*4(A-H,O-Z)                                    LOG00600
          DIMENSION A(20000),B(20000)                                 LOG00650
          READ(1,200)XF,YF,IS                                         LOG00651
  200      FORMAT(2F4.2,I2)                                           LOG00700
          NR=-499                                                     LOG00900
          READ(9,END=10)N                                             LOG00902
          READ(9)(B(I),I=1,N)                                         LOG00910
          DO 240 I=1,N                                                LOG00911
          IF(B(I).LT.2000) GO TO 240                                  LOG00912
          B(I)=4096-B(I)                                              LOG00913
  240     CONTINUE                                                    LOG00922
  50      DO 222 I=1,N                                                LOG00923
          A(I)=B(I)                                                   LOG00924
  222     CONTINUE                                                    LOG00930
          NR=NR+500                                                   LOG00931
          NQ=NR+499                                                   LOG00932
          IF(NQ.GT.N) GO TO 10                                        LOG00970
  98      FAX=NQ-NR+1                                                 LOG00971
          FAX=500.*XF/(1.*FAX)                                        LOG01911
  600      CONTINUE                                                   LOG01912
          FAC=1.2                                                     LOG01913
          GO TO 800                                                   LOG01915
          FAC=0.                                                      LOG01920
          DO 800 I=NR,NQ                                              LOG01921
          ZX=ABS(A(I))                                                LOG01922
          IF(ZX.LT.FAC)GO TO 800                                      LOG01923
          FAC=ZX                                                      LOG01924
  800     CONTINUE                                                    LOG01940
          OF=FAC                                                      LOG01942
          WRITE(3,111)OF                                              LOG01943
  111     FORMAT(' ','MAXIMUM IS  ',E11.4)                            LOG01950
          FAC=1000.*YF/FAC                                            LOG01960
          READ(1,242)DATE,TIME,SPEED                                  LOG01970
  242     FORMAT(A5,A5,A4)                                            LOG02400
          CALL GPSEND(1,1)                                            LOG02500
          CALL GPLOT(62.5,200.,2)                                     LOG02600
          CALL GPLOT(0.,0.,1)                                         LOG02700
          Y=A(NR)*FAC + 400.*YF                                       LOG02800
          CALL GPLOT(0.,Y,3)                                          LOG02850
          NB=NR+1                                                     LOG02900
          DO 100 K=NB,NQ                                              LOG03000
          X=K-NB+1                                                    LOG03100
          X=X*FAX                                                     LOG03200
          Y=A(K)*FAC + 400.*YF                                        LOG03300
          CALL GPLOT(X,Y,4)                                           LOG03400
  100     CONTINUE                                                    LOG03500
          CALL GPLOT(0.,400.*YF,3)                                    LOG03600
          CALL GPLOT(500.*XF,400.*YF,4)                               LOG03700
          CALL GPLOT(500.*XF,1400.*YF,4)                              LOG03800
          CALL GPLOT(0.,1400.*YF,4)                                   LOG03900
          CALL GPLOT(0.,400.*YF,4)
```

```
      CALL GPLOT(450.*XF,1350.*YF,3)                                    LOG03902
      CALL GPTEXT(DATE,4,IS,0)                                          LOG03903
      CALL GPLOT(450.*XF,1300.*YF,3)                                    LOG03904
      CALL GPTEXT(TIME,5,IS,0)                                          LOG03905
      CALL GPLOT(450.*XF,1250.*YF,3)                                    LOG03906
      CALL GPTEXT(SPEED,4,IS,0)                                         LOG03907
      CALL GPLOT(400.*XF,1350.*YF,3)                                    LOG03910
      CALL GPTEXT('DATE  ',6,IS,0)                                      LOG03920
      CALL GPLOT(400.*XF,1300.*YF,3)                                    LOG03930
      CALL GPTEXT('TIME  ',6,IS,0)                                      LOG03940
      CALL GPLOT(400.*XF,1250.*YF,3)                                    LOG03950
      CALL GPTEXT('SPEED ',6,IS,0)                                      LOG03960
      CALL GPSEND(2)                                                    LOG04000
      GO TO 50                                                          LOG04100
 10   STOP                                                              LOG04200
      END                                                               LOG04300
/*                                                                      LOG04400
//GO.SYSIN    DD   *                                                    LOG04450
C.75C.7502                                                              LOG04451
 22.7 0935 264                                                          LOG04462
 22.7 0945 264                                                          LOG04472
 22.7 1040 324                                                          LOG04482
 22.7 1130 324                                                          LOG04492
 30.8 0900 324                                                          LOG04502
 30.8 0930 324                                                          LOG04512
 30.8 1030 324                                                          LOG04522
 30.8 1130 228                                                          LOG04532
 30.8 1230 264                                                          LOG04542
 30.8 1330 274                                                          LOG04552
 30.8 1420 287                                                          LOG04562
 30.8 1510 223                                                          LOG04572
 30.8 1540 370                                                          LOG04582
 30.8 1540 341                                                          LOG04592
 30.8 1640 357                                                          LOG04602
 30.8 1735 357                                                          LOG04612
 30.8 1810 218                                                          LOG04622
 31.8 0750 309                                                          LOG04632
 31.8 0910 262                                                          LOG04642
 31.8 1040 280                                                          LOG04652
 31.8 1140 252                                                          LOG04662
 31.8 1230 299                                                          LOG04672
 31.8 1335 365                                                          LOG04682
 31.8 1520 373                                                          LOG04692
 31.8 1600 373                                                          LOG04702
 31.8 1630 375                                                          LOG04712
 00.C 0000 000                                                          LOG04722
//GO.AEPLOT   DD   SYSOUT=C                                             LOG04732
//GO.FT09F001   DD   DSN=RWH.S1T027.SPECS,DISP=SHR                      LOG04742
```